CORRELATION BETWEEN GEOTECHNICAL AND ACOUSTIC PROPERTIES OF MARINE SEDIMENTS- OUTER PLACENTIA BAY, NEWFOUNDLAND

CENTRE FOR NEWFOUNDLAND STUDIES

TOTAL OF 10 PAGES ONLY
MAY BE XEROXED

(Without Author's Permission)

SHADEN TAWFIK ABDEL-GAWAD

MEMORIAL UNIVERSITY
LIBRARY
AUG 17 1982
OF NEWFOUNDLAND

CORRELATION BETWEEN GEOTECHNICAL AND ACOUSTIC PROPERTIES OF MARINE SEDIMENTS - OUTER PLACENTIA BAY, NEWFOUNDLAND

by

© SHADEN TAWFIK ABDEL-GAWAD, B.Sc.

A Thesis submitted in partial fulfillment
of the requirements for the degree of
Master of Engineering

Faculty of Engineering and Applied Science
Memorial University of Newfoundland

April 1980

St. John's Newfoundland

Canada

CORRELATION BETWEEN GEOTECHNICAL AND ACOUSTIC PROPERTIES OF MARINE SEDIMENTS - OUTER PLACENTIA BAY, NEWFOUNDLAND

TO MY PARENTS

ABSTRACT

Marine sediment samples collected by a Benthos piston corer and a Van Veen grab sampler from the floor of outer Placentia Bay have been subjected to a wide range of acoustic and geotechnical measurements. The parameters determined were subjected to a correlation analysis as part of a comprehensive study to determine relationships between geotechnical properties and the parameters measured by various investigation techniques. The regional and surficial geology of the Placentia Bay area is briefly reviewed.

Measurements of sound velocity on eight sediment core samples and related values of acoustic impedance are reported. Consolidation and shear strength data, as well as determinations of the index properties and particle size characteristics of the sampled sediments are presented. The output from impact cone penetrometer tests in the seabed near the core locations has been evaluated in light of the measured geotechnical properties. An expression to relate the dynamic resistance of the impact cone penetrometer to quasi-static cone resistance is postulated.

Both linear and non-linear regression analyses, using digital computation, have been used to establish relationships between various parameters and the degree of correlation in each case. The analysis has, for the sediment data evaluated, identified relationships between a) various geotechnical properties, b) acoustic and geotechnical properties and c) cone parameters and acoustic and geotechnical properties. In addition, a number of elastic constants of the sediments have been determined.

ACKNOWLEDGEMENTS

This dissertation was completed at the Faculty of Engineering and Applied Science, Memorial University of Newfoundland. The writer wishes to acknowledge with thanks the receipt of a Memorial University Fellowship during the period of this study.

The writer is very grateful to her supervisor Mr. W.L. White, Associate Professor of Engineering, for his excellent guidance, valuable suggestions, encouragement and continuous support with the provision of reference materials through the project.

The writer would like to express her gratitude to Dr. A. Zielinski, the late Dr. A.D. Dunsiger, Dr. N. Cochrane, Dr. P. Simpkin, and Dr. T.R. Chari for their keen interest in the work, for the facilities afforded to use their data, and for help on problems encountered during the progress of the work.

Thanks are due to Dean R.T. Dempster, Dean of Engineering, for the facilities provided and to Dean F.A. Aldrich, Dean of the Graduate School, for his constant encouragement.

Appreciation and gratitude are extended to the writer's parents, Mr. and Mrs. T. Abdel-Gawad, for their encouragement and inspiration. The writer is most fortunate in having a very understanding husband, special thanks are due to him for his assistance, patience and encouragement.

TABLE OF CONTENTS

LIST OF TABLES

LIST OF FIGURES

NOTATION

The symbols listed below and used in this thesis generally confirm to those suggested by the American Society of Civil Engineers (Nomenclature for Soil Mechanics, Journal of Soil Mechanics and Foundations Division, June 1962) and the Canadian Geotechnical Society, 1978. SI units are used throughout.

I – English Letters

a_c	– activity
a_o , a_1	– constants
C	– soil cohesion
C_c	– compression index
C_{Is}	– cone index of a standard cone
C_{Ix}	– cone index of penetration velocity V_x with cone diameter d_x
c_v	– coefficient of consolidation
D_R	– relative density
e	– void ratio
e_o	– initial void ratio
E	– Young's modulus
F_s	– sleeve friction
g	– acceleration
I_L	– liquidity index
I_P	– plasticity index
K	– water-mineral bulk modulus
K_f	– dynamic frame bulk modulus
K_s	– aggregate bulk modulus of mineral grains
K_w	– bulk modulus of pore water

M	- exponent of shear rate factor
$M_{d\phi}$	- median diameter
M_z	- graphic mean diameter
M_ϕ	- mean diameter
n	- porosity
N_c	- bearing capacity factor for cohesion
N_d	- dynamic bearing capacity factor
p	- pressure
p_c	- preconsolidation pressure
p_o	- effective overburden pressure
Q	- constant
Q_d	- dynamic cone tip resistance
Q_s	- theoretical quasi-static cone resistance
r	- correlation coefficient
R	- correction factor
S_r	- degree of saturation
S_u	- undrained shear strength
u_1	- clay fraction
u_2	- sand fraction
u_3	- silt fraction
v_s	- sediment sound velocity
v_w	- sound velocity in water
w	- moisture content
w_L	- liquid limit
w_p	- plastic limit
x	- independent variables
$\bar{x}$, $\bar{y}$	- mean values

y	- dependent variables
Z	- acoustic impedance

II - Greek Letters

α	- semi-apex angle
β	- compressibility
γ	- wet unit weight
ρ_s	- bulk density of soil
ρ_w	- density of water
σ_ϕ	- phi deviation
λ	- Lame's constant
μ	- Poisson's ratio
ν	- rigidity (shear) modulus

III - Units

mm	- millimeter
cm	- centimeter
m	- meter
gm	- gram
kg	- kilogram
kN	- kilonewton
kPa	- kilopascal
s	- second
log	- logarithm base 10

CHAPTER I

INTRODUCTION

1.1 General

There is an increased interest in the exploration, development and utilization of offshore resources. Marine geotechnical engineering is an important aspect in all these operations. Because of the conditions prevailing in the ocean environment, the tools and methods of sampling and in-situ testing are often different from the techniques used for soil and geological investigations on land. Since conventional terrestrial methods are expensive and of limited use in the offshore environment, a need exists for rapid, reliable and preferably remote methods of determining the composition and engineering properties of the seabed.

Methods currently being developed and used for offshore investigations include sampling (corers, etc.), in-situ testing (shear vanes, quasi-static cone penetrometers, impact penetrometers, etc.) and indirect methods (acoustic, seismic, etc.).

Indirect acoustic techniques provide a rapid, non-intrusive method of remotely sensing the ocean floor. To a large extent, the procedures have been subjective and practised by a few experienced marine geologists who have relied primarily on the interpretation of acoustic grey scale graphic records. Quantitative measurements of reflection coefficient and sound velocity using acoustic techniques (Hampton, 1974) have been employed mainly for the eventual determination of geophysical properties; e.g., bulk modulus, porosity and density. Although acoustic methods have the advantage of being fast they lack immediate correlation with the geotechnical

properties of marine sediments.

In terms of sediment classification, advances have been made in recent years with ground truthing being done by conventional techniques. Thus, grabs, dredges, boreholes and corers can then be used to retrieve what are hoped to be representative samples for laboratory analysis. Grabs and dredges retrieve only surficial materials, thus affecting the validity of the laboratory assessment of their geotechnical properties. Corers readily penetrate soft seafloor materials, and can recover disturbed samples with varying degrees of disturbance up to 10 meters in length. However, the presence of the water medium with large hydrostatic pressure and the frequent underconsolidation of surficial sediments make the task of high-quality sample recovery difficult. In-situ tests are thus becoming an indispensable component of offshore site investigation.

Among in-situ methods, the cone penetrometer is now finding greater application in both terrestrial and underwater investigations. The use of an impact penetrometer as a quick method of in-situ soil testing of the ocean floor has been demonstrated by Allen at al, (1975). As a part of the ongoing research on the penetrometer at Memorial University of Newfoundland, a completely redesigned version of the penetrometer was developed (Chari et al, 1978) and successfully deployed at sea during May, 1978.

1.2 C.S.S. HUDSON Cruise 1978 - M.U.N.

During the second half of May 1978, the Ocean Engineering Group at Memorial University of Newfoundland in cooperation with the Bedford Institute of Oceanography (BIO) undertook a multi-device, high-density seafloor survey in the outer Placentia Bay area at the northern extremity of the Newfoundland

Grand Banks, using the BIO ship C.S.S. HUDSON (Cruise 78-012). HUNTEC ('70) ltd. and the Geological Survey of Canada also contributed to this data-gathering effort.

One of the principal objectives of the cruise was to obtain data on ocean sediments in order to relate acoustical measurements to soil properties determined by conventional techniques. Other objectives were to perform sea trials of a prototype free fall penetrometer, and to assess a penetrometer descent-rate measuring device.

A site bounded by latitudes 46°N to 47°N and longitudes 54° 10'W to 55° 10'W at the southerly end of Placentia Bay, Newfoundland, was chosen. This site provides the required variety of sediments. A quick-look survey was first undertaken, in which the HUNTEC Deep Tow Seismic system (DTS), side scan sonar and air gun were used continuously. Based on this information, six locations overlain with five different sediment types were chosen for more intensive investigation (Fig. 1). The intensive study included an acoustic survey using the DTS system, the side scan sonar, the echo sounder and ground truth stations using a Benthos piston corer, Van Veen bottom grab sampling equipment and remote bottom photography. An impact penetrometer developed at Memorial University of Newfoundland was used at 20 stations. Table 1 summarizes the type and amount of data gathered at the various stations (Peters, 1978).

A transverse sound velocity profile of each core, in its plastic lining, was obtained immediately after removal from the core barrel. Laboratory tests were conducted later for natural moisture content, Atterberg limits, wet density, relative density, particle size distribution, vane shear strength and consolidation characteristics.

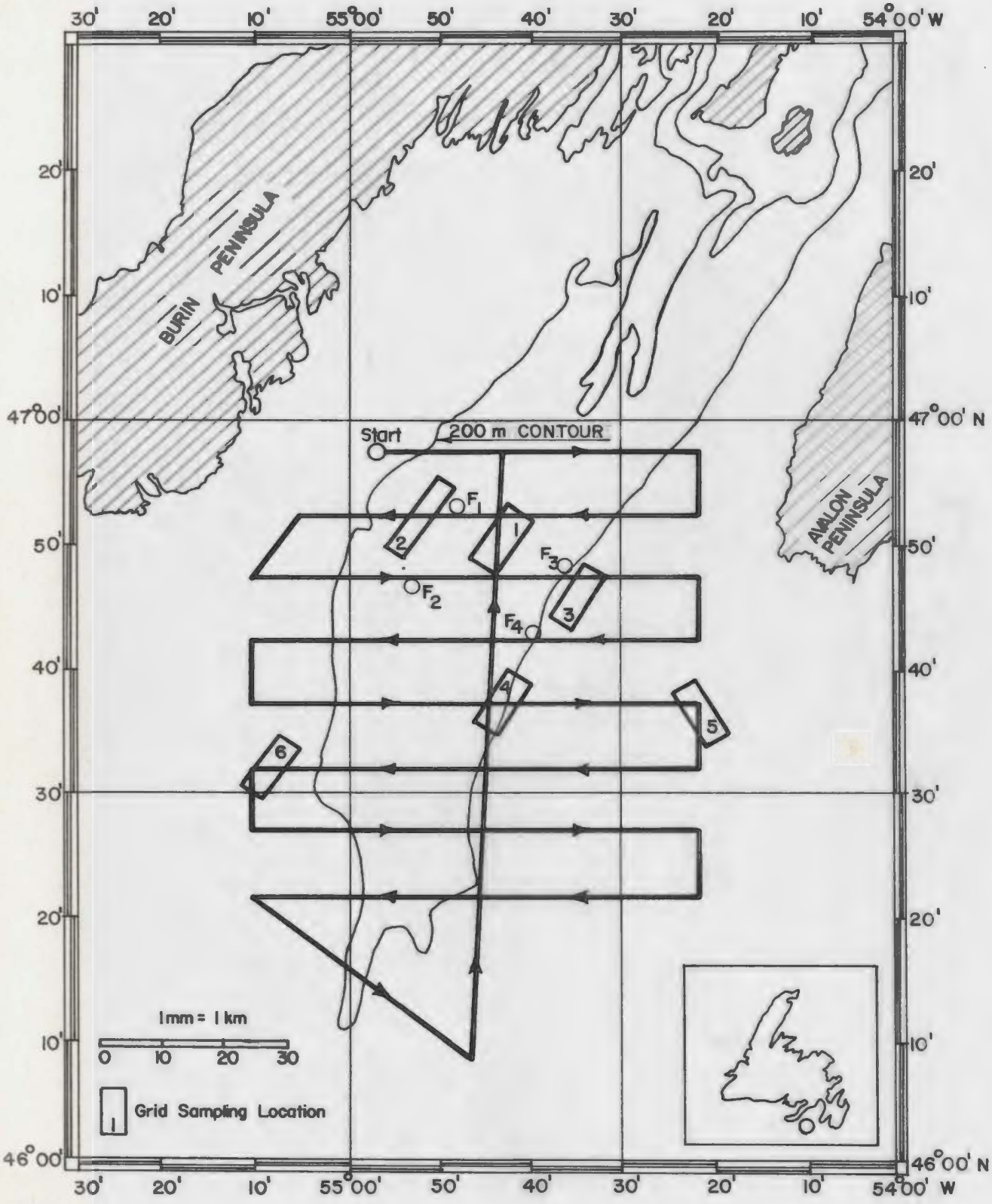

Fig. 1. Track Chart, C.S.S. HUDSON Cruise (78 - 012),

1 - 6 Intensive Study Areas. (Ref. 12)

TABLE 1. SUMMARY OF THE TYPES OF DATA GATHERED DURING C.S.S. HUDSON CRUISE (78 - 012). (Ref. 52)

Grid No.	Van Veen grab	Corer	Penetro-meter	DTS	Bottom photos	Density probe	Refraction array
1	14	9	6	1	2	1	2
2	16	5	2	1	2	1	1
3	15	4	4	2	1	1	0
4	15	11	8	1	3	1	1
5	15	0	0	3	6	0	0
6	15	0	0	1	3	0	0
other							
F_1	1	1	0	0	0	0	1
F_2	1	1	0	0	0	0	0
F_3	0	1	0	0	0	0	0
F_4	0	1	0	0	0	0	1
Total	92	33	20	9	17	4	6

The free fall impact penetrometer received extensive testing in this cruise. Cone tip resistance, sleeve friction and deceleration records were obtained for different soil targets. A doppler telemetry device was used in each penetrometer drop to independently measure the velocity of penetration during free fall.

1.3 Objectives and Organization of this Study:

The purpose of the research described in this thesis is to determine where correlation exists between acoustic and geotechnical properties of ocean sediments using field results obtained by Hudson cruise (78-012). An analysis of the output data from the free fall penetrometer formed part of this study to relate the geophysical, geotechnical and acoustic properties of ocean sediments. In this research, the acoustic properties of the cores are only included. The overall plan of Ocean Engineering Group is also to compare DTS acoustic data with the geotechnical and penetrometer data, but at the time of writing this thesis, this data has not been reduced to a form in which it could be compared.

Data from eight stations representing four grids in the test area are examined, and the results are reported in this dissertation. These locations are indicated in Table 2, and acoustic and geotechnical core data, grab, and penetrometer data is available for all sites.

It is worth mentioning that, in addition to the laboratory tests carried out by the author, some of the results reported herein were conducted by a group of research assistants. Geotechnical test results on 6 core samples and 4 free fall penetrometer tests were made available to the author with permission to use them in the analysis by the Ocean Engineering Group at Memorial University of Newfoundland.

The specific objects of this study are to present quantitative

TABLE 2. STATION LOCATIONS, WATER DEPTH AND CORE LENGTH

grid no.	position		water depth (m)	core length (m)
	Latitude N	Longitude W		
G 132	46° 50.3'	54° 43.5'	263	8.82
G 141	46° 48.4'	54° 44.2'	230	7.06
G 233	46° 52.9'	54° 50.5'	241	3.02
G 243	46° 52.6'	54° 49.5'	247	2.75
G 332	46° 46.1'	54° 34.5'	165	3.68
G 341	46° 44.5'	54° 35.2'	157	2.30
G 432	46° 36.9'	54° 43.3'	196	3.50
G 441 A	46° 35.6'	54° 43.4'	188	5.65

relationships between the following three data sources from the areas investigated:

1. the basic geotechnical properties of the sediments from conventional laboratory analyses of the cores; e.g. moisture content, Atterberg limits, wet density, relative density, particle size distribution, vane shear strength and consolidation tests.
2. the sound velocity and acoustic impedance profiles of the cores.
3. the free fall penetrometer records of cone tip resistance, sleeve friction and deceleration as well as the penetrometer velocity measured directly by doppler telemetry.

There is also a basic need to have the considerable amount of data obtained during this investigation assimilated and presented in this manner as a record for future reference.

The state-of-the-art of the methods used for evaluating geotechnical and acoustic properties of ocean floor sediments is reviewed in Chapter II. Chapter III presents information to the geology, bottom topography and surficial geology of the Placentia Bay test area. Chapter IV presents data acquisition, methods and summarized results of this investigation. Analysis of laboratory results, correlation between available data sources, and an interpretation of the free-fall penetrometer results are presented in Chapter V. Finally, the summary and conclusions from this study are presented in Chapter VI together with recommendations for further work. Additional details of the procedures and methods actually used for measuring sediments properties are explained in Appendices A and B, while Appendix C presents details of the correlation analysis and the computer program used.

CHAPTER II

THE STATE-OF-THE-ART AND LITERATURE REVIEW

2.1. General

Activities related to the design and construction of offshore structures have gained great momentum in the last two decades. Detailed information on the properties of sea floor soils is essential for safe and economical design of foundations on the ocean floor. The development of most seabed resources including the methods and economics is influenced by the nature and type of the ocean floor materials as well as the extent to which the geotechnical properties of the ocean bed can be evaluated. Methods for offshore evaluation are mostly extensions of conventional procedures used onshore. With the expansion of offshore activities, new techniques are needed for both preliminary and detailed evaluation of ocean bed characteristics.

This chapter briefly reviews the methods currently used for measuring and evaluating geotechnical properties of the ocean floor including indirect techniques (acoustics, seismic, etc.) and direct methods (sampling and in-situ testing). Various attempts relating sediment properties with acoustic properties are also presented.

2.2. Indirect Methods

One of the byproducts of offshore exploration is the rapid development of indirect methods to determine sub-bottom characteristics, such as; acoustic, sub-bottom profiling and electrical logging.

The use of acoustic surveys dates back to the 1920s, when geophysicists used a sound refraction method to detect the depth of rock formations in oil fields.

2.2.1. Acoustics

Knowledge of the acoustical properties of sediments is important in its own right. Direct acoustic probe measurements can be made on two parameters, the velocity of sound transmitted through sediments and its attenuation. Surface probes, containing a transmitter and variable distance receiver, have been constructed and can measure acoustic properties within the top 10 cm of seafloor sediment.

During the past two decades, extensive studies have been carried out to measure sound velocities on core samples and in-situ (Hamilton, 1963 and 1965). Test results on a wide range of marine sediments indicate a range of typical sound velocities from 1500 m/s for medium clays to 1780 m/s for sands. It has been well demonstrated that sound velocity is inversely related to porosity. For porosities more than 0.55, sound velocities were lower than that in sea water which is 1533 m/s (Noorany and Gizienski, 1970). In 1962, the first deep-water in-situ measurements of sound velocity in seafloor sediments at water depths of 338 m to 1240 m were made using special probes attached (Hamilton, 1963). The results of wave velocity measurements from the submersible Deepstar-4000 in bottom deposits at water depths up to 915 m have been reported by Hamilton (1969). During these dives, samples were taken also by corers deployed from the submersible. Laboratory measurements of sound velocities on soil samples agreed closely with the in-situ measurements (Hamilton, 1963 and 1969).

Knowledge of the relationships between acoustical and physical properties of sediments permits the use of acoustical techniques for determination of the physical and some engineering properties of sediments.

2.2.2. Seismic Reflection Profiling

Seismic methods are routine operations in geophysical exploration, onshore and offshore. A state-of-the-art survey of sub-bottom profiling is given by Saucier (1970). Seismic reflection profiling systems consist of a source for generating a pulsed acoustic energy, detection of the reflection at the various boundaries and continuous recording on a suitable recorder. Use of this method in geotechnical investigations is confined to obtaining high-resolution bottom profiles, detecting surficial topography, layering and buried glacial channels. High-resolution sub-bottom reflection profiling (less than 200 m penetration) presents little difficulty in areas of soft sediment cover. However, in areas of hard bottom, large amounts of energy scatter result in poor penetration.

2.2.3. Side Scanning Sonar

A side scan sonar (SSS) is typically used in conjuction with sub-bottom profiling (Hitchings, et al. 1976) and the combined techniques are commonly used for site selection surveys for marine structures. SSS is used to image the surface macrofeatures of the seafloor, and to characterize the general distribution of different types of bed materials (e.g. muds, sands, gravels, bedrock and hard glacial till). The presence of these features may sometimes be used as an indicator of both subsurface conditions and environmental conditions.

Although data from acoustic profiling techniques is quite useful for preliminary site evaluation, sufficient soils information for

foundation and geotechnical design is not provided. The required physical and mechanical properties of submarine soils at present can be assessed only by direct sampling or in-situ testing.

2.3. Direct Methods

2.3.1. Underwater Sampling

Underwater sampling in the ocean predates the days of the Challenger expeditions (1872 - 1876). With the growing interest in marine geotechnology during recent years, various types of improved samplers have been developed. A survey of bottom samplers of different types is given by Noorany (1972) and Fukuoka and Nakase (1973). The techniques of underwater sampling may be subsumed under two major categories:

a) Shallow penetration samplers having penetration depths of a few meters up to nearly 30 m.

b) Deep penetration sampling and drilling used for greater depths up to 1000 m.

2.3.1.1 Shallow Penetration Sampling

Shallow penetration samples may be obtained by hand tools and simple samplers operated by divers. Various types of samplers are available for near surface as well as sub-bottom sampling.

a. Near Surface Sampling

Several types of samplers for scooping up surface sediments have been used such as: orange peel sampler, Shipek sampler, Van Veen sampler, box dredge and clamshell snapper. For undisturbed sampling of near surface soils, two types of samplers are most commonly used; the gravity corer and the free fall piston corer. The gravity corer is an open barrel corer, with weight and is strung by wire and winch to the ship. The falling speed

is in the range of 1 - 3 m/s (Fukuoka and Nakase 1973). The free fall piston corer is a modified version of the gravity corer. The corer is lowered by a wire and winch, and when a trigger weight touches the sea bottom, a release mechanism comes into action and the corer falls freely down and penetrates into the bottom soils. An advantage of this corer as compared to the gravity corer is to be able to use a piston sampler, which is favourable in reducing the degree of sample disturbance. Piston samplers can be used to obtain cores of maximum 150 mm diameter and 3 m length and gravity corers for obtaining 300 mm diameter and 6 m long (Richards 1966). The spade corer is considered to be a special type of free fall corer (Rosfelder and Marshall 1967). This sampler built in a tripod frame is lowered by a wire and winch down in the water. When it hits the sea bottom, the draw wire slacks and the sampler penetrates into the soil by its own weight, then a swinging spade closes the bottom of the box type sampler. This sampler has been successfully used for soft soils. Another types of corers such as rocket fueled samplers, rotary corers and giant piston corer (Silva and Hollister 1973) have been successfully used.

b. Sub-bottom Sampling

The samples obtained by the oceanographic samplers are generally not satisfactory for structure foundation design because of the following short-comings:

1. the length of the core is short.
2. a detailed location of sample in the sediment column is not always known because the core penetration is not controlled.
3. a vertical orientation of samples is not always ascertained.
4. a degree of sample disturbance is often relatively high.

In order to overcome these short-comings, several types of bottom resting cores have been devised. These tend to be elaborate in construction and are generally mounted on a frame resting on the ocean floor. U.S. Navy's (Taylor and Demars 1970) DOTIPOS (Deep Ocean Tests In-Place and Observation System), university of Rhode Island's DOSP (Deep Ocean Sediment Probe) and the vibrocorer are examples under this category. These bottom resting corers are able to perform an incremental coring by the use of manipulators.

2.3.1.2 Deep Penetration Drilling and Sampling

Site investigations for major structures at sea require deep penetration borings. Drilling and sampling operations may be carried out from a fixed platform constructed on piles, a jackup platform, an anchored barge or a positioned ship.

The drilling and sampling procedure from fixed or jackup platforms resembles deep drilling on land, however, when an anchored barge or a drilling boat is used, special offshore drilling techniques become necessary. Two major problems which must be coped with are ship movement and difficulties involved in sampling at great depths. One method which has proved effective is the use of drill pipe to advance the boring and to serve as a guide pipe for a wire line sampler and testing equipment. Drilling mud is commonly used to stabilize the sides of the boreholes which would otherwise collapse, particularly if the sediment penetrated is weak. Emrich (1971) has described the principles of operation of wire line corers, and has given details of applications in offshore boreholes.

The engineering literature contains a number of accounts of deep penetration sampling operations for foundation investigations.

2.3.2. In-Situ Testing

A variety of techniques used for terrestrial in-situ measurements are available for adoption to ocean floor work. In-situ devices generally measure a characteristic property of the soil in its natural environment which is then related to the shear strength and bearing capacity. The in-situ test results frequently supplement laboratory tests on recovered samples. The following techniques have been successfully used but most are in an ongoing stage of development.

2.3.2.1 Vane Shear Tests

For the purpose of obtaining the undrained shear strength of fine grain sediments, the vane test seems preferable. Fenske (1957) has reported the use of vane shear tests in the Gulf of Mexico. Taylor and Demars (1970) have developed an instrument "The Deep Ocean Test In-Place and Observation System" (DOTIPOS) for measuring in-situ shear strength with the help of vane shear and a static cone penetrometer. This instrument is capable of measuring shear strength to a sediment depth of 3 m at water depth to 180 m. McNary and Frolich (1970) have reported vane shear devices which can be operated by divers, for testing surficial sediment deposits. A remote-controlled vane probe has been developed and tested by Doyle, et al. (1971). Richards, et al. (1972) have reported an in-situ vane shear testing equipment capable of testing up to 3 m depth of surficial sediments in water depths of 4500 m.

2.3.2.2 Plate Bearing Tests

Harrison and Richardson (1967) have performed plate bearing tests (i.e. model footing tests) in shallow water (5 to 6 m deep). This system is not yet suitable for deep water testing unless some modifications are made. Kretschmer and Lee (1969) have reported a device developed by Naval Civil Engineering Laboratory (NCEL) for performing in-situ plate bearing

tests on sea floor sediments. NCEL has also developed two devices for monitoring long term sea floor foundation settlement and tilting.

2.3.2.3 Pressuremeters

Pressuremeter tests have been used mostly in Europe to evaluate the stress-strain behaviour of soils. Gambin (1971) has reported the use of a pressuremeter at 45 m below the mudline in water depths of 90 m. The technique involves the expansion of a cylindrical membrane in a prepared cavity in the soil. The membrane forces the walls of the hole to expand as a result of internal fluid pressure. Both the pressure and corresponding volume changes are measured and plotted to evaluate the in-situ soil elastic modulus directly and the shear strength and compressibility indirectly.

2.3.2.4 Accelerometers

Scott (1967) suggested the use of an accelerometer mounted on a gravity-type corer, to obtain information about both the performance of the corer and the in-place properties of the sediment. The acceleration applied to the corer and recorded by the accelerometer can be converted directly into forces by multiplying by the appropriate mass for the corer in the water. Integration of the acceleration - time record yields the velocity of the corer, and a second integration yields the displacement.

Data of the force and displacement can be related to the adhesion of the soil on the inside and outside surface of the corer and thus to the shear strength of the soil.

2.3.2.5 Electrical and Nuclear Methods

Electrical resistivity studies on soils to predict different geotechnical properties have been reported by Erchul (1974) and Wang, et al. (1976).

Nuclear density meters (Keller 1965) may be used to determine the in-situ bulk density and water content of sediments. These devices may be either shallow probes or inserted in previously drilled boreholes.

2.3.2.6 Cone Penetrometer Tests

Various types of penetrometer tests are finding greater application in both terrestrial and underwater investigations. The resistance offered by the soil to advancement of the penetrometer device can be correlated to the soil properties.

Penetrometers used in the ocean environment can be classified according to the mode of operation as; a) static or quasi-static penetrometers, b) dynamic penetrometers and c) free fall penetrometers.

a. Quasi-Static Penetration Test

The idea of static or quasi-static penetration test is simple, a rod is advanced into soil at a constant speed (1 - 2 cm/s) and the load required to produce such an advance is measured. The "FUGRO" electrical cone penetrometer (De Ruiter 1971) capable of measuring the tip resistance and sleeve friction through load cells inside the penetrometer is now popularly used as a standard penetrometer.

Cone penetrometer tests in a quasi-static mode have been used for more than thirty years, mostly in Europe, in terrestrial geotechnical engineering (Sanglert 1972). A review of the various methods and the state-of-the-art in different countries is given in ESOPT (1974).

Static penetrometers require seabed rigs (De Ruiter 1975, Zuidberg 1975) to test marine sediments and a drill string attachment (Ferguson, et al. 1977) for tests inside boreholes. A number of cone penetrometers have been used in the North Sea, for which the "Seacalf" and "Stingray"

investigation systems are probably best known for their deep penetration capabilities. The "Seacalf" is a 20 ton sea bed jack which drives a fixed length of cone rod into the seafloor sediments at a rate of 2 cm/s, (Zuidberg 1975). The "Seacalf" has achieved a maximum penetration of 25 m in soft sediments and 6 to 8 m in hard clays. The recently developed "Stingray" seabed jack has achieved 25 m penetration in very hard clays.

For site-specific foundation studies, static penetration tests appear to be extremely relevant and useful. The only limitation associated with static penetration tests in the marine environment is the need for suitable reaction rigs to perform the test.

b. Dynamic Penetration Test

In recent years, several studies of a projectile directed at low and high velocities into seafloor have been reported. Scott (1967) built an accelerometer monitored corer which collects the soil sample and records the deceleration of corer simultaneously. Preslan (1970) has made use of accelerometer records in calculating the drag force and added mass of a free falling corer. Colp, et al. (1975) reported measurements with a 75 mm diameter, 1500 mm long disposable penetrometer with a tapered nose section. True (1975) reported studies with dynamic penetrometers of different shapes. Beard (1977) developed a disposable penetrometer with Doppler telemetry for velocity measurement. A 50 mm diameter dynamic penetrometer driven by repeated blows of a freely falling weight was reported by Kolbe (1975). Standardization and interpretation of dynamic penetration tests is still an area for further work.

Another variety of dynamic cone penetration test commonly forming a part of nearshore investigations consists of a drop weight progressively advancing a cone tip attached to drill rods.

c. Free Fall Penetrometer

With a view to developing a quick and economical way of testing surficial soils over large areas, the use of the standard "FUGRO" penetrometer with some modification in free fall mode was suggested, and a laboratory free fall penetrometer was developed (Dayal 1974) at Memorial University of Newfoundland. A penetration of 10 meters of the ocean floor is envisaged with such an instrument. This has a good potential in geotechnical surveys and investigation of large tracts such as those of pipeline routing. There were some operational and structural problems when this penetrometer was tried at sea (Jones 1976).

A completely redesigned version of the field penetrometer is now 76.2 mm (3 inch) diameter. A description of the penetrometer and preliminary results from its sea trials south of Newfoundland during May 1978 are reported by Chari, et al. (1978, 1979).

As part of the ongoing research on penetrometer characteristics, laboratory experiments were conducted to facilitate interpretation of the output from the 76.2 mm diameter model. Results from these penetrometer tests in quasi-static mode were reported by Abdel-Gawad (1979), and in free fall mode by Chaudhuri (1979). The correlation of the tests using this penetrometer in the free fall and quasi-static modes with the results from triaxial and direct shear tests is reported by Chari, et al. (1979).

2.4. Geotechnical and Acoustic Property Inter-Relationship

Various attempts have been made to relate sediment properties with acoustic properties. The following discussion describes the relationship of acoustic properties with the geotechnical properties of sediments. Hamilton (1965) and Horn, et al. (1968) revealed in their studies that for

sediment bulk properties a decrease in porosity, moisture content and void ratio is matched by an increase in sound velocity.

A definitive relationship has been reported between sound velocity and mean grain size. Sound velocity increases with an increase in mean grain size (Hamilton, 1965 and Horn, et al. 1968). They also reported a relationship between wet density and sound velocity in water-saturated sediments. Sutton, et al. (1957) showed definite positive correlation between sound velocity and carbonate content. This correlation described by Sutton et al. was discounted by Hamilton (1965) as being due to cementation within the sediment sample. The results of Buchan, et al. (1972) investigation on 84 cores showed that an increase in the percentage of calcium carbonate present, could be associated with an increase in sound velocity, acoustic impedance and attenuation coefficient.

Several regression analyses have been carried out mainly on core samples, relating acoustic properties to certain geotechnical parameters. Sutton, et al. (1957) obtained a relationship between sound velocity and certain geotechnical properties for ocean bottom consolidated sediments which be expressed as;

$$v_s = 1.653 - (0.414 \pm 0.006)M_{d\phi} + (0.00135 \pm 0.00038)\gamma - (0,44 \pm 0.15)n \quad \ldots\ldots(1)$$

where: v_s = the observed sound velocity in km/s

γ = the percent of carbonate by weight of dried sample

$M_{d\phi}$ = the median diameter

n = porosity

Buchan, et al. (1972) related sound velocity with many geotechnical parameters and the more relevant correlations obtained were;

$$v_s = 1.336 + 0.092\ u_2 + 0.101\ \rho \quad \ldots\ldots\ (2)$$

$$v_s = 1.616 + 0.09\ u_2 + 0.002\ n \quad \ldots\ldots\ (3)$$

$$v_s = 1.416 - 0.007\ M_\phi + 0.091\ \rho \quad \ldots\ldots\ (4)$$

where: u_2 = sand fraction > 62.5 microns

ρ = bulk density, gm/cm^3

M_ϕ = mean diameter, (phi units)

Acoustic impedance is a fundamental geotechnical – acoustic parameter which is equal to the product of sound velocity and bulk density. The relationship between acoustic impedance and wet density is very well defined for most sediments (Hamilton 1965 and Buchán, et al. 1972) as is its relationship with porosity. Buchan, et al. (1972) obtained the best prediction equations for acoustic impedance from a regression analysis of;

$$Z = 2.733 + 0.0014\ S_u + 0.721\ w_L \quad \ldots\ldots\ (5)$$

where: S_u is the shear strength (gm/cm^2) and w_L is the liquid limit. They also reported relationships between attenuation coefficient and geotechnical parameters with the total correlation coefficients for 84 sets of results.

CHAPTER III

GEOLOGY, BOTTOM TOPOGRAPHY AND SURFICIAL GEOLOGY - PLACENTIA BAY

3.1 Regional Geology

The island of Newfoundland represents the North American extremity of the Appalachian Orogen, a northeast - trending belt of deformed rocks extending along the Atlantic seaboard of the United States and Canada. The orogen includes the major portion of the adjacent offshore shelf areas, including the northern half of the Grand Banks and the Scotian Shelf.

Five major stratigraphic zones are recognized within the Orogen in insular Newfoundland, (Williams, 1979). Placentia Bay and an area extending southward to about Latitude 45°N are located within the Avalon zone, which is separated from the adjacent Gander zone to the northwest by the major Hermitage/Dover fault. The Avalon zone is underlain primarily by late Precambrian volcanic and sedimentary rocks that have undergone relatively little metamorphism. Over much of the area sedimentary rocks of Cambrian or Lower Devonian age overly the Precambrian, which plutonic Devonian rocks are also present throughout the zone.

The terrestrial geology around Placentia Bay is complex. Along the western and eastern shorelines siliceous mudstones, shales and sandstones of late Hadrynian and Cambrian age predominate. Volcanic rhyolites of similar age are common on the Burin Peninsula along the western side of the bay. Plutonic rocks comprising granites, syenite, diorite and related rocks are common north and northwest of the bay.

3.2. Submarine Topography

Placentia Bay is within the submerged Atlantic Uplands region of the Appalachian Orogen. It is the largest bay in insular Newfoundland, and is about 130 km long and 90 km wide at its mouth which is adjacent to the northerly limit of the Grand Banks. The longitudenal axis of the bay and the deeper channels extend in a NNE - SSW orientation. Placentia Bay has the characteristics of a fiord with a predominantly U - shaped cross-section and relatively deep water, both features which indicate glacial scouring.

The floor of Placentia Bay is characterized by a deep trough, arbitrarily defined by the 200 m depth contour, which extends the full length of the bay and 50 km to the south. Towards the northerly end, the trough divides into three narrow channels which are overdeepened and separated by three islands. Near the mouth of the bay, the deep trough widens to a large overdeepened basin about 20 km wide and 80 km long. The minimum depth of water beyond the southerly limit of the basin varies from 100 to 130 m in channels between individual banks. The greatest water depth within Placentia Bay is about 450 m immediately southwest of Merasheen Island, while within the study area the greatest water depth is about 265 m (Canada, Hydrographic Service, 1973).

In addition to the main trough and channels already described, the floor of the bay contains several other U - shaped channels and a number of small, overdeepened depressions. Small banks and shelf areas characterize the irregular surface morphology along the western side of the bay. In contrast the bottom configuration along the eastern side comprises more uniform and consistent slopes. Southward from Placentia Bay, the bottom topography is typically more uniform.

3.3. Oceanography

Relatively little information on currents and other oceanographic parameters has been published for the Placentia Bay area although data from several localized studies is available. From the limited information reported surface currents move predominantly counterclockwise, but are variable in both directions. Wind appears to have a greater influence on these surface currents than tidal activity, but all observations indicate low velocity currents in the order of 1 knot. Observations of surface drift along the easterly side of the bay suggest strong northeasterly surface currents in this area , although velocity determinations were not made (Stehman, 1976).

South of Placentia Bay, surface currents move in a westerly direction at about 0.5 knot resulting from general ocean circulation.

Virtually no information on deep water currents is available near the mouth of the bay, but bottom topographic features such as megaflutes and sand waves confirm that significant bottom currents exist.

3.4. Glacial and Surficial Geology

The extent of present knowledge and methods used to determine regional surficial geology in the eastern Canadian offshore area have recently been reviewed by King (1979). The surficial sediment characteristics and distribution in northern Placentia Bay have been reported by Stehman (1976). However, virtually no details on sediment composition and distribution over the southern half of the bay are available.

Much of the northwest Atlantic continental shelf area was glaciated during the Pleistocene epoch. In the vicinity of Placentia Bay, it is postulated that the last continental ice sheet deposited glacial

debris some 150 km south of the mouth of the bay (Sen Gupta and McMuller 1969). It is interpreted that Wisconson ice from central Newfoundland moved southeastward across the northerly part of Placentia Bay. There is also evidence that another large ice mass moved westward from the southern Avalon Peninsula out into Placentia Bay (Henderson, 1972). The presence of ice in the Grand Banks area is thought subsequently to have blocked the southward flow of ice in the bay.

It is thus probable that the majority of surficial sediments in the bay and to the south were derived from bedrocks and glacial debris transported by ice from the north and west. However, some of the present sediments undoubtedly originated in the St. Mary's Bay area of the Avalon. Petrographic evidence confirms the local source of the majority of Placentia Bay sediments (Slatt and Gardiner, 1976).

The surficial sediments in outer Placentia Bay are direct deposits of the last major glacial advance and / or the result of the subsequent marine transgression from the late Pleistocene sea level to the present level. Extensive areas of exposed till have been mapped in the bay but an absence of glacial till below about the 200 m contour indicates a possible isobath or lower limit of glacial ice (Stehman, 1976).

The Pleistocene shoreline is characterized by beachlike feature at about 110m contour. Nearshore marine activity at this time modified the bottom materials adjacent to the beach strand. Reworking of the previously-deposited glacial marine took place as the sea level rose from the Pleistocene minimum, with a transgression beach zone formed at successive levels of the rising sea. During this process, fine particles were removed from the glacial deposits leaving the coarser fragments in

the beach zone. The silt and clay size particles were transported to deeper water where deposition occured as predominantly fine-grained sediment. Evidence of this marine transgression and deposition of fines in deeper channels and basins of Northern Placentia Bay was verified by Stehman (1976).

3.5. Local Subsurface Conditions at Grid Locations

A preliminary determination of the sub-bottom stratigraphy in each of the grid areas selected for detailed study (Fig. 1) was made during the Hudson cruise 78-012. An interpretation of data from the following sources comprised this initial evaluation: air gun seismic reflection profiles, Kelvin-Hughes MS-26B echo sounder profiles, Huntec '70 DTS high resolution seismic reflection profiles, side scan sonar profiles and a visual examination of surficial grab samples and piston cores.

The results of this interpretation suggest the following stratigraphical sequences in the unconsolidated sediments and related surface topography (Chari et al. 1979):

Grid No. 1: Clay (mud) about 15m thick, overlying 20 m of silt which in turn overlies about 10 m of glacial till which extends to the bedrock surface.

Grid No. 2: Typically clay (mud) overlies about 10 m of proglacial silt which extends to glacial till. Several areas of glacial till outcrop exist.

Grid No. 3: A surficial sand and gravel layer overlies the clay stratum which in turn overlies the proglacial silt which is in excess of 10 m thick. Sand waves also occur in this area, and towards the south gas was detected. The surface is relatively smooth with little relief.

Grid No. 4: Similar to grid no. 1, but the clay appears to have been eroded in places and several slight longitudinal depressions exist. A number of sand waves were also detected on the surface.

Grid No. 5 and 6: Sand and gravel, less than 10 m thick, overlies bedrock in grid no. 5, Shell accumulations are also common. Within grid no. 6, glacial till less than 10 m thick generally overlies bedrock. The surface contains a number of apparent iceberg furrows.

CHAPTER IV

DATA ACQUISITION - EQUIPMENTS, METHODS AND SUMMARIZED RESULTS

4.1. Introduction

Sediment samples collected by a Benthos piston corer and a Van Veen grab sampler at four test sites in the outer Placentia Bay area have been subjected to a wide range of geotechnical and acoustic measurements. Penetration resistance and acceleration data from a free fall penetrometer has also been obtained at these sites and evaluated. Comparisons of the data available have been carried out as part of a comprehensive study of the engineering properties of marine sediments and alternate methods of evaluation.

Data presented and evaluated in this study have been obtained from 8 cores, 10 grab samples and 6 free fall penetrometer test locations. This chapter presents results of geotechnical laboratory testing, penetrometer test results and core velocity logging, and describes procedures followed to obtain the data presented herein. Actual data are summarized in this chapter while additional details of test procedures and methods actually used are presented in Appendix A.

4.2. Geotechnical Properties of Sediments

The geotechnical parameters of sediments can be listed under three main headings; parameters which describe the particles themselves, parameters which relate the index properties and those which describe engineering properties. Descriptive parameters of the first type are

those concerned with grain size, grain shape and mineralogy. Index properties include water content, density and physical properties, while engineering properties include mechanical strength and elastic constants.

The more commonly used classifications of sediments are those based on particle size. Descriptive terms such as silt, mud, clay and sand are often used in general conversation, but for scientific and commercial purposes, these terms must be quantified.

4.2.1. Particle Size Analysis

Folk (1966) gives a detailed description of the various techniques in common use for particle size analysis. Sediments coarser than very fine sand are graded by sieving whilst sediments containing significant amount of clay and silt are analyzed by a combination of sieving and hydrometer or pipette methods.

The data from particle size analyses are normally expressed in the form of percentages by weight of the sample within various size ranges. Gravel is considered to have a maximum dimension in the range of 60.0 mm to 2.0 mm, sand 2.0 mm to 0.06 mm, silt 0.06 mm to 0.002 mm and clay in the range smaller than 0.002 mm. It is convenient to present the data in the form of a cumulative frequency curve. From this curve, median diameter $M_{d\phi}$, mean diameter M_{ϕ}, graphic mean M_z and phi deviation σ_{ϕ} could be obtained. These quantities are defined in Appendix A.

The bulk of published data on the physical properties of submarine soils have been obtained by marine geologists, who have chosen a modified triangular soil classification system shown in Fig. 2.

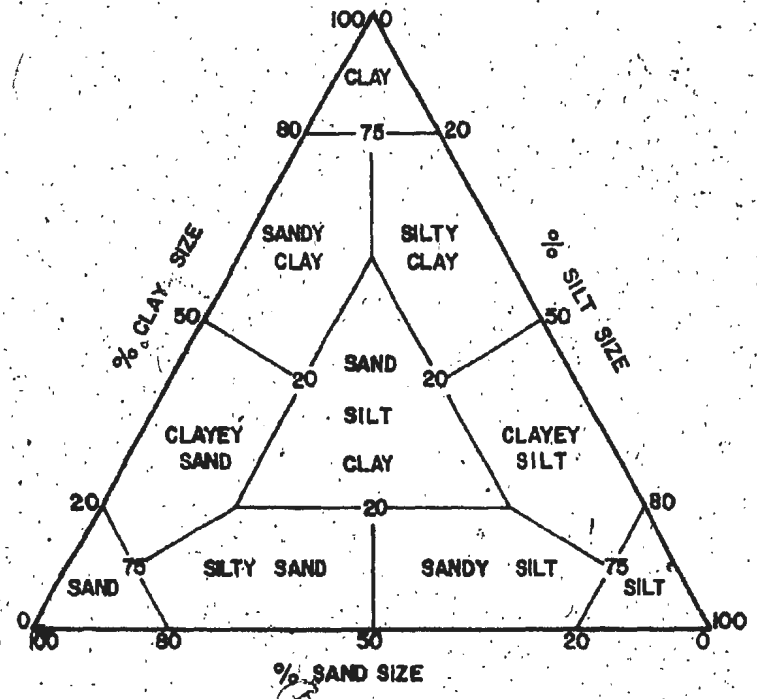

Fig. 2. Classification of Marine Sediments

4.2.2. Index Properties

A typical element of sediment comprises three distinct phases; solid, liquid and gas. The most common index properties determined which describe the inter-relationship of these phases are: moisture content, Atterberg limits, wet density, and relative density of solids. Other basic parameters can be computed from these properties such as: plasticity index, liquidity index, degree of saturation, activity, void ratio and porosity.

Definitions of the index properties obtained from the samples tested are included in Appendix A. The test results are presented in Figures 3 to 10 together with additional test data.

4.2.3. Engineering Properties

Several parameters which measure the strength and compressibility characteristics of sediments can be determined in the laboratory. These include:

a. Shear Strength: shear strength measurements are important for all types of soils and sediments in loading stability computations. Various test methods are in common use to measure the shear strength of fine grained soils under laboratory conditions such as direct shear, unconfined compression and triaxial tests. The undrained shear strength S_u was measured by the vane shear test in this study. The relatively low shear strength of soils tested made triaxial and unconfined compression tests impractical to conduct.

b. Consolidation: consolidation is the process of gradual reduction in the volume of a soil mass resulting from an expulsion of pore water. It is the major process by which compression or settlement within saturated

fine-grained sediment occurs after a load has been applied. During this testing program, the compression index C_c and the coefficient of consolidation c_v were computed from the results of conventional one-dimensional odeometer tests. In this study, the coefficient of consolidation for the second load increment has been computed and reported.

4.3. Geotechnical Tests on Cores

A total of eight cores representing four grid locations have been tested in this program. The grid locations are indicated in Table 1.

During storage, the core samples as well as the grab samples have been humidified and refrigerated to prevent dessication or biological breakdown. The storage temperature was arbitrarily set at 4 ^{o}C $\pm$ to simulate natural conditions.

The cores were subdivided in 0.5 m segments and standard laboratory tests were conducted on each segment to determine the following geotechnical properties: natural moisture content, Atterberg limits, wet density, relative density, particle size distribution by wet analysis, vane shear strength, and consolidation characteristics. Other basic parameters were calculated from the properties measured such as plasticity index, liquidity index, degree of saturation, activity, porosity, etc. The full series of tests were performed on the total length of each core.

The natural moisture content of the cores was measured at sea immediately after recovery. Subsequent laboratory tests show the loss of water was less than 2 % after 6 months in storage.

The measured and calculated geotechnical properties of eight cores have been plotted graphically with respect to depth below mud-line, and are shown in Figs. 3 to 10. This summarized data has been presented

in two figures for each core to facilitate comparison of the various parameters. The particle size composition and selected index properties are included in the first figure. Graphical plots of the shear strength and consolidation parameters are presented on the second figure together with free fall penetrometer output records. Detailed results of the parameters measured by the penetrometer are presented later in this chapter.

The range and average of particle size composition of the eight cores as well as their median diameter, mean diameter, graphic mean and phi deviation are presented in Table 3. The range of the particle size distribution for each core is shown as a composite plot in Figs. 11 to 18. Additional details regarding the particle size characteristics of each core are shown in Tables 12 to 19 in Appendix A. In the second presentation, the range and average of selected properties are listed for all samples from the eight cores in Table 4.

In addition to the laboratory tests carried out by the author, some of the results reported herein were obtained by part-time laboratory assistants. All the laboratory tests have been performed in accordance with methods outlined in applicable ASTM standards.

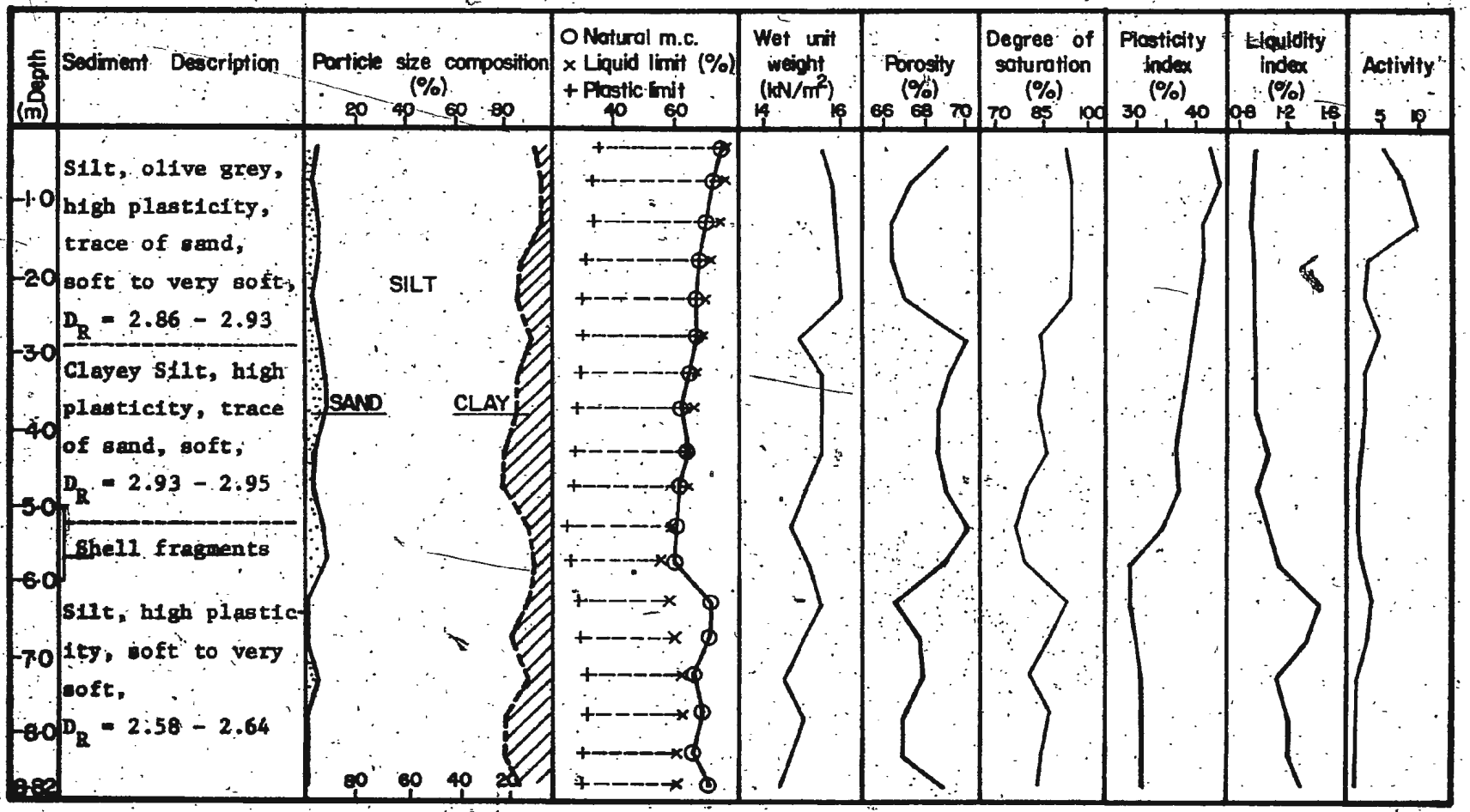

Fig. 3a. Station G 132 - Particle Size Distribution and Index Properties

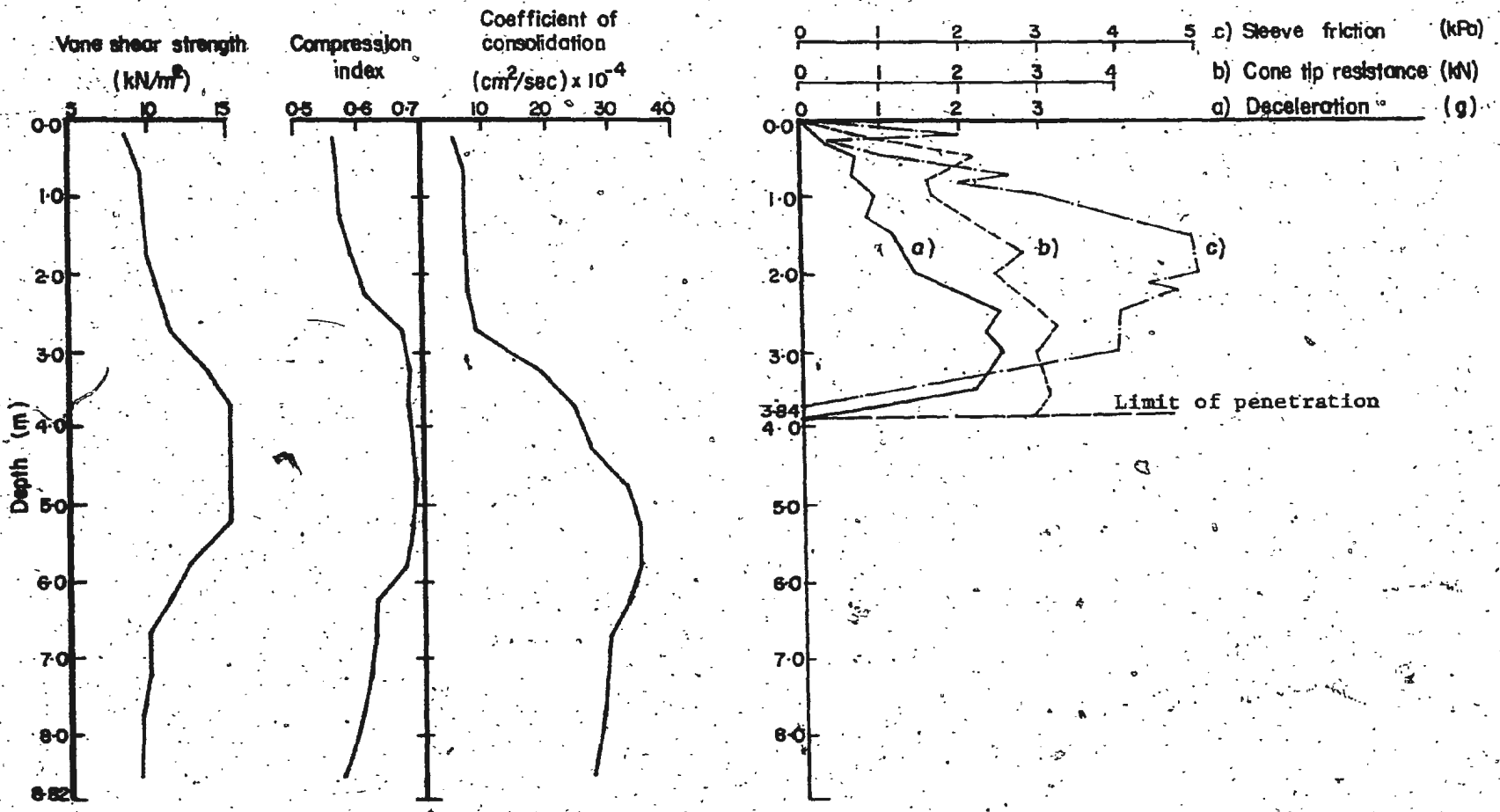

Fig. 3b. Station G 132 - Engineering Properties and Penetrometer Records

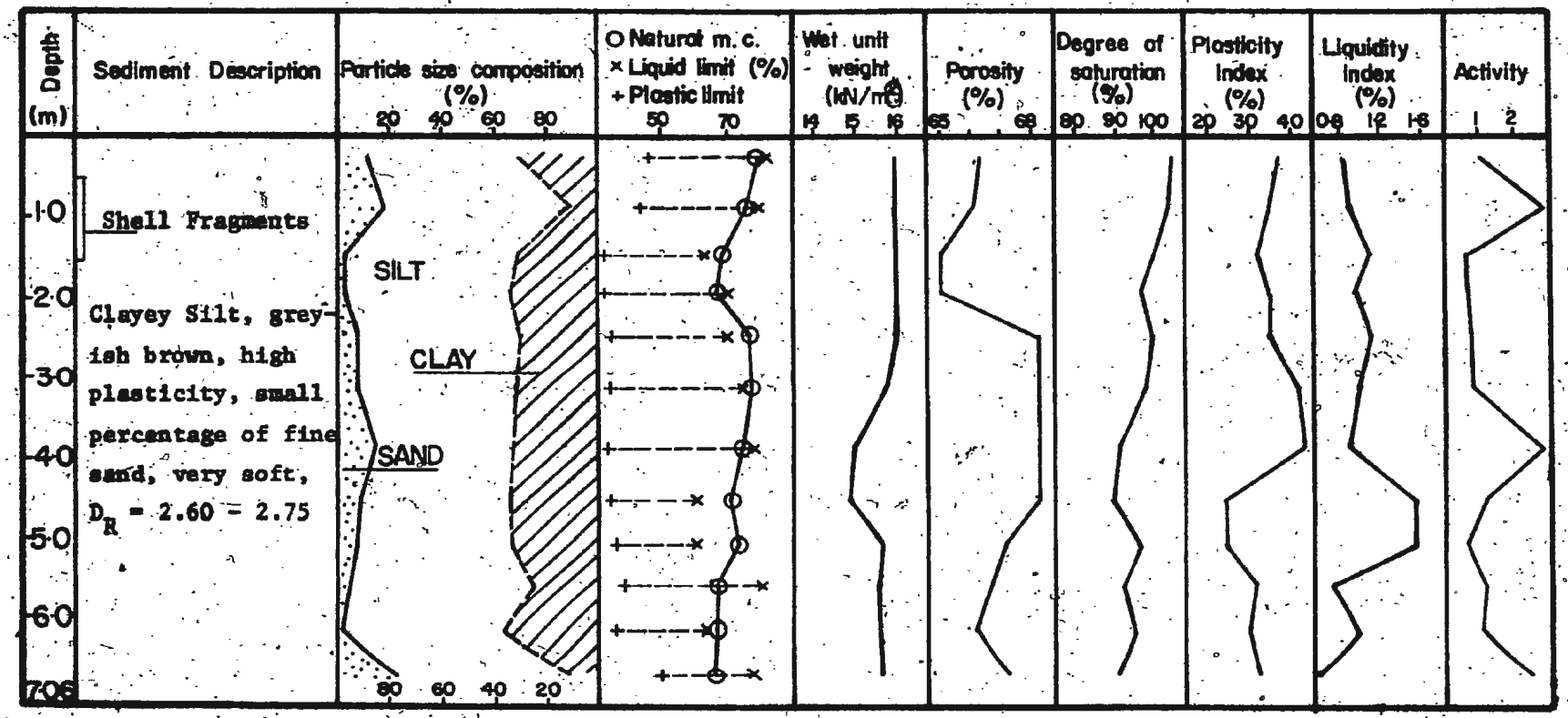

Fig. 4a. Station G 141 – Particle Size Distribution and Index Properties

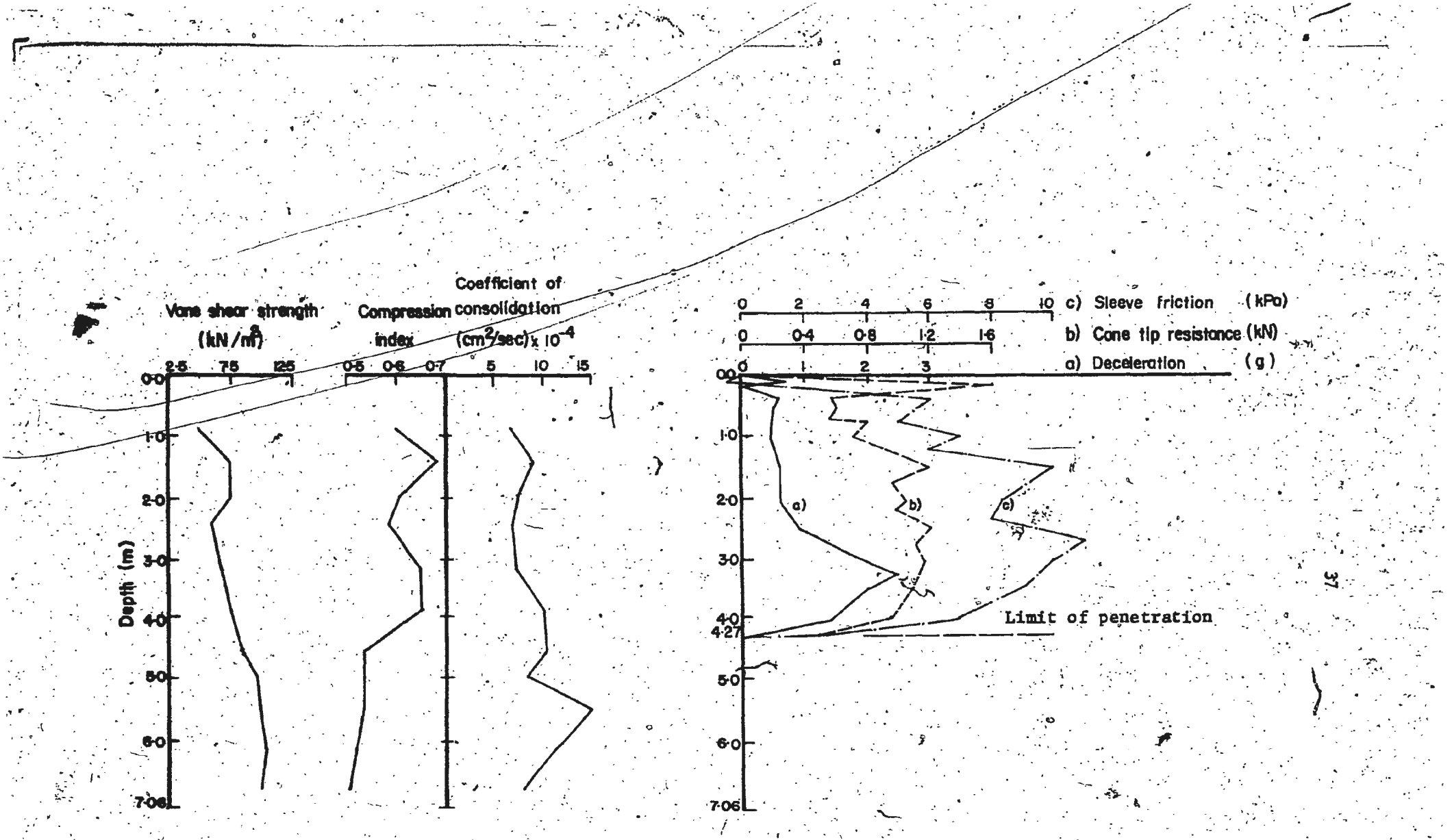

Fig. 4b. Station G 141 – Engineering Properties and Penetrometer Records

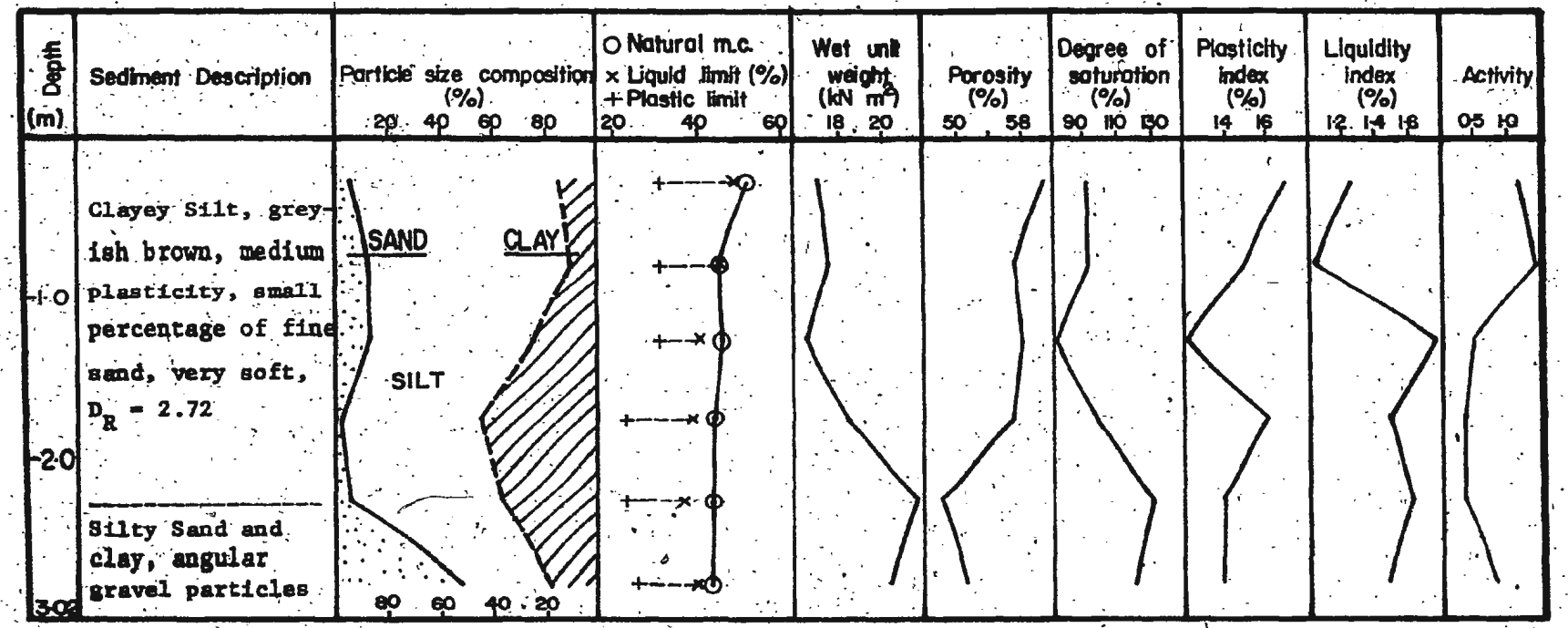

Fig. 5a. Station G 233 - Particle Size Distribution and Index Properties

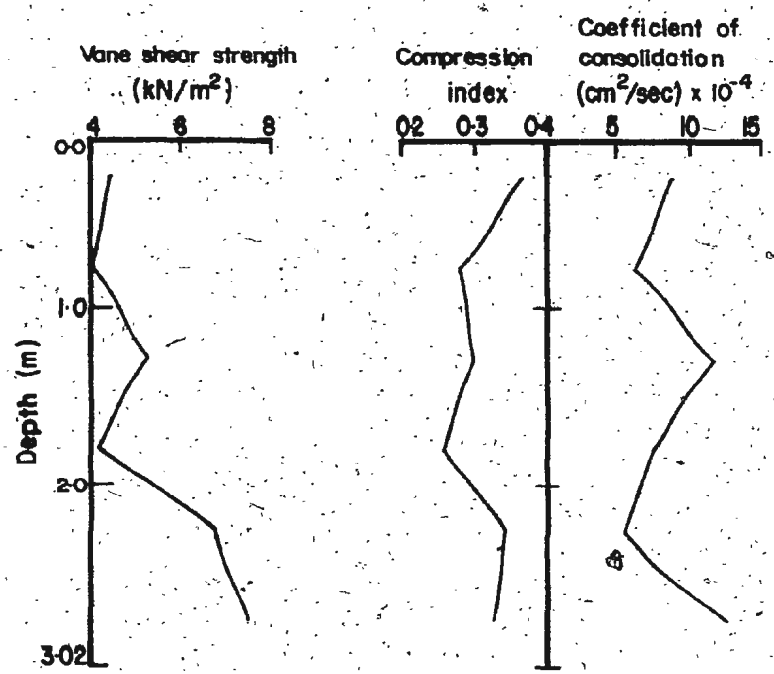

* Penetrometer records not obtained at this location.

Fig. 5b. Station G 233 - Engineering Properties and Penetrometer Records

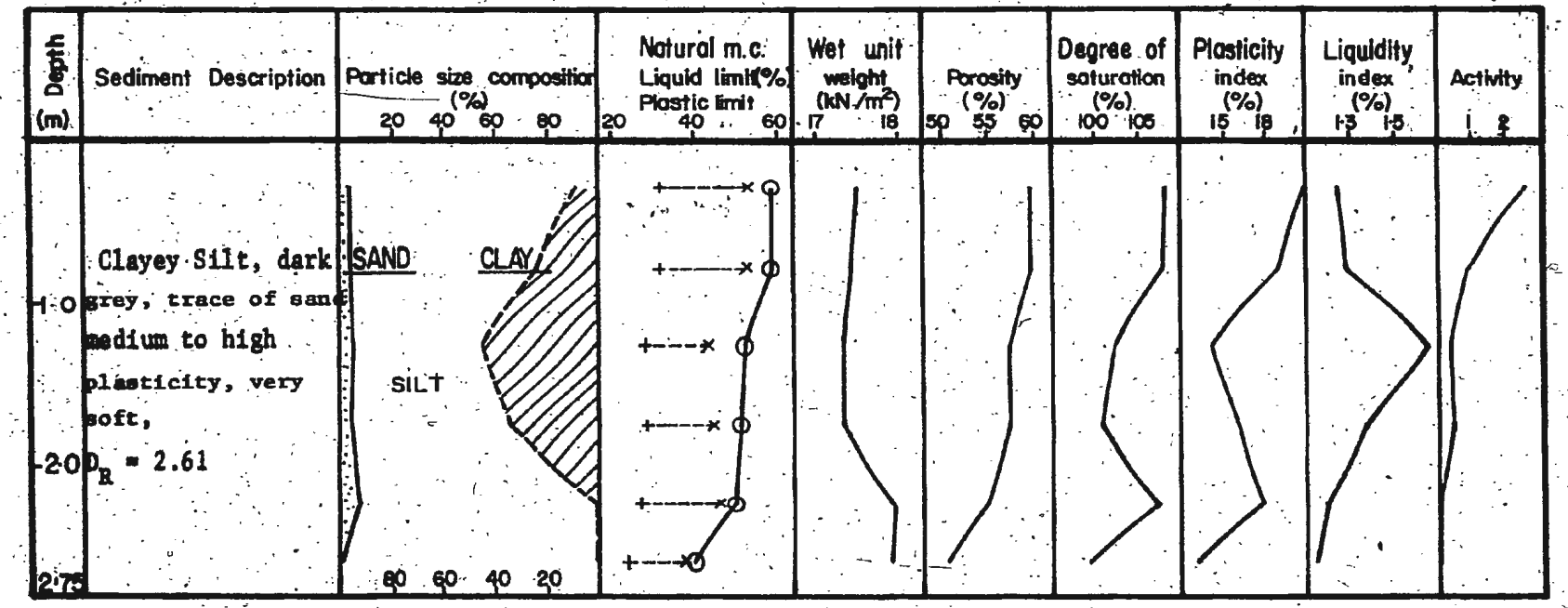

Fig. 6a. Station G 243 – Particle Size Distribution and Index Properties

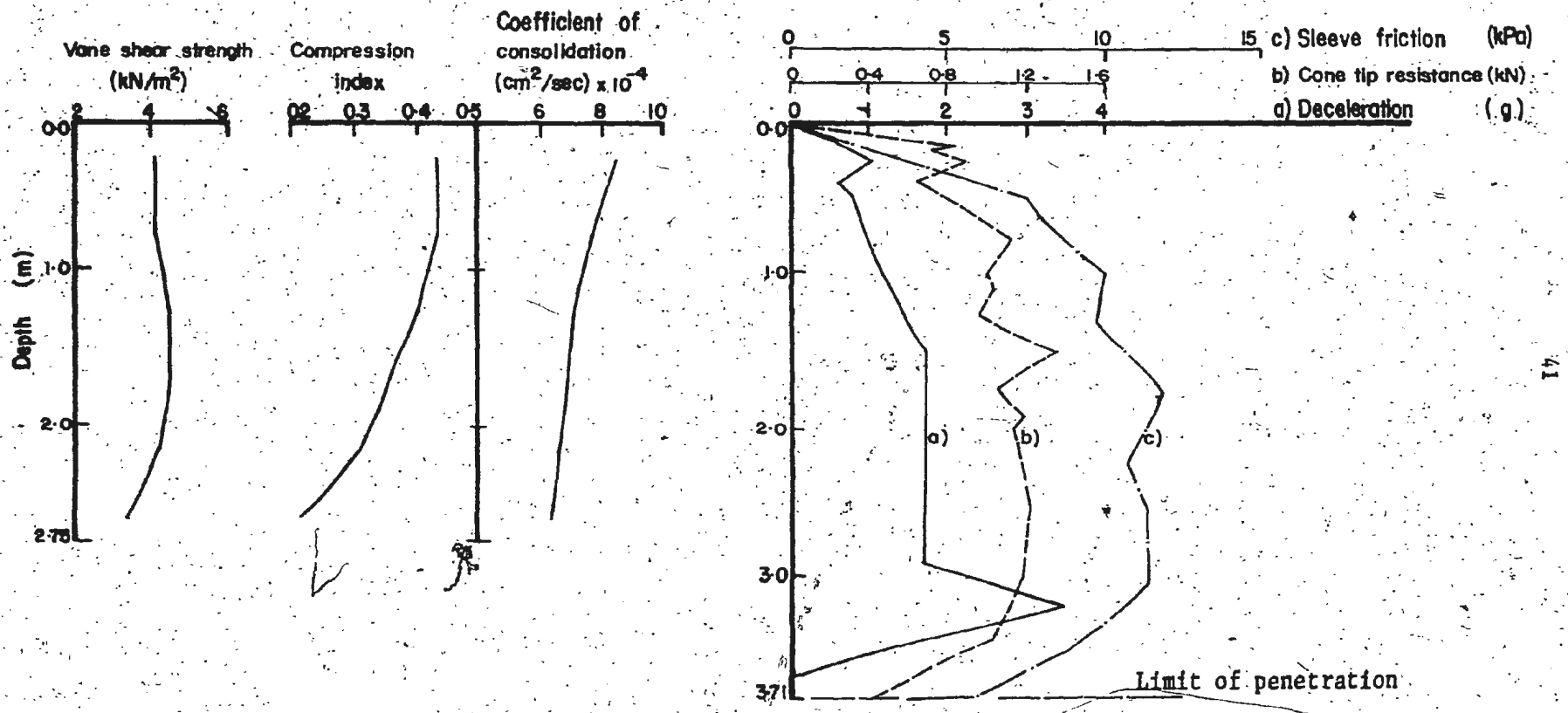

Fig. 6b. Station G 243 - Engineering Properties and Penetrometer Records

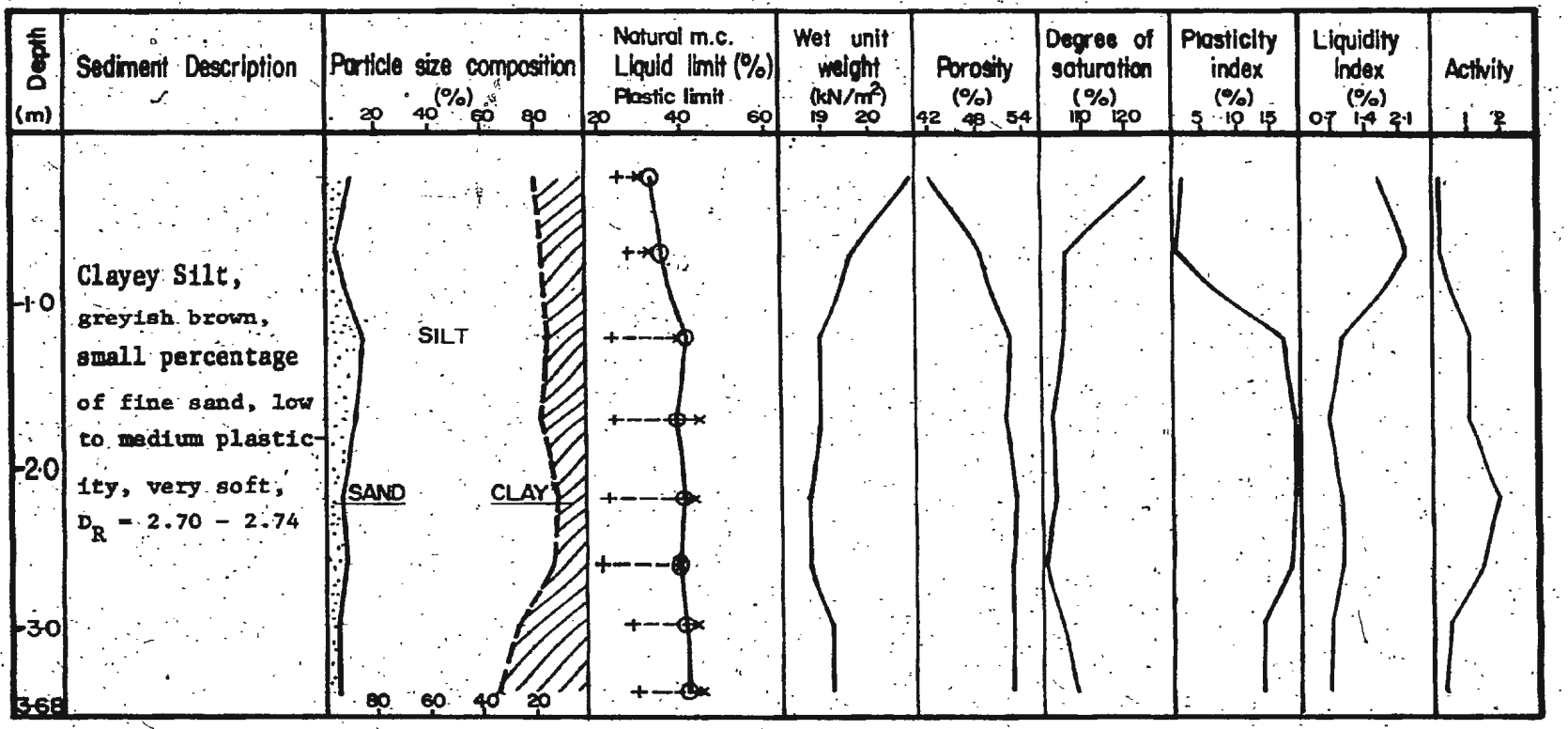

Fig. 7a. Station G 332 - Particle Size Distribution and Index Properties

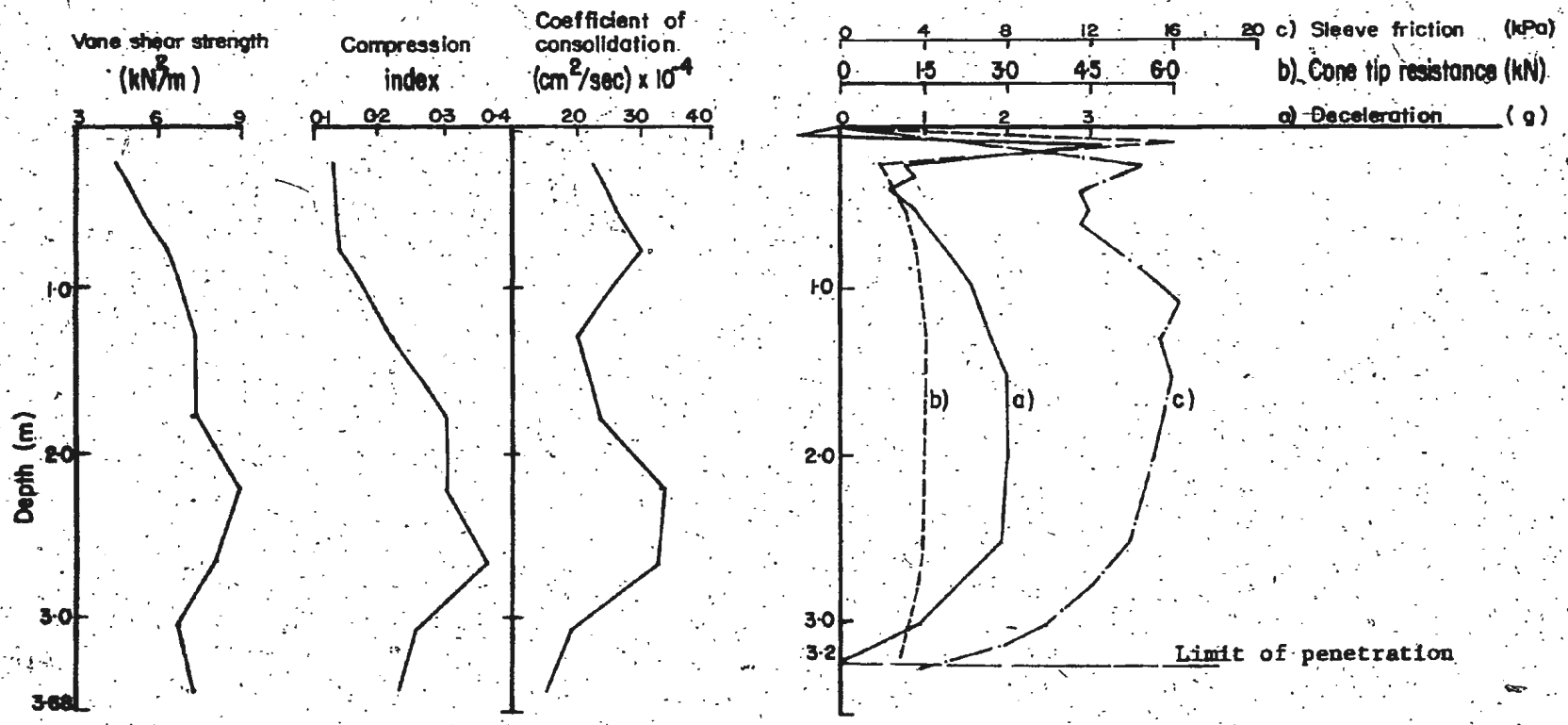

Fig. 7b. Station G 332 - Engineering Properties and Penetrometer Records

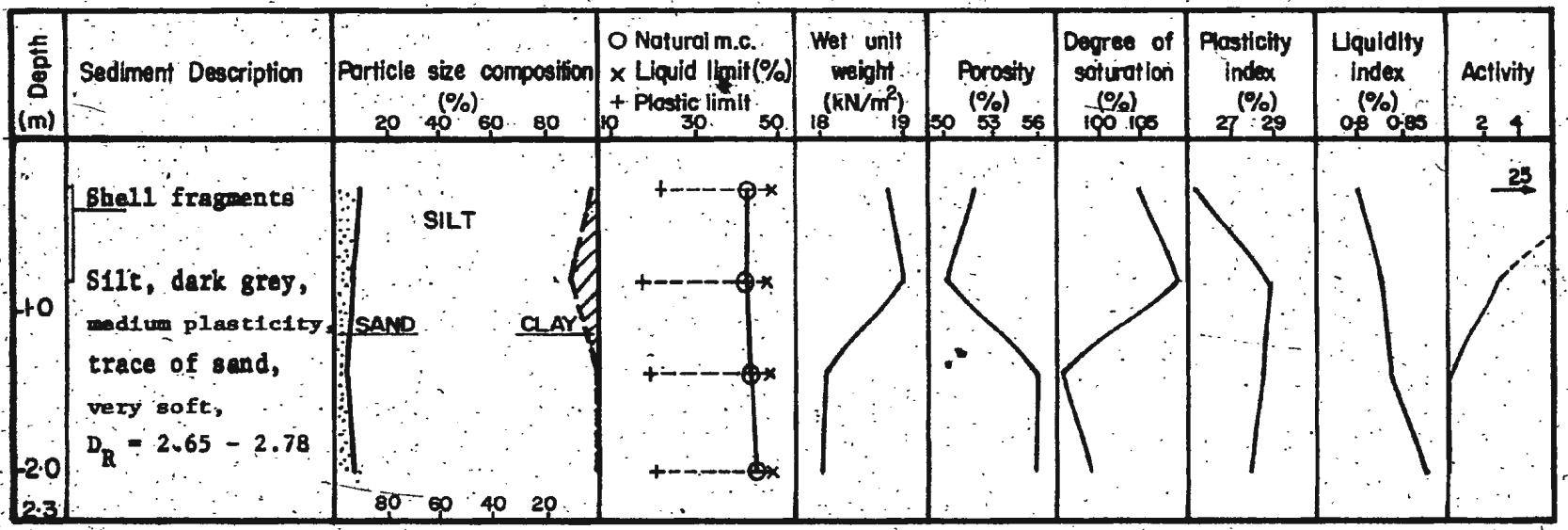

Fig. 8a. Station G 341 - Particle Size Distribution and Index Properties

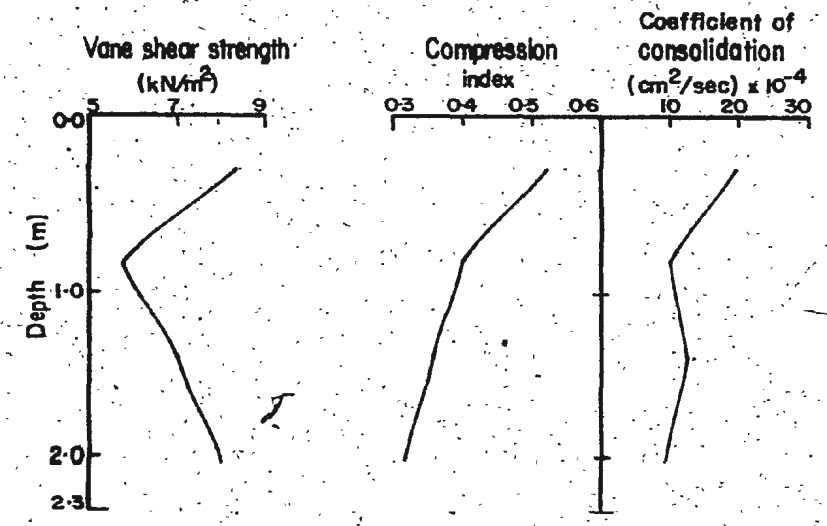

* Penetrometer records not obtained at this location.

Fig. 8b. Station G 341 - Engineering Properties and Penetrometer Records

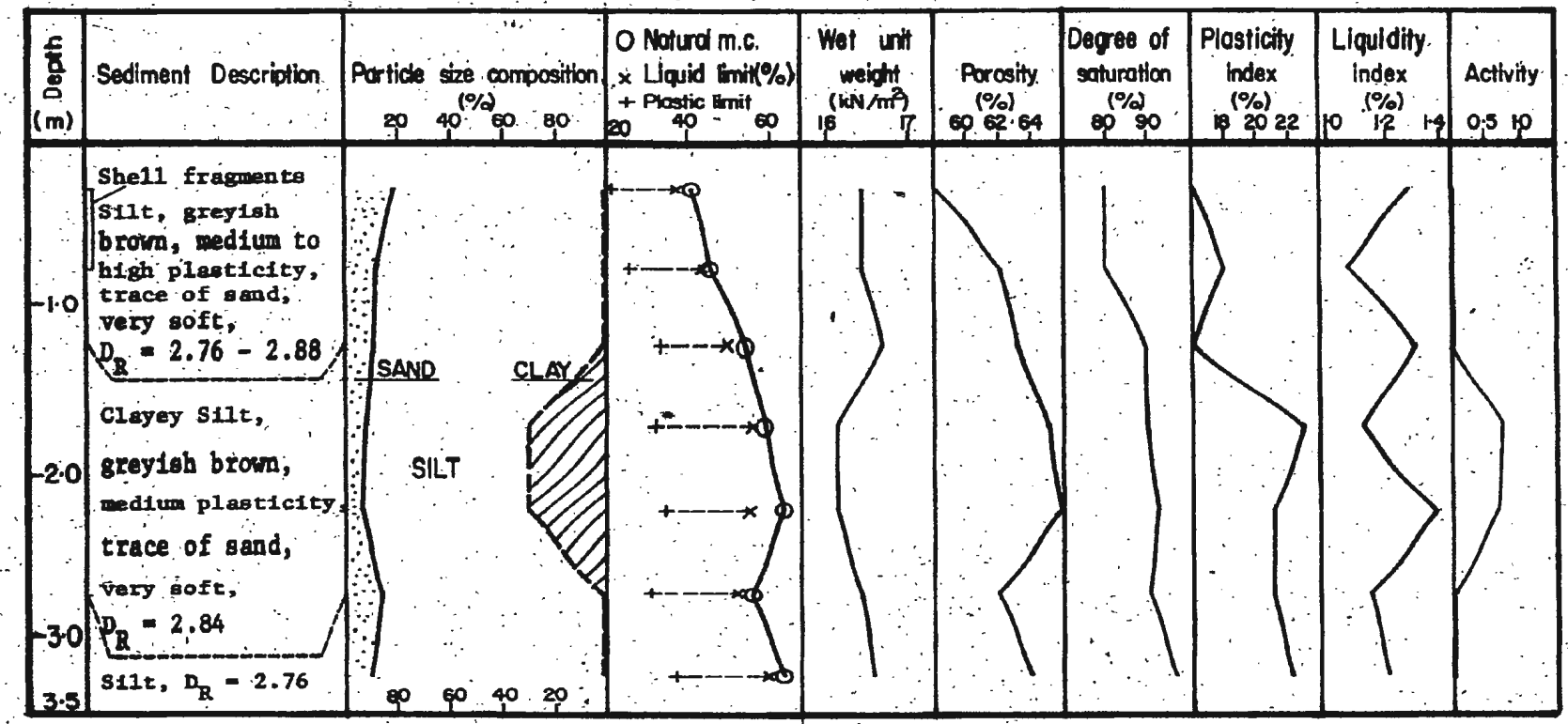

Fig. 9a. Station G 432 - Particle Size Distribution and Index Properties

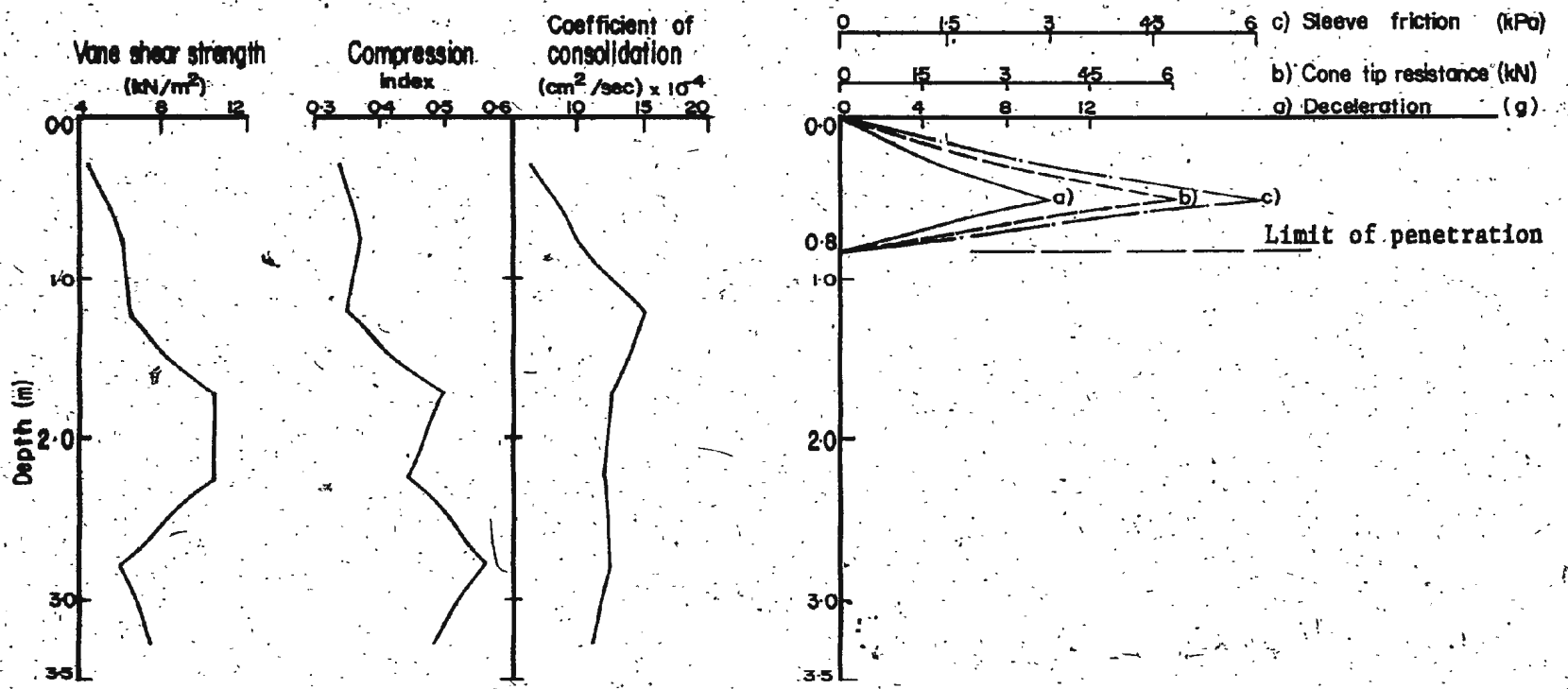

Fig. 9b. Station G 432 – Engineering Properties and Penetrometer Records

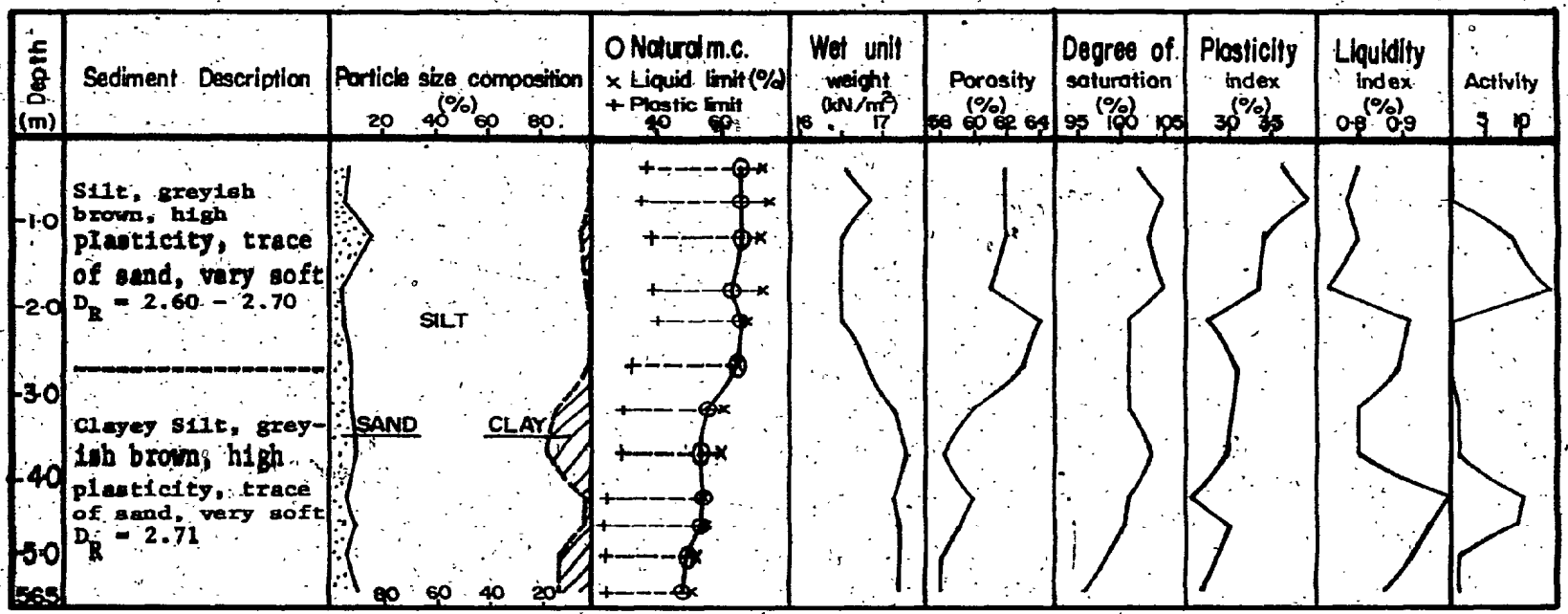

Fig. 10a. Station G 441A – Particle Size Distribution and Index Properties

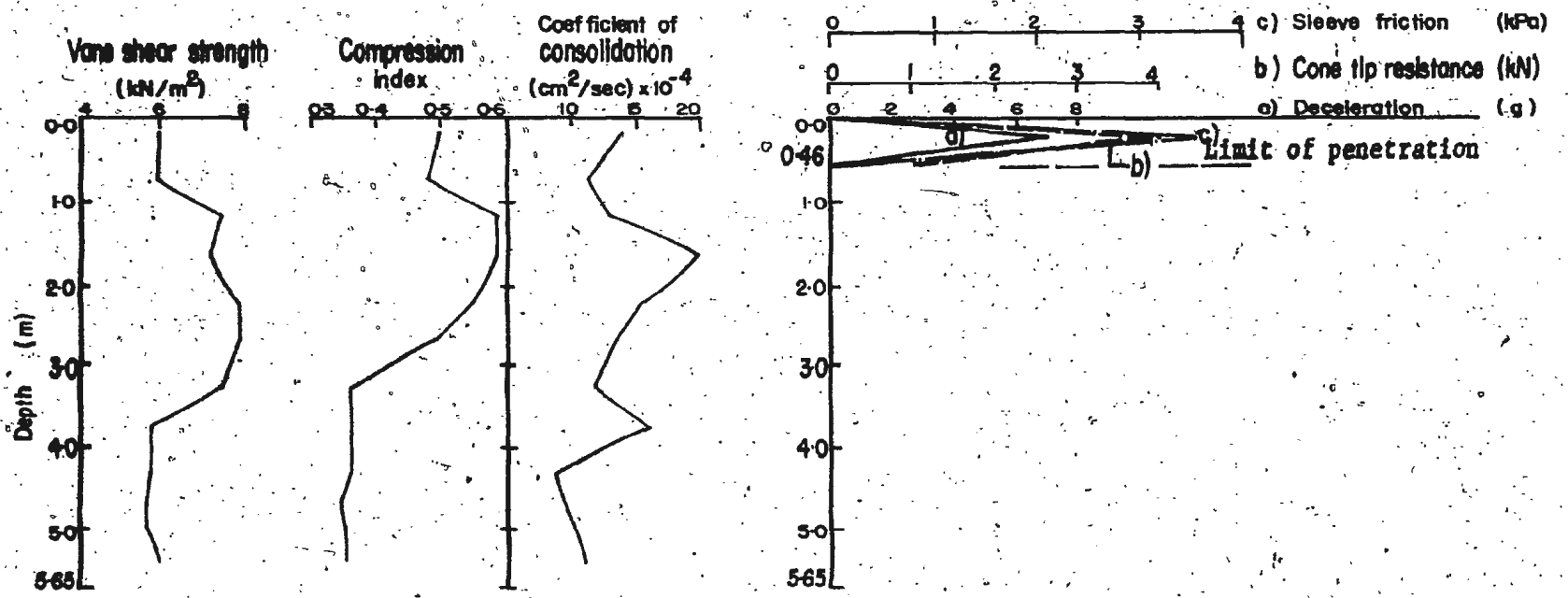

Fig. 10b. Station G 441A - Engineering Properties and Penetrometer Records

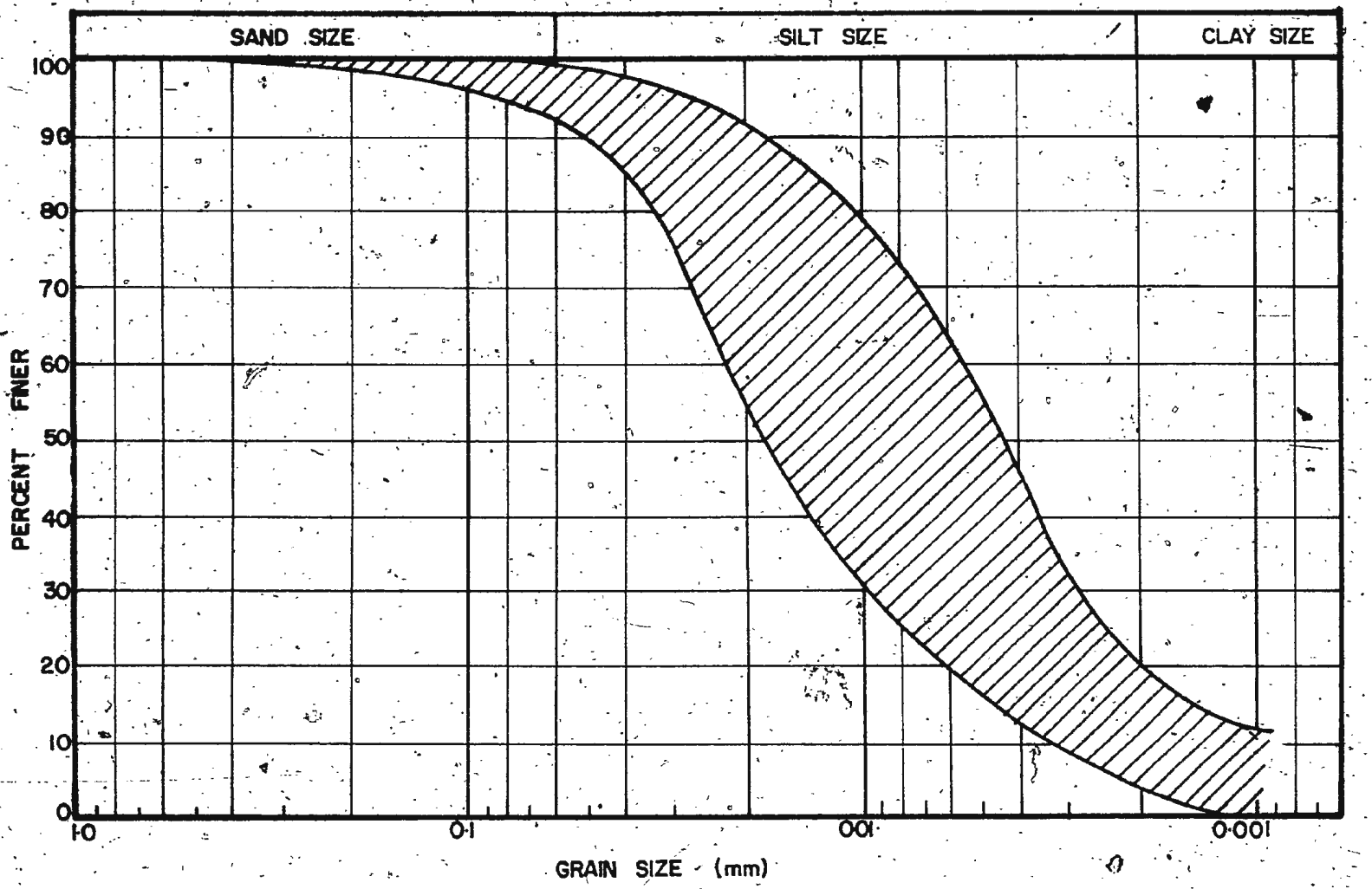

Fig. 11. Core G 132 – The Range of Particle Size Distribution

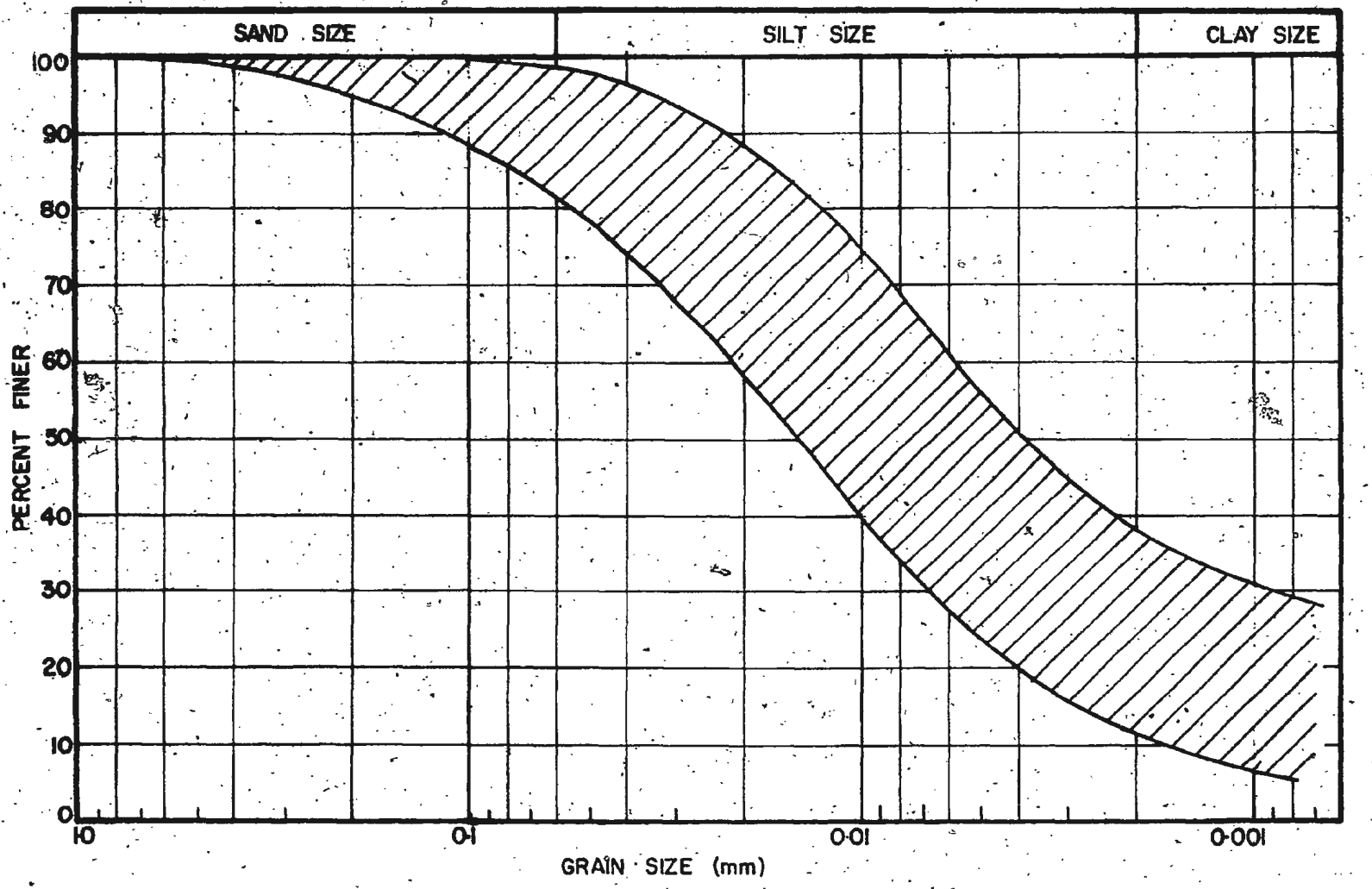

Fig. 12. Core G 141 - The Range of Particle Size Distribution

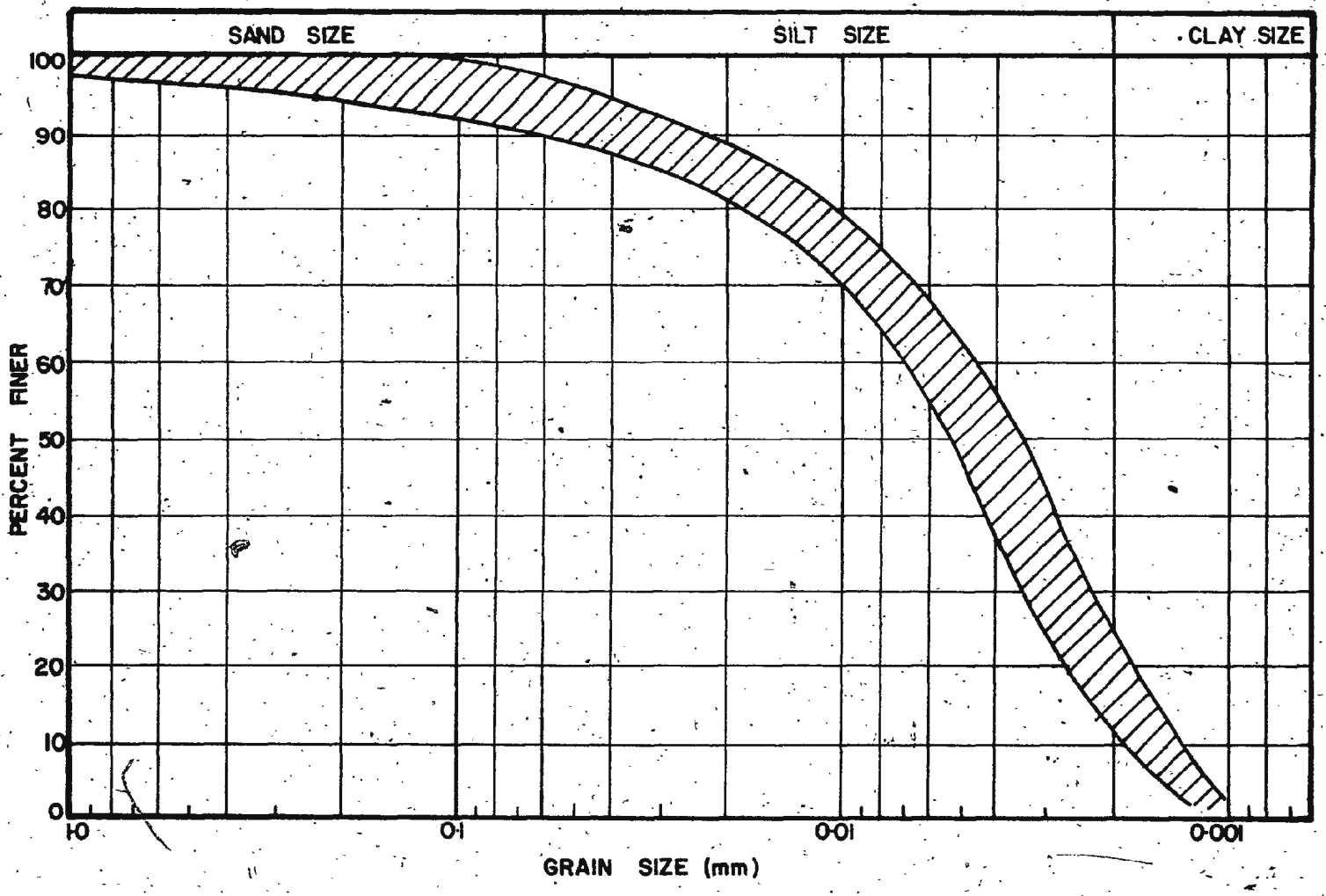

Fig. 13. Core G 233 – The Range of Particle Size Distribution

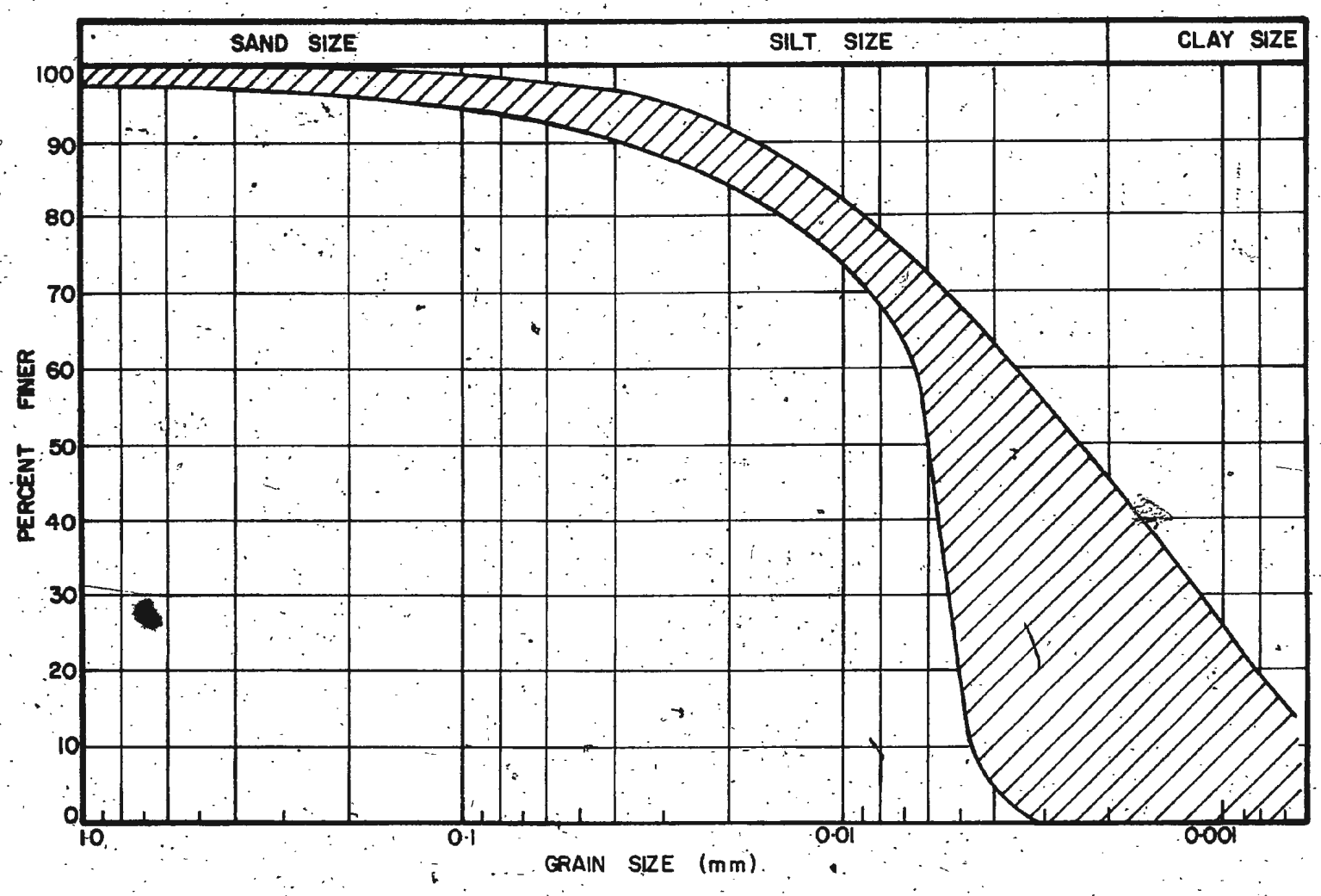

Fig. 14. Core G 243 - The Range of Particle Size Distribution

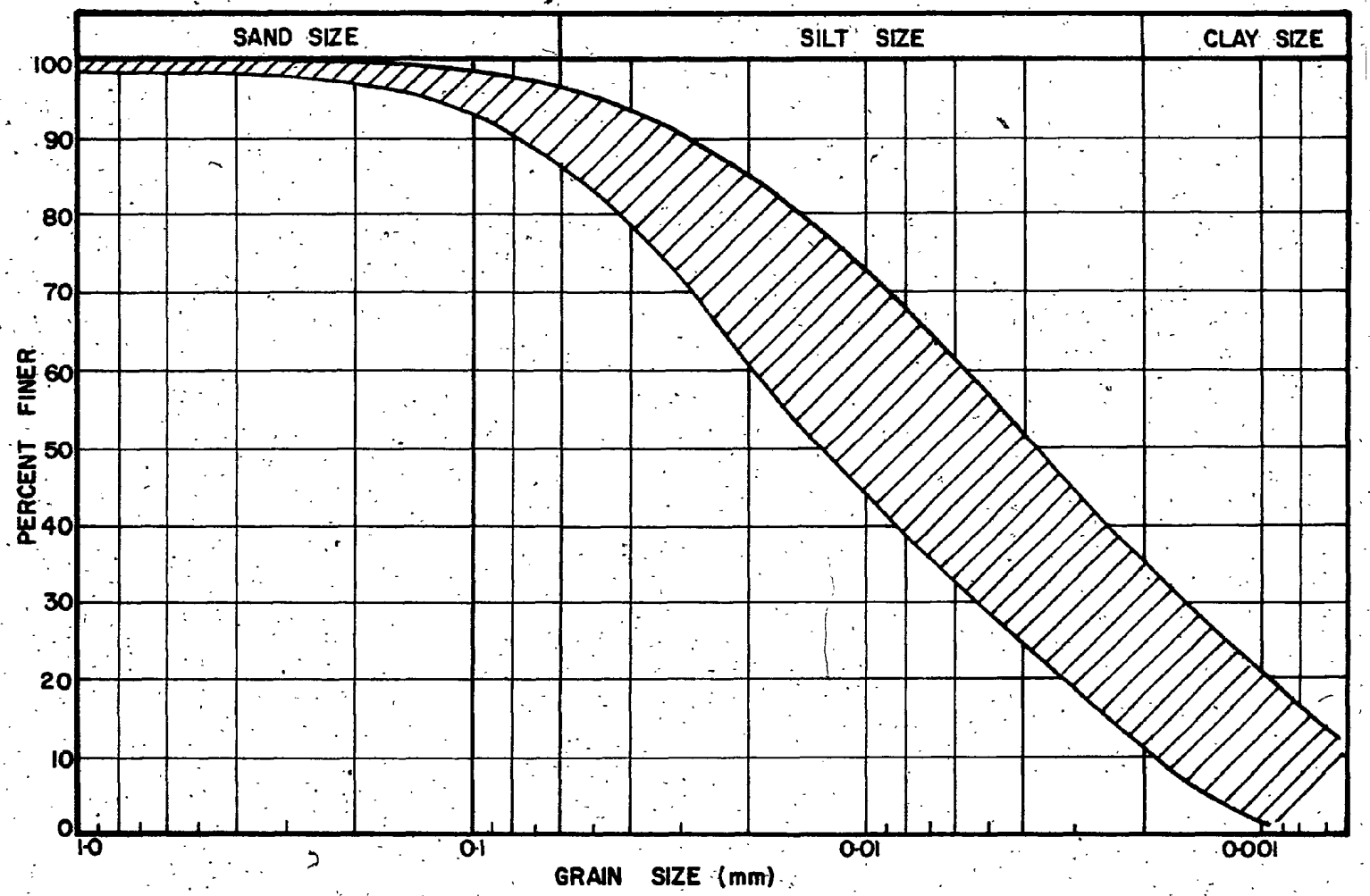

Fig. 15. Core G 332 – The Range of Particle Size Distribution

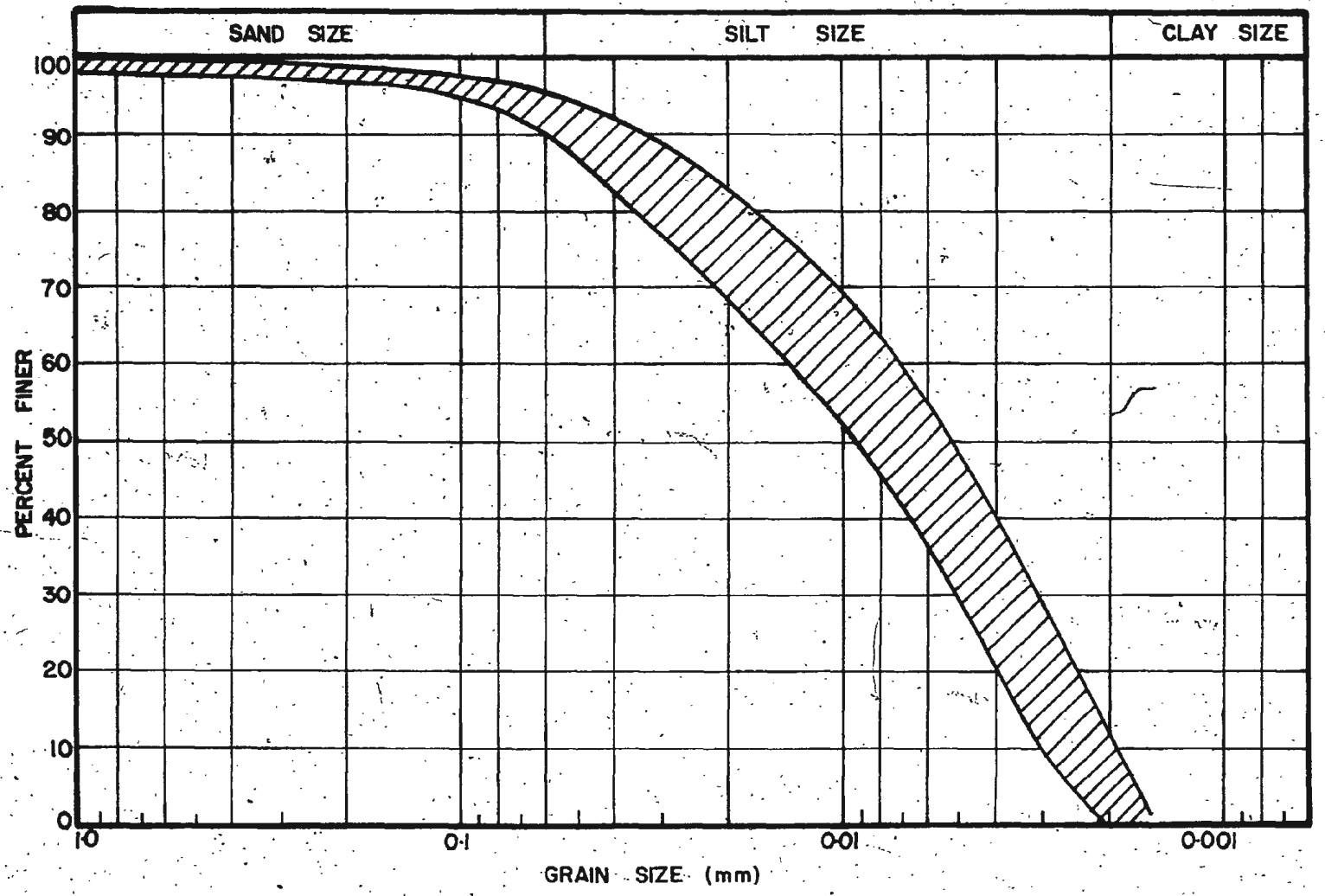

Fig. 16. Core G 341 - The Range of Particle Size Distribution

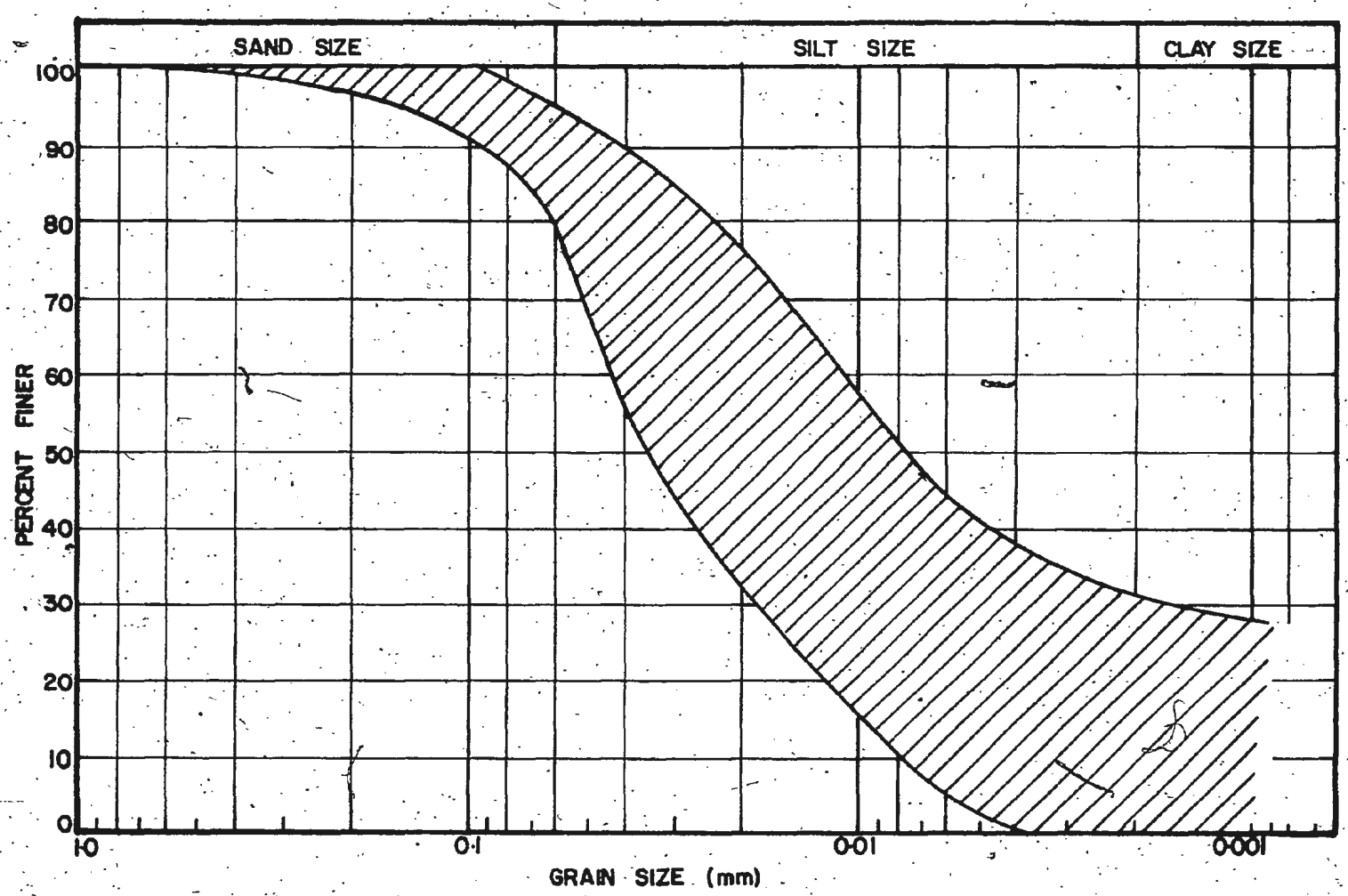

Fig. 17. Core G 432 - The Range of Particle Size Distribution

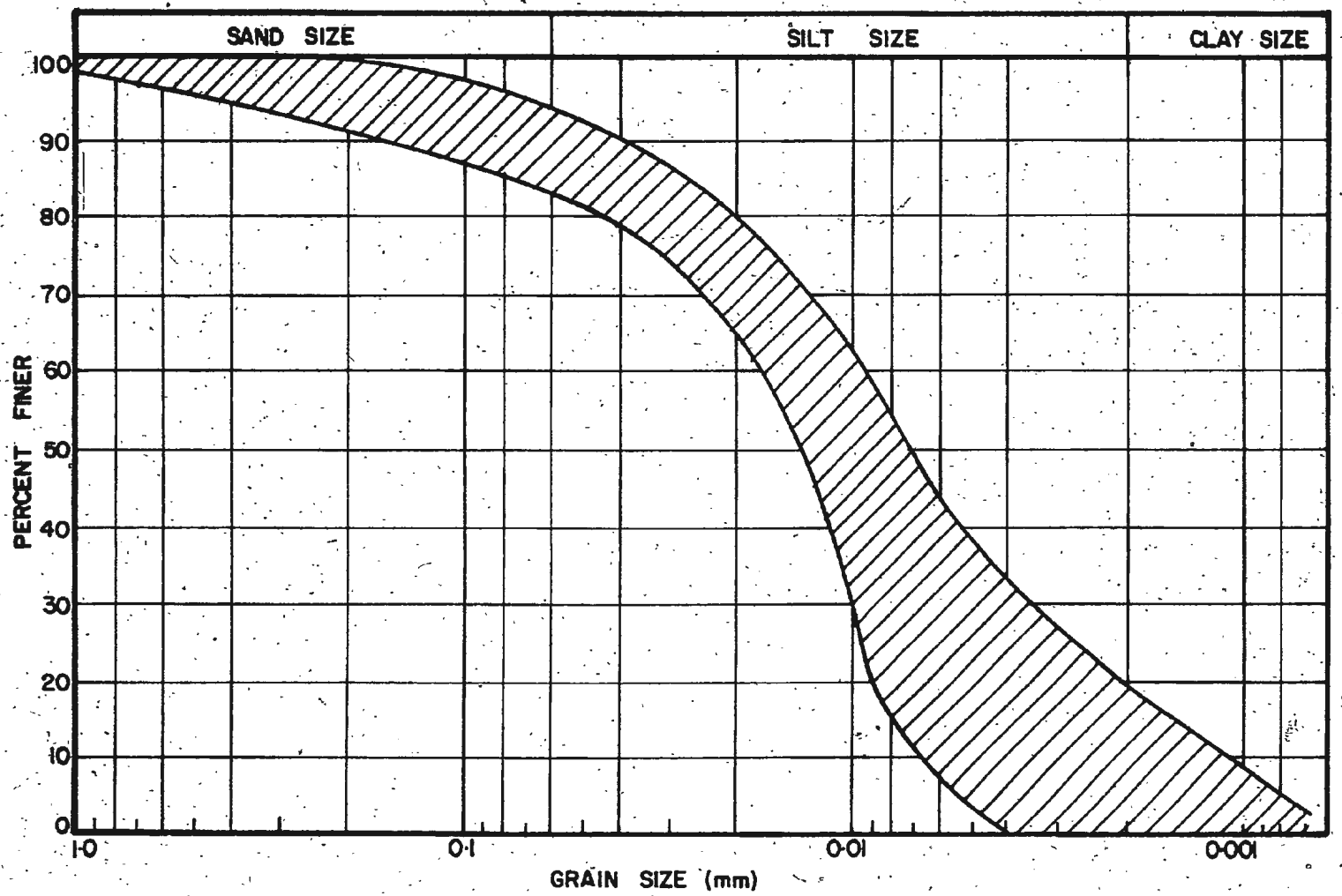

Fig. 18. Core G 441A – The Range of Particle Size Distribution

TABLE 3. SUMMARY OF PARTICLE SIZE CHARACTERISTICS FOR EACH CORE

particle size parameters	number of samples	minimum	maximum	mean	standard deviation
G 132- sand size, u_2 %		0.0	7.5	3.4	2.67
silt size, u_3 %		77.0	95.0	83.7	4.95
clay size, u_1 %		4.0	20.0	13.0	5.27
median diameter, $M_{d\phi}$ mm	18	0.005	0.016	0.007	0.0027
mean diameter, M_ϕ mm		0.007	0.021	0.015	0.0056
graphic mean, M_z mm		0.006	0.017	0.012	0.0042
phi deviation, σ_ϕ mm		0.005	0.019	0.012	0.0048
G 141- sand size, u_2 %		2.0	25.0	9.5	6.8
silt size, u_3 %		53.0	71.0	62.25	5.7
clay size, u_1 %		12.0	37.0	28.25	8.38
median diameter, $M_{d\phi}$ mm	12	0.004	0.01	0.014	0.019
mean diameter, M_ϕ mm		0.01	0.08	0.022	0.019
graphic mean, M_z mm		0.012	0.07	0.023	0.016
phi deviation, σ_ϕ mm		0.01	0.06	0.019	0.014
G 233- sand size, u_2 %		2.0	50.0	13.7	17.7
silt size, u_3 %		34.0	82.0	62.3	17.9
clay size, u_1 %		10.0	41.0	23.5	12.58
median diameter, $M_{d\phi}$ mm	6	0.003	0.06	0.013	0.013
mean diameter, M_ϕ mm		0.001	0.016	0.01	0.0051
graphic mean, M_z mm		0.009	0.031	0.018	0.0083
phi deviation, σ_ϕ mm		0.001	0.013	0.01	0.0044
G 243- sand size, u_2 %		2.0	8.0	4.33	2.07
silt size, u_3 %		50.0	98.0	75.7	18.6
clay size, u_1 %		0.0	45.0	20.5	18.6
median diameter, $M_{d\phi}$ mm	6	0.002	0.005	0.003	0.0011
mean diameter, M_ϕ mm		0.006	0.01	0.008	0.0014
graphic mean, M_z mm		0.008	0.018	0.011	0.0037
phi deviation, σ_ϕ mm		0.003	0.009	0.006	0.002

Continued

TABLE 3. (CONTINUED)

particle size parameters	number of samples	minimum	maximum	mean	standard deviation
G 332- sand size, u_2 %		5.0	15.0	8.9	3.6
silt size, u_3 %		60.0	80.0	72.0	6.7
clay size, u_1 %		12.0	34.0	19.25	7.46
median diameter, $M_{d\phi}$ mm	8	0.005	0.015	0.01	0.0037
mean diameter, M_ϕ mm		0.011	0.029	0.02	0.0057
graphic mean, M_z mm		0.013	0.037	0.025	0.0071
phi deviation, σ_ϕ mm		0.01	0.027	0.018	0.0052
G 341- sand size, u_2 %		5.0	9.0	7.0	1.63
silt size, u_3 %		83.0	95.0	90.25	5.25
clay size, u_1 %		0.0	10.0	2.75	4.86
median diameter, $M_{d\phi}$ mm	4	0.005	0.009	0.007	0.0021
mean diameter, M_ϕ mm		0.014	0.024	0.018	0.0053
graphic mean, M_z mm		0.011	0.018	0.014	0.0048
phi deviation, σ_ϕ mm		0.011	0.021	0.015	0.0048
G 432- sand size, u_2 %		8.0	18.0	11.7	3.77
silt size, u_3 %		62.0	91.0	79.7	12.4
clay size, u_1 %		0.0	30.0	8.57	14.6
median diameter, $M_{d\phi}$ mm	7	0.008	0.043	0.015	0.012
mean diameter, M_ϕ mm		0.016	0.066	0.032	0.017
graphic mean, M_z mm		0.02	0.07	0.034	0.018
phi deviation, σ_ϕ mm		0.014	0.05	0.025	0.012
G 441A-sand size, u_2 %		6.0	14.0	8.33	2.87
silt size, u_3 %		71.0	94.0	85.9	8.34
clay size, u_1 %		0.0	18.0	5.75	6.7
median diameter, $M_{d\phi}$ mm	12	0.009	0.012	0.011	0.001
mean diameter, M_ϕ mm		0.018	0.039	0.021	0.006
graphic mean, M_z mm		0.023	0.044	0.026	0.0051
phi deviation, σ_ϕ mm		0.011	0.03	0.016	0.0054

TABLE 4. SUMMARY OF GEOTECHNICAL PROPERTIES OF SOILS TESTED – ALL CORES

parameter	number of analyses	minimum	maximum	mean	standard deviation
sand size, u_2 %	73	0.0	50.0	9.0	6.4
silt size, u_3 %	73	34.0	98.0	76.0	14.7
clay size, u_1 %	73	0.0	51.0	15.5	14.5
moisture content, w %	219	33.0	77.0	54.0	23.0
liquid limit, w_L %	219	30.0	82.0	53.0	25.0
plastic limit, w_p %	219	18.0	50.0	29.0	10.0
plasticity index, I_p %	73	3.0	45.0	24.0	15.0
liquidity index, I_L %	73	0.5	2.3	1.1	0.3
degree of saturation, S_r %	73	72.7	136.8	96.3	10.5
activity, a_c	73	0.0	25.0	2.8	4.46
bulk density, ρ gm/cm^3	73	1.4	2.1	1.6	0.25
relative density, D_R	146	2.6	2.95	2.7	0.22
porosity, n %	73	42.0	70.0	59.0	16.0
shear strength, S_u kN/m^2	146	3.4	15.0	7.9	2.82
compression index, C_c	73	0.1	0.7	0.5	0.15
coeff. of consolidation, c_v ($cm^2/sec \times 10^{-4}$)	73	5.3	33.0	13.6	9.36

4.4. Plasticity and Activity of the Sediments

One of the familiar means for classification and comparison of different samples of fine-grained soil within a deposit, or comparing one deposit with another, is the plasticity chart. Such a chart usually is shown with a diagonal line termed the "A - Line" which represents the relationship of:

$$I_P = 0.73\ (w_L - 20) \qquad \ldots\ldots\ldots \quad (6)$$

where: I_P = plasticity index

w_L = liquid limit

The results of 73 Atterberg limit determination carried out on the samples obtained from different locations in the Placentia Bay area are summarized in Fig. 19a. Almost all the data plots within the "A-Line" which indicate the organic nature of the soils.

The activity a_c (plasticity index / clay size fraction< 2 microns) of all samples investigated is plotted in Fig. 19b. The range of these data is surprisingly wide, from inactive clays to highly active clays. The samples from stations G 132, 341 and 441A are very active and samples from stations G 233 and 432 are inactive while samples from stations G 141, 243 and 332 range between active and normal.

4.5. Surficial Grab Samples

There are various types of grab samplers such as Eckman, Orange-peel, Shipek and Van Veen. All are composed of essentially a set of jaws which snap shut upon reaching the surface of the sea bottom, taking a bite of sediment. The sample generally is somewhat mixed and disturbed by the sampling process and will always be a surficial one.

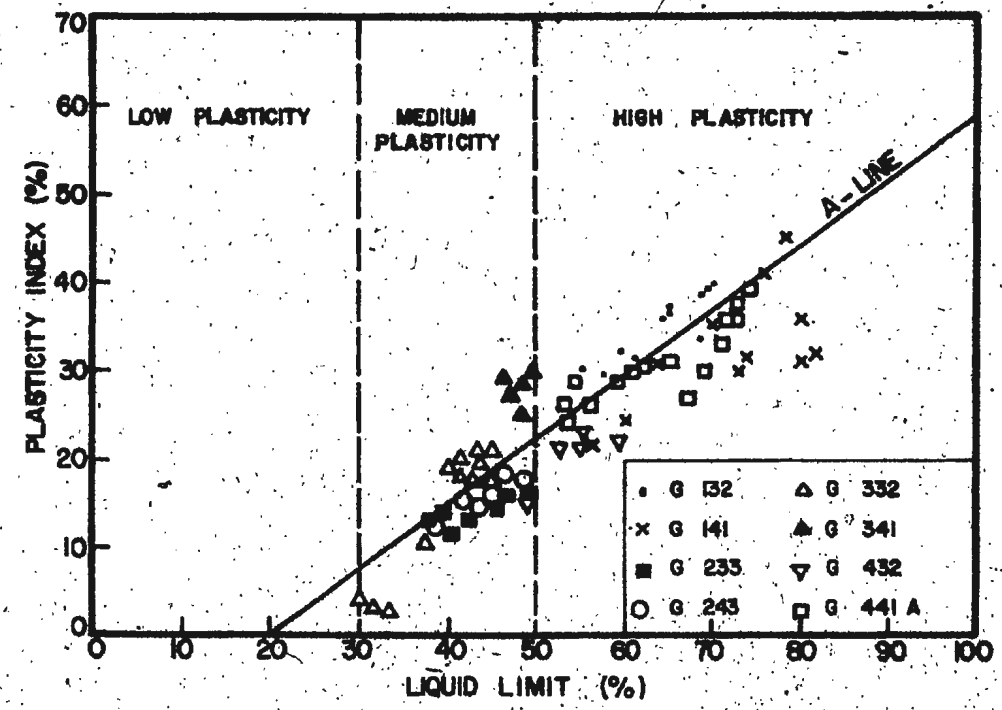

Fig. 19a. Plasticity Chart

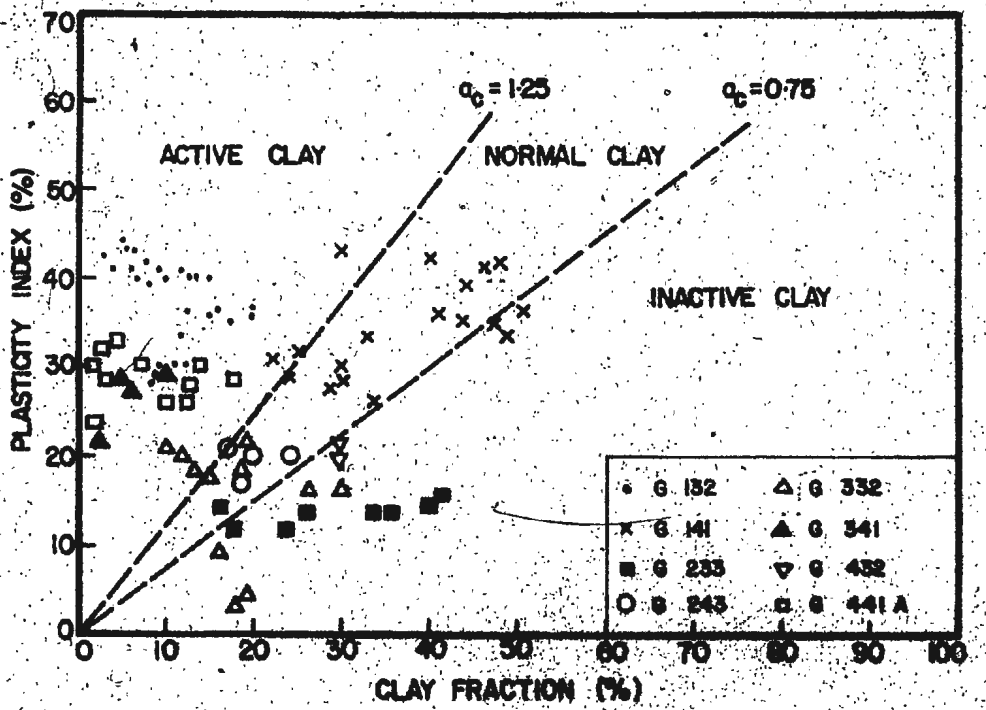

Fig. 19b. Activity Chart

The Van Veen sampler, which was used on the Hudson Cruise, is a large, heavy and robust apparatus which collects samples from sandy bottoms as well as soft ones. Some washing out of fine sediment often occurs however during sampling and raising the sampler to the ship.

Grab samples are always disturbed and have relatively little use in determination of engineering properties of the soil. They give only a preliminary and quick indication regarding the type and properties of surficial ocean sediments.

The grab samples representing grids no. 1,2,3,4 and 6 have been tested in this study, with the results summarized in Table 5. Samples from grid no. 5 were not tested since they comprised shells and cobble-size fragments only.

Comparing the results of the grab samples with the upper 0.25 m of corresponding core samples, a discrepancy in the order of 3 to 4 % is evident for most parameters. However, considerable differences in the results of particle size composition were noted. This is attributed to washing out of fine particles during the grab sampling process.

4.6. Free Fall Cone Penetrometer

A free fall cone penetrometer, designed and developed at Memorial University of Newfoundland, has the potential to make a rapid and economical evaluation of the geotechnical properties of the upper few meters of surficial ocean sediments. A brief description of this instrument, and the results from six test drops in the study area are presented in this section.

4.6.1. Description of the Cone Penetrometer and Instrumentation

The free fall penetrometer is a cone tipped cylindrical projectile which is allowed to impact on a soil target from a pre-determined height

TABLE 5. SUMMARY OF LABORATORY TEST RESULTS ON GRAB SAMPLES

sample no.	moisture content (%)	liquid limit (%)	plastic limit (%)	relative density	gravel (%)	sand (%)	silt (%)	clay (%)	other
G 132	80	75	35	2.74	0	47	50	3	-
G 141	80	78	39	2.60	0	53	45	2	-
G 233	55	48	30	2.60	20	55	24	1	shells
G 243	65	55	35	2.57	10	64	24	2	worms
G 312	41	N/A	20	2.68	5	92	3	0	shells
G 332	32	N/A	21	2.70	0	92	8	0	-
G 411	48	N/A	22	2.80	0	88	12	0	-
G 432	39	N/A	21	2.75	0	96	4	0	shells
G 641	37	N/A	N/A	2.65	32	57	10	1	shells
G 653	26	N/A	N/A	2.66	22	68	9	1	shells

(Fig. 20). It is instrumented with load cells for measuring both the cone tip resistance and friction on the side sleeve independently during penetration. An accelerometer is also mounted within the penetrometer for recording the deceleration profile, up to the full depth of penetration.

The physical dimensions of the free fall penetrometer used is as follows:

Nose diameter	76.2 mm
Nose length (tip + sleeve)	450 mm
Base area of the cone	45.62×10^2 mm^2
Cone apex angle	60°
Sleeve diameter	76.2 mm
Area of sleeve	645.2×10^2 mm^2
Material	stainless steel

Details of the tip and instrumentation are indicated in Fig. 21. Additional details of the free fall penetrometer have been presented by Chari, et al. 1979 and Chaudhuri 1979.

4.6.2. Field Operations

The penetrometer, which weighed 1.56 kN, was slowly lowered from a winch and tripped by a pilot-weight to give a free fall of 15 meters before striking the ocean floor (Fig. 20). The total length of the penetrometer body including the nose assembly is 3.7 m. The entire unit is topped with a stabilizer section which is 0.75 m long and has a larger cross section. The cone resistance and sleeve measurements obtained from the strain gages were transmitted via a cable to an eight-channel, FM analog

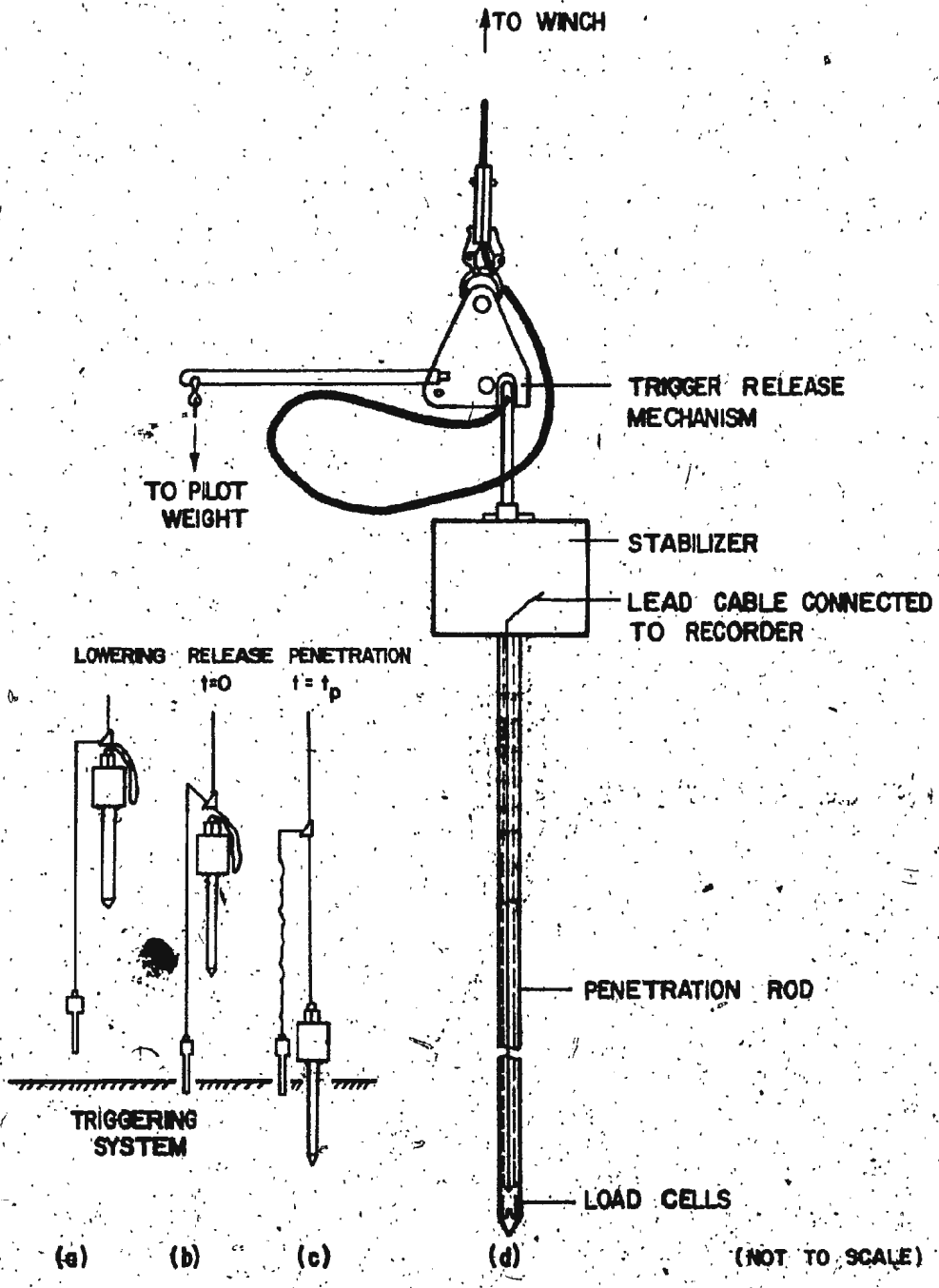

Fig. 20. Free Fall Cone Penetrometer (Ref. 13)

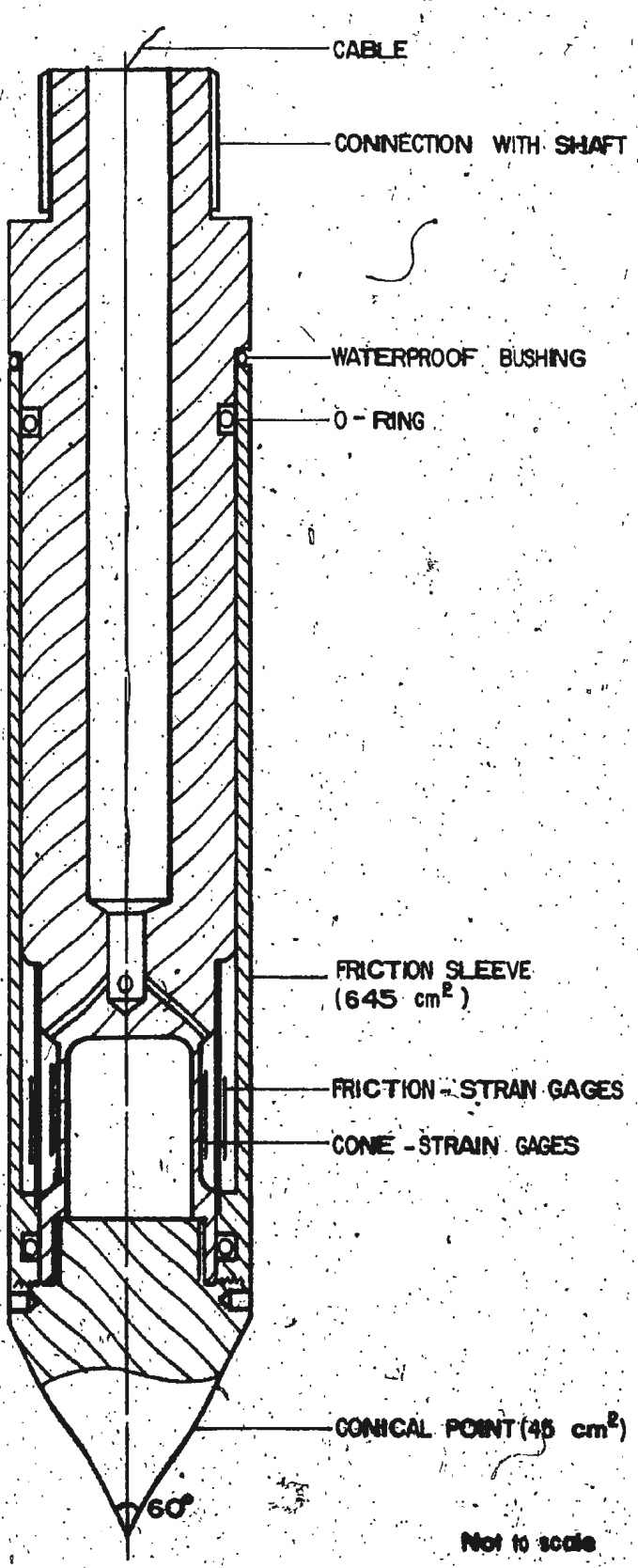

Fig. 21. Free Fall Cone Penetrometer Tip Details
(Ref. 16)

tape recorder on the ship.

A seperate Doppler telemetry unit was attached on the top of the penetrometer assembly. The Doppler telemetry system was used to obtain velocity profiles of the unit independently. Comparison of the direct velocity profiles from the Doppler system with the integrated results of the accelerometer records was later carried out. A chart recorder was used in parallel with the tape recorder to determine whether the system was operating properly.

4.6.3. Data Processing and Cone Penetrometer Output Results

Data from the penetrometer instrumentation was recorded on the analog recorder, and subsequently digitized in a H.P. 5451-B Fourier Analyzer. The record obtained from the accelerometer, cone load cell and sleeve load cell is a voltage output as a function of time. Calibration was necessary to convert cone and sleeve output to pressure and the deceleration output to displacement.

- for cone scale 1 volt = 6.005 kN
- for sleeve scale 1 volt = 0.5938 kN
- for deceleration scale 1 volt = $\frac{\text{voltage} \times 100}{16.7}$ g
- for velocity from Doppler telemetry

$$1 \text{ volt} = \frac{\text{voltage} \times v}{800}$$

where: v = sound velocity = 1445 m/s (assumed)

From the accelerometer output, time histories of velocity and displacement were calculated by a double integration program in accordance with the following relationships:

$$v(t) = \int_o^t a(t)\, dt + v_o \qquad \ldots\ldots\ldots \quad (7)$$

$$d(t) = \int_o^t \left\{ \int_o^t a(t)\, dt + v_o \right\} dt + d_o \qquad \ldots\ldots\ldots \quad (8)$$

where: $v(t)$ = velocity at time t

$a(t)$ = acceleration at time t

v_o = impact velocity

$d(t)$ = displacement at time t

d_o = displacement at t = 0 ($d_o = 0$)

From the Doppler telemetry record, the velocity of penetration versus time was obtained as an independent measurement. This measured velocity was then re-plotted as a function of the depth and was compared with the integrated result of the acceleration record. The agreement between the two velocity profiles was good as it is shown in Figs. 22,23.

The cone tip resistance, sleeve friction and deceleration profiles were re-plotted as functions of the soil depth. Figs. 24 to 29 show each of these profiles for stations G 132, 141, 243, 332, 432 and 441A respectively. No records were obtained from stations G 233 and 341 due to flooding of the cable connector. The depth of penetration varies between 3.0 to 4.5 m for stations G 132, 141, 243 and 332, while for stations G 432 and 441A, the depth of penetration was only 0.8 and 0.46 m respectively. For these two stations, the penetrometer obviously hit a very hard object or layer and came to rest within these depths. In stations G 141 and 332, on initial impact, the penetrometer recorded high initial cone tip resistance and deceleration. This means that the penetrometer contacted a hard object or layer. The cone tip resistance and sleeve friction then increase uniformly with further depth suggesting soil of reasonably consistent properties.

Correlation of the free fall penetrometer output results with parameters determined by other methods is presented in Chapter V.

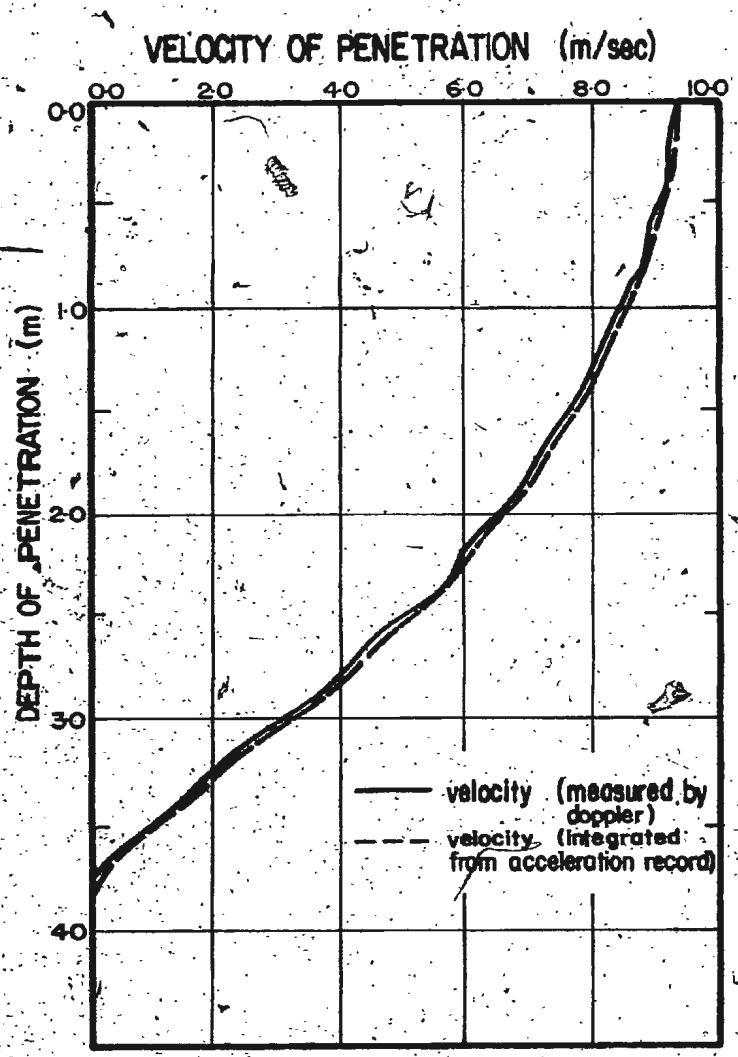

a. G 132

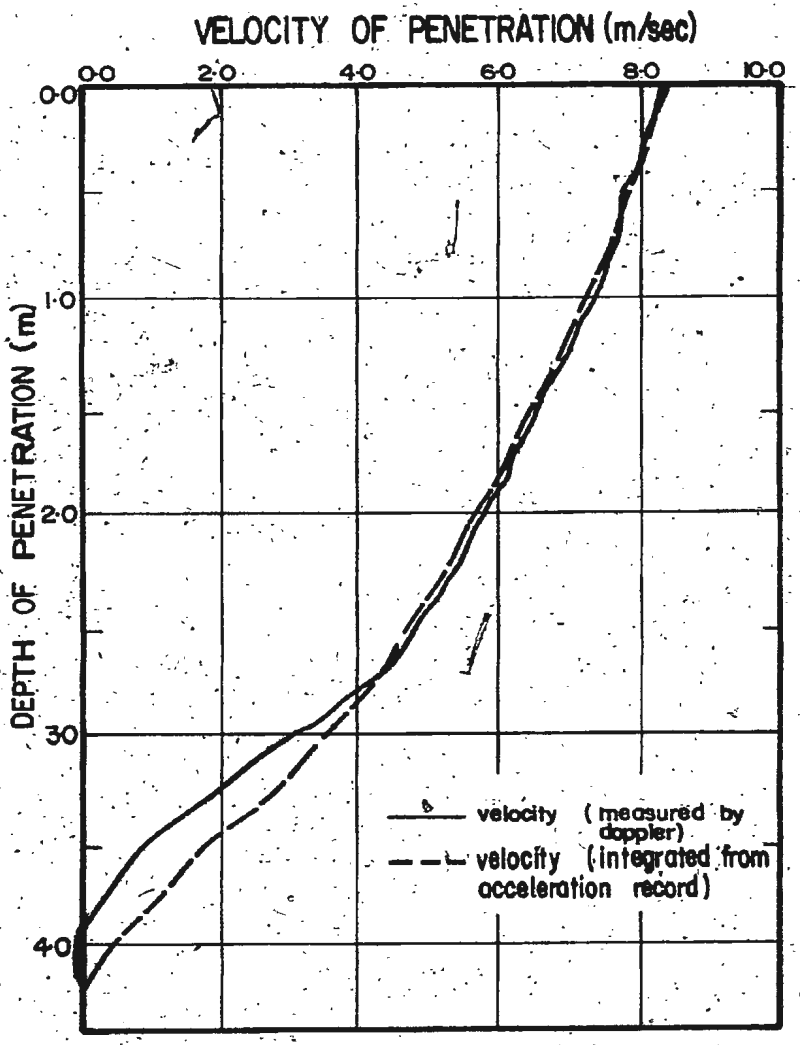

b. G 141

Fig. 22. Comparison of Cone Penetrometer Velocities - Doppler Telemetry and Accelerometer - Stations G 132, 141

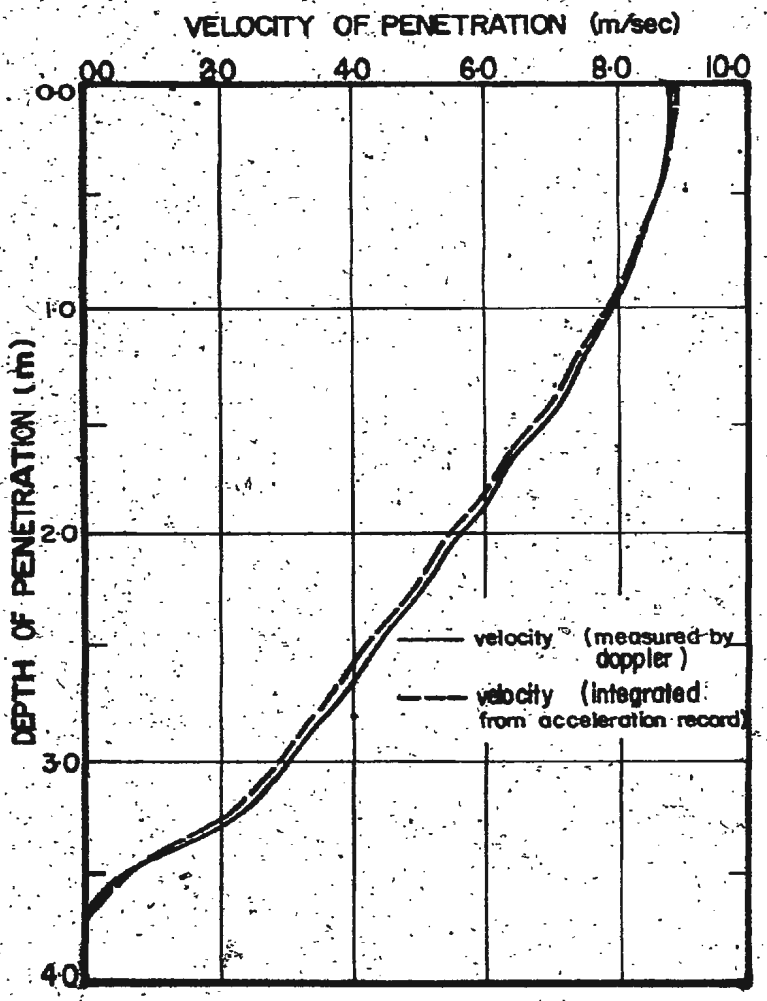

a. G 243

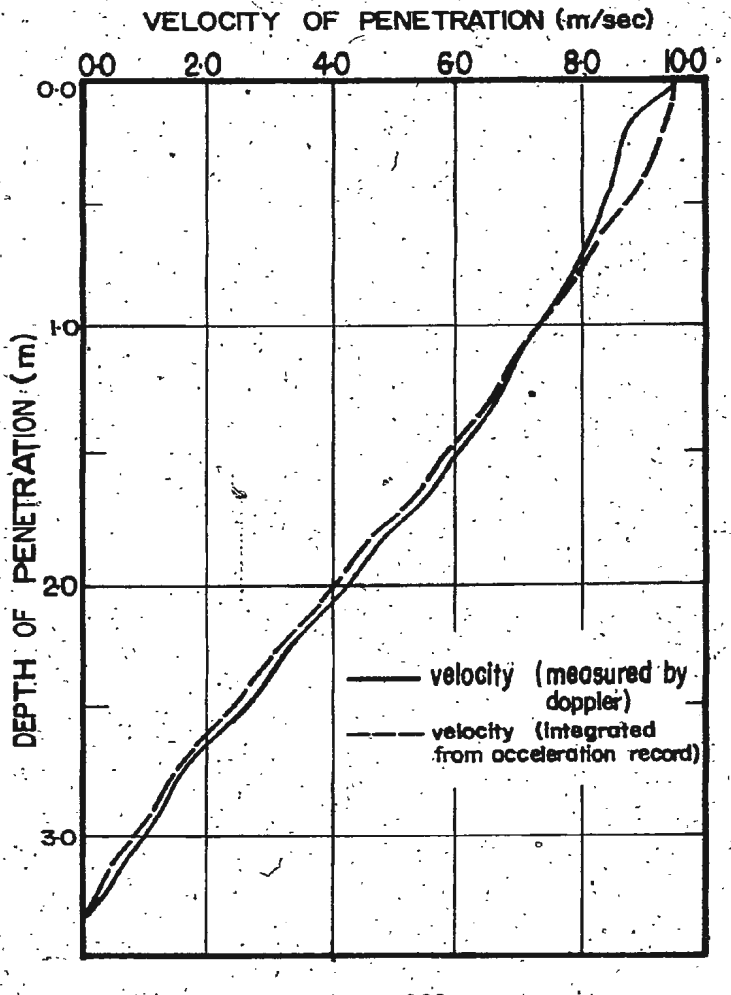

b. G 332

Fig. 23. Comparison of Cone Penetrometer Velocities - Doppler Telemetry and Accelerometer - Stations G 243, 332

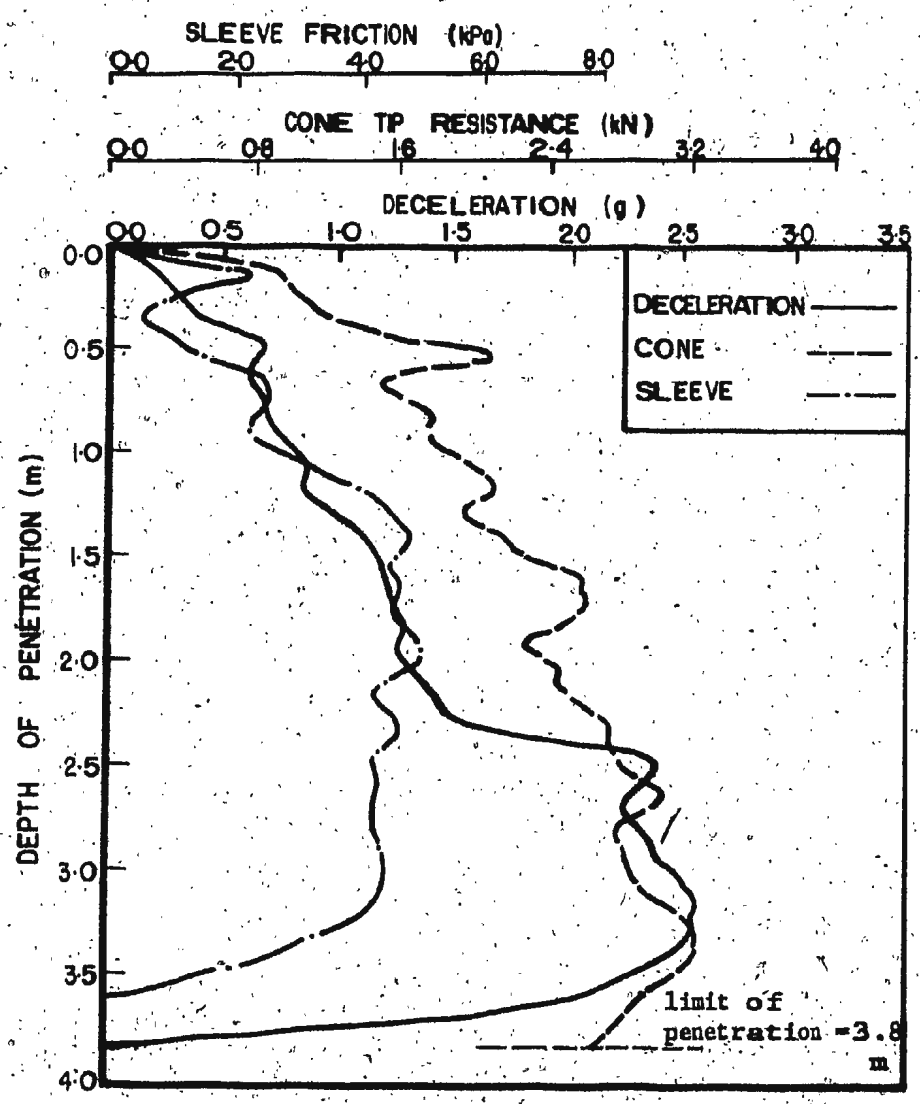

Fig. 24. Cone Penetrometer Output - Station G 132

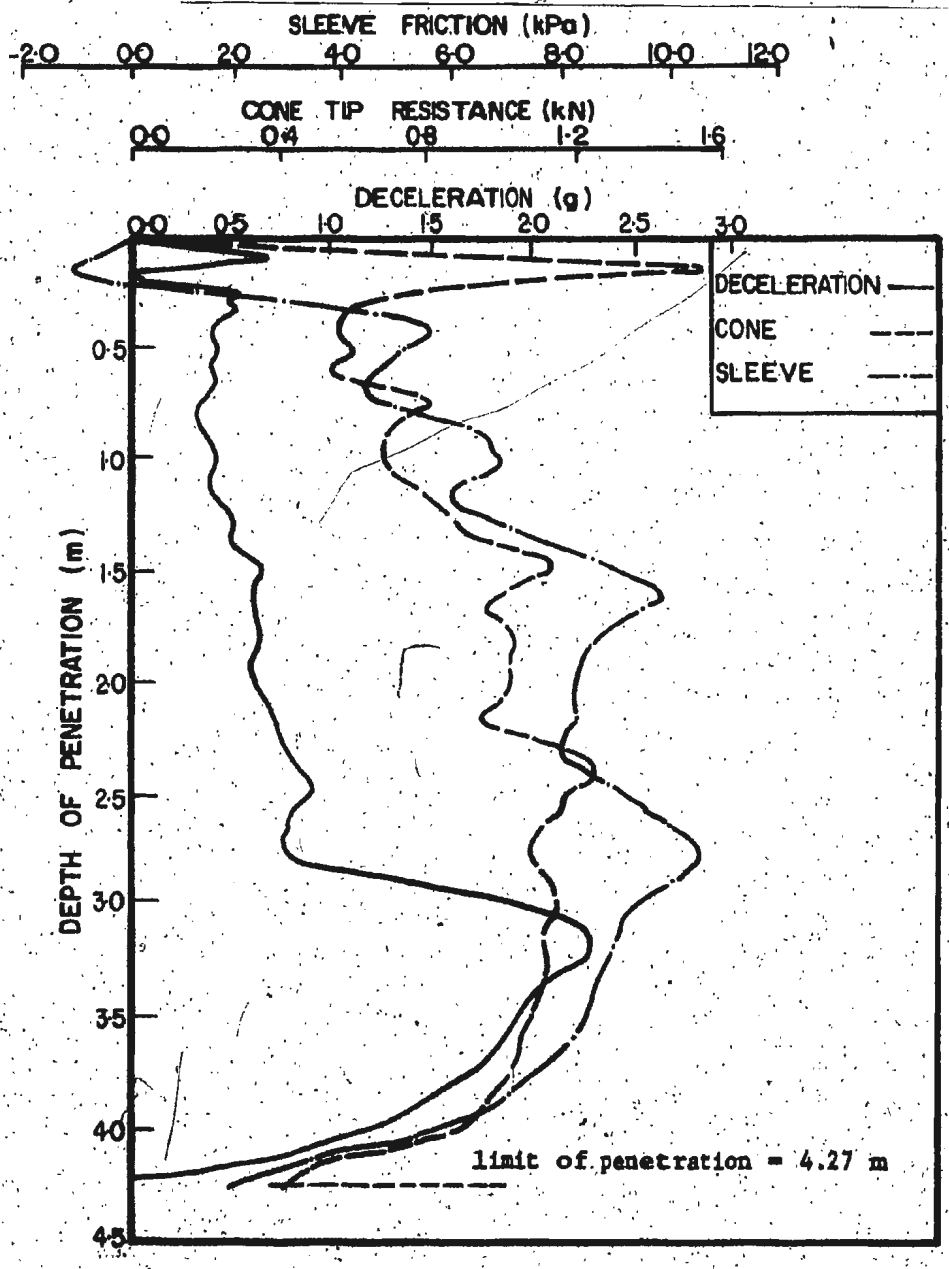

Fig. 25. Cone Penetrometer Output - Station G 141

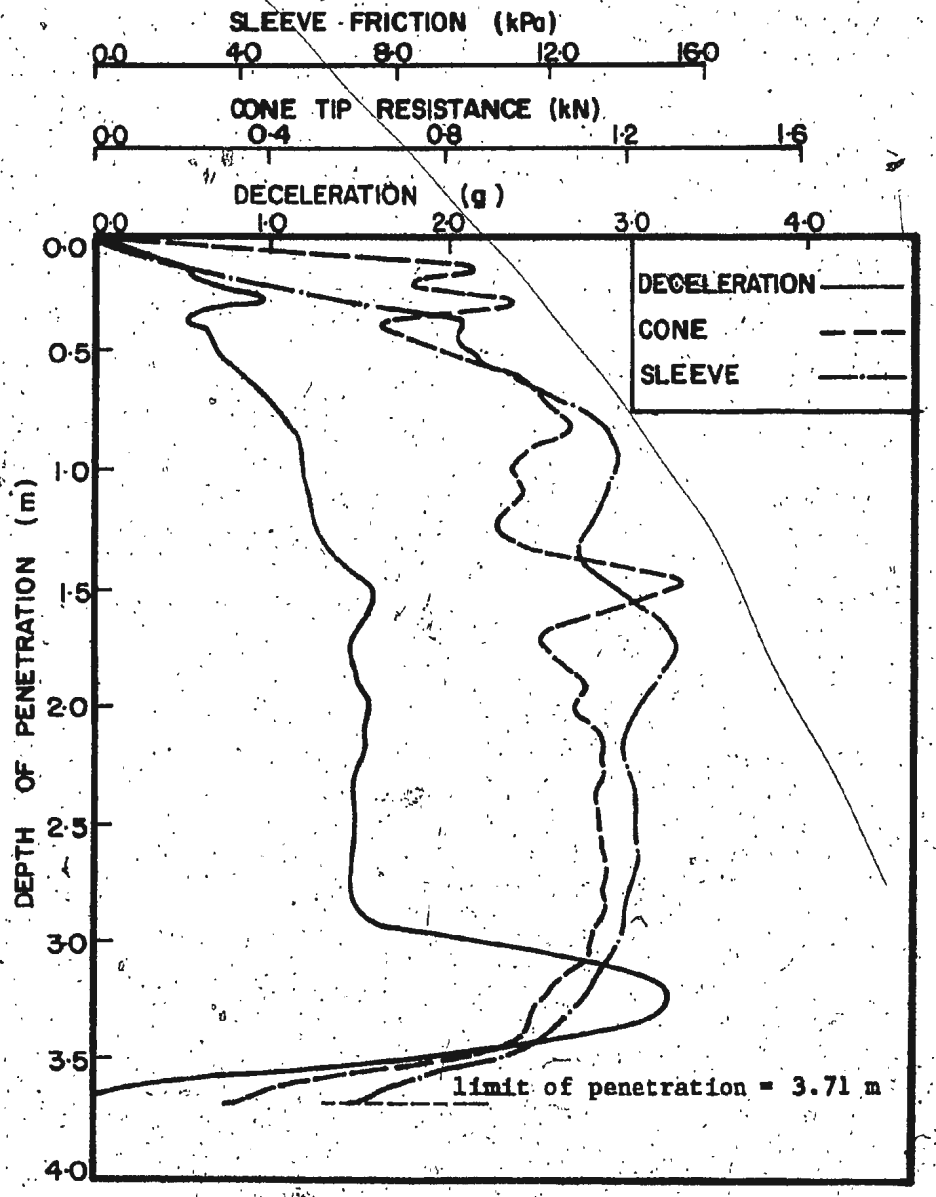

Fig. 26. Cone Penetrometer Output - Station G 243

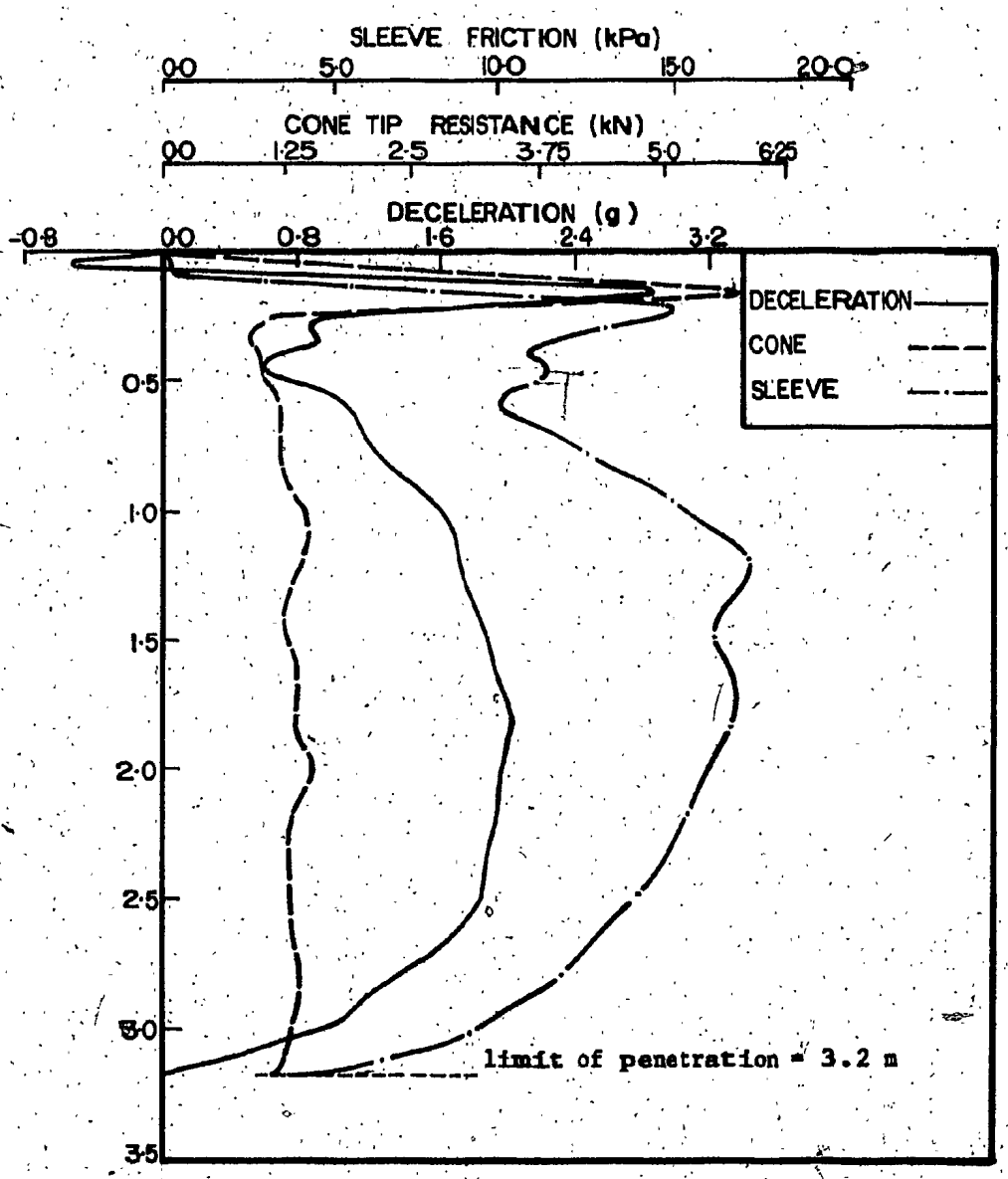

Fig. 27. Cone Penetrometer Output – Station 0 332

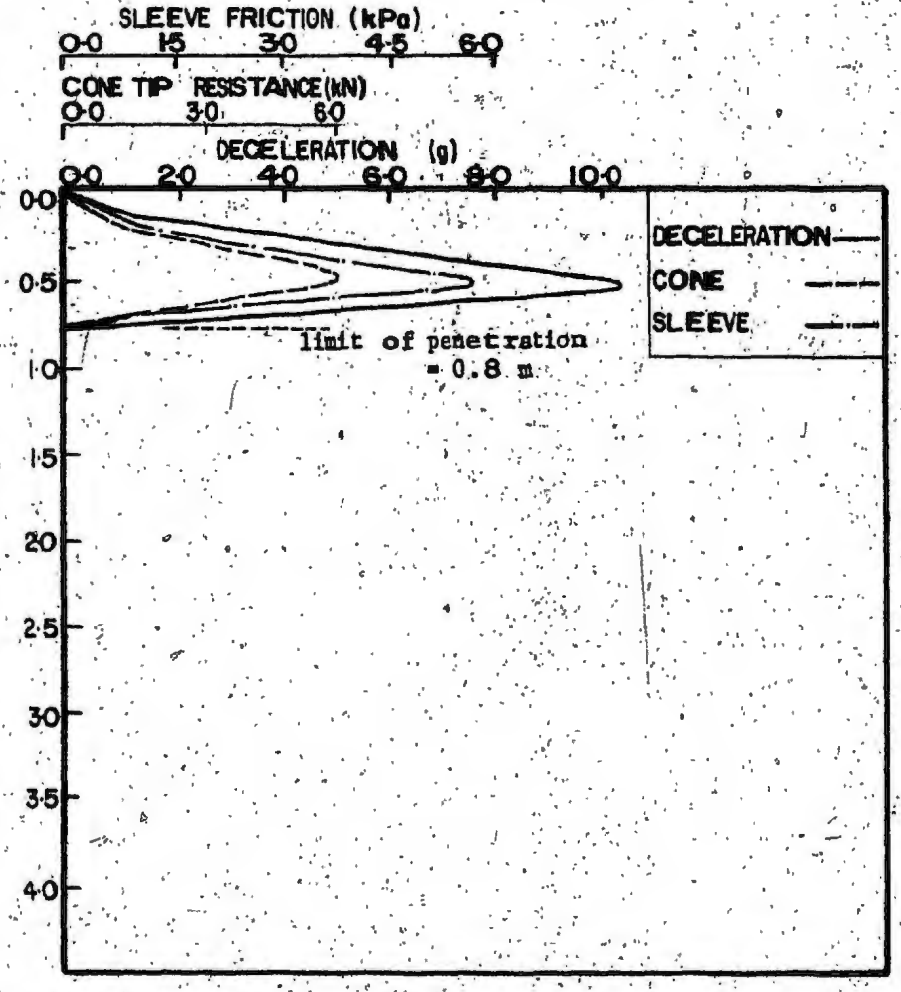

Fig. 28. Cone Penetrometer Output - Station G 432

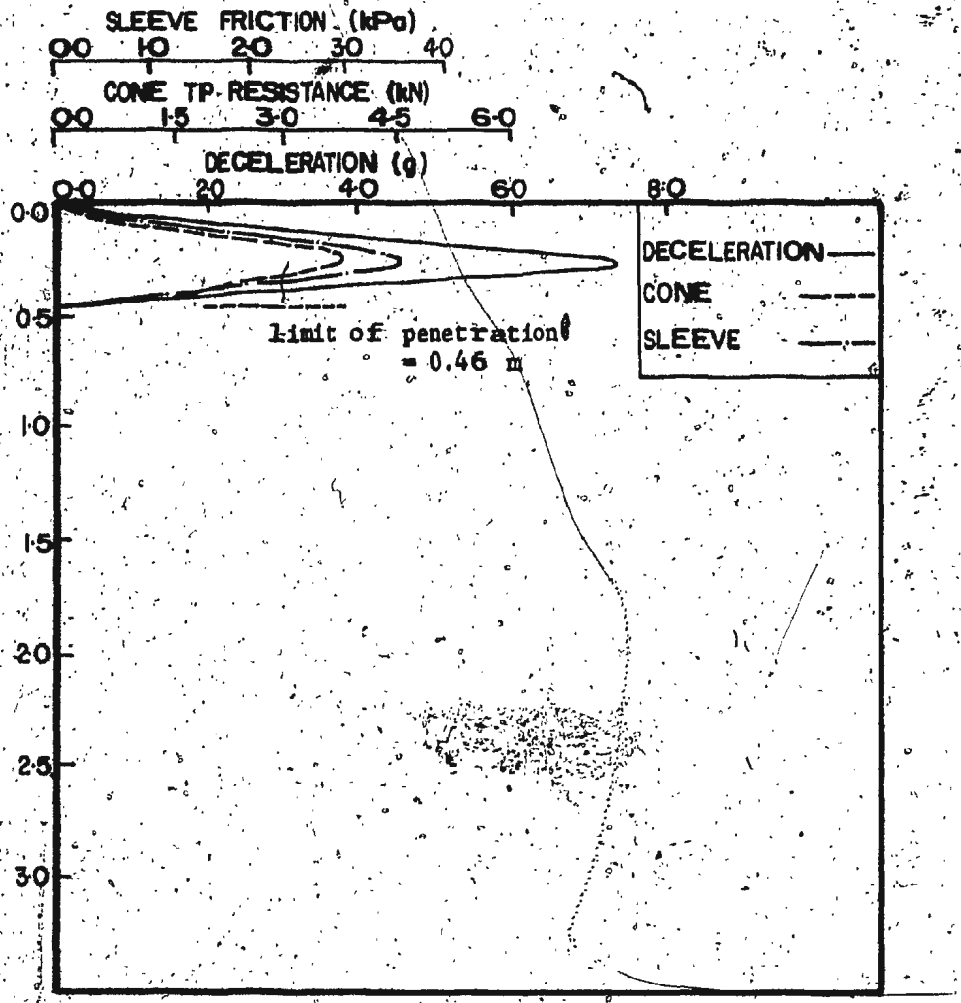

Fig. 29. Cone Penetrometer Output - Station G 441A

4.7. Acoustic Properties

Marine sediments can be regarded as a three phase media; solid, liquid and gas and the whole can be considered as a mixture of these phases. The acoustic properties are dependent upon the relative proportions of the phases. The experimental technique developed for the measurement of the sound velocity in sediment samples is based upon the measurement of the transit time and amplitude of an acoustic pulse transmitted directly through the medium.

4.7.1. Sound Velocity Determination

To determine sound velocity, the time for a compressional wave to travel through a certain thickness of sediment is compared to the time for it to travel through the same thickness of a known velocity medium. From the time difference, the velocity of sound in the sediment can be calculated.

The fundamental equation for the velocity of propagation of a compressional wave through a perfectly elastic, homogenous and isotropic solid is given by:

$$v^2 = \frac{3K + 4\mu}{3\rho} \qquad \ldots\ldots\ldots\ldots \quad (9)$$

where: K = the bulk modulus = $\frac{1}{\beta}$

μ = the rigidity or shear modulus

ρ = the bulk density

β = the compressibility

Basically the measurement of the transverse sound velocity of a core takes the form of a comparison of the travel times of a sound impulse across a core liner filled with sediment to one filled with water of known velocity. This technique eliminates the unknown yet

fixed electrical delays and acoustic delays associated with the transducers.

Velocity measurements were made on the cores immediately after removal from the core barrel on the ship. The apparatus used to measure the velocity is described in Appendix A together with additional details related to the measurements made.

In this study, velocity measurements were taken across the core diameter at 100 mm intervals, along the core length. Measurement of the water standard were made twice during the sampling phase. The sound velocity in the core was calculated using the formula:

$$v_s = \frac{(L_2 - L_p)\, v_w}{\Delta T\, v_w + (L_1 - L_p)} \qquad \ldots\ldots\ldots \quad (10)$$

where: v_s = sound velocity of sediment

v_w = sound velocity in water = 1463.7 m/s

L_p = 2 x liner wall thickness

L_1 = outside diameter of liner

$\Delta T = T_2 - T_1$ = difference in the elapsed time for both the sediment and water cases.

The direct velocity measurements quoted in this study were conducted by Dr. P. Simpkin, and have been used with his permission. The velocity logs obtained from the cores are presented in Figs. 30 to 37. In some cases, large variations in sound velocity have been recorded. There are several reasons why large anomalies can occur such as;

a. poor coupling between transducers and core liner.

b. poor coupling between core liner and core caused by air space or air bubble.

c. internal structure of core such as gassing, cracks, pebbles or shells or sampling disturbance.

The temperature/salinity profiles obtained during the cruise indicated a bottom water temperature between 0 and $-1^{\circ}C$ with a salinity between 32.5 and 33 %. This gives values of sound velocity for the near bottom water in the range 1442 - 1445 m/s.

The velocity logs show the uncorrected sound velocity, meaning that they are not referred to any standard temperature. It is usual to refer seafloor measurements of velocity to a standard temperature, and the most common method is to add the difference in the velocity of sound in sea water at $20^{\circ}C$ and the velocity at the in-situ temperature. In our case, this would require 70 m/s added to the measured velocities.

4.7.2. Acoustic Impedance

The acoustic impedance of the sediment is defined as

$$Z = \rho \times v \qquad \ldots\ldots\ldots\ldots \quad (11)$$

where ρ = bulk density of the material

v = acoustic velocity through the material

It is the controlling property in acoustic energy transmission across a boundary. The bulk density of the soil has been measured as the wet unit weight at 500 mm intervals along the core. From these measured values, interpolated values of bulk density have been estimated at 100 mm intervals along each core to correspond with velocity measurements obtained. Figs. 30 to 37 show the acoustic velocity, density and the acoustic impedance for each core.

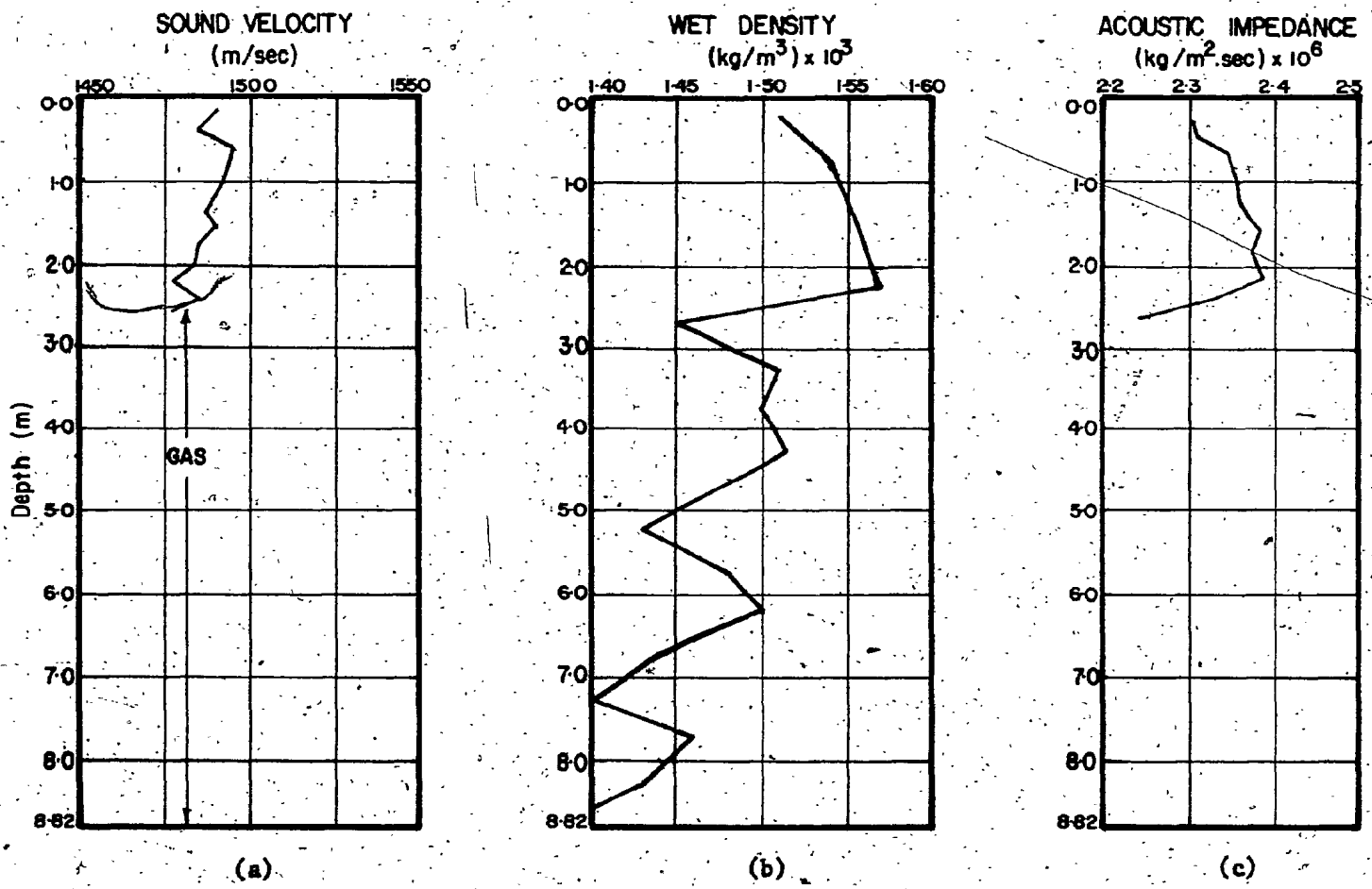

Fig. 30. Measured Acoustic Properties along Core G 132, (a) Acoustic Sound Velocity (uncorrected), (b) Wet Density and (c) Acoustic Impedance

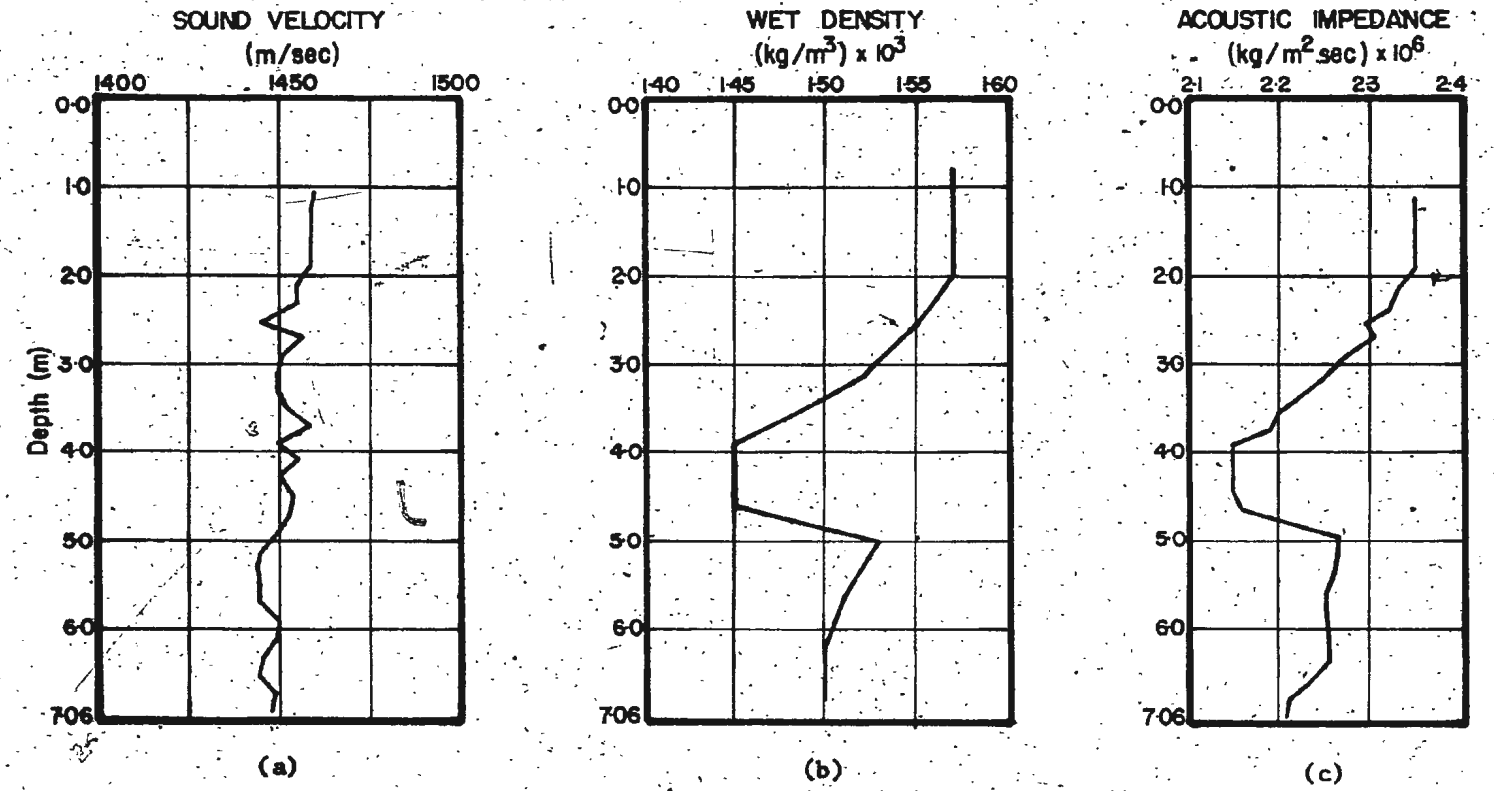

Fig. 31. Measured Acoustic Properties along Core G 141, (a) Acoustic Sound Velocity (uncorrected), (b) Wet Density and (c) Acoustic Impedance

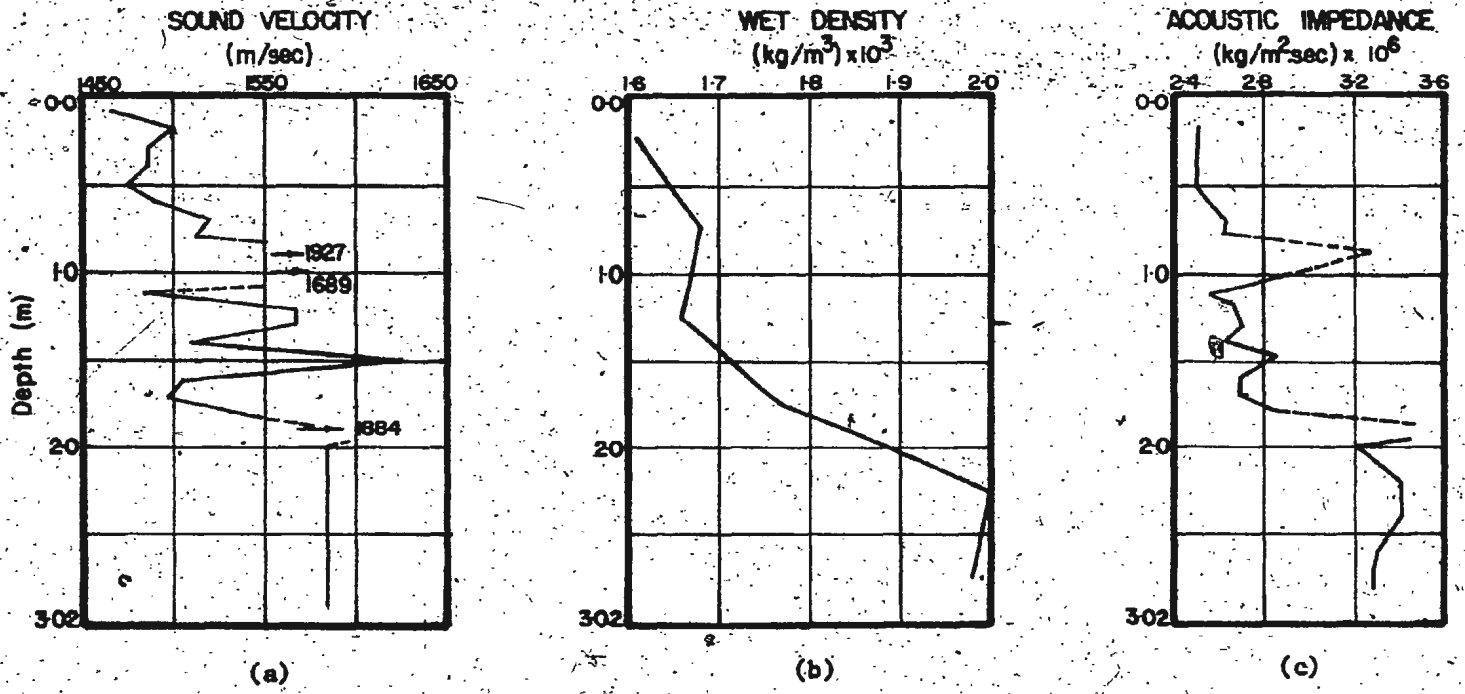

Fig. 32. Measured Acoustic Properties along Core G 233, (a) Acoustic Sound Velocity (uncorrected), (b) Wet Density and (c) Acoustic Impedance

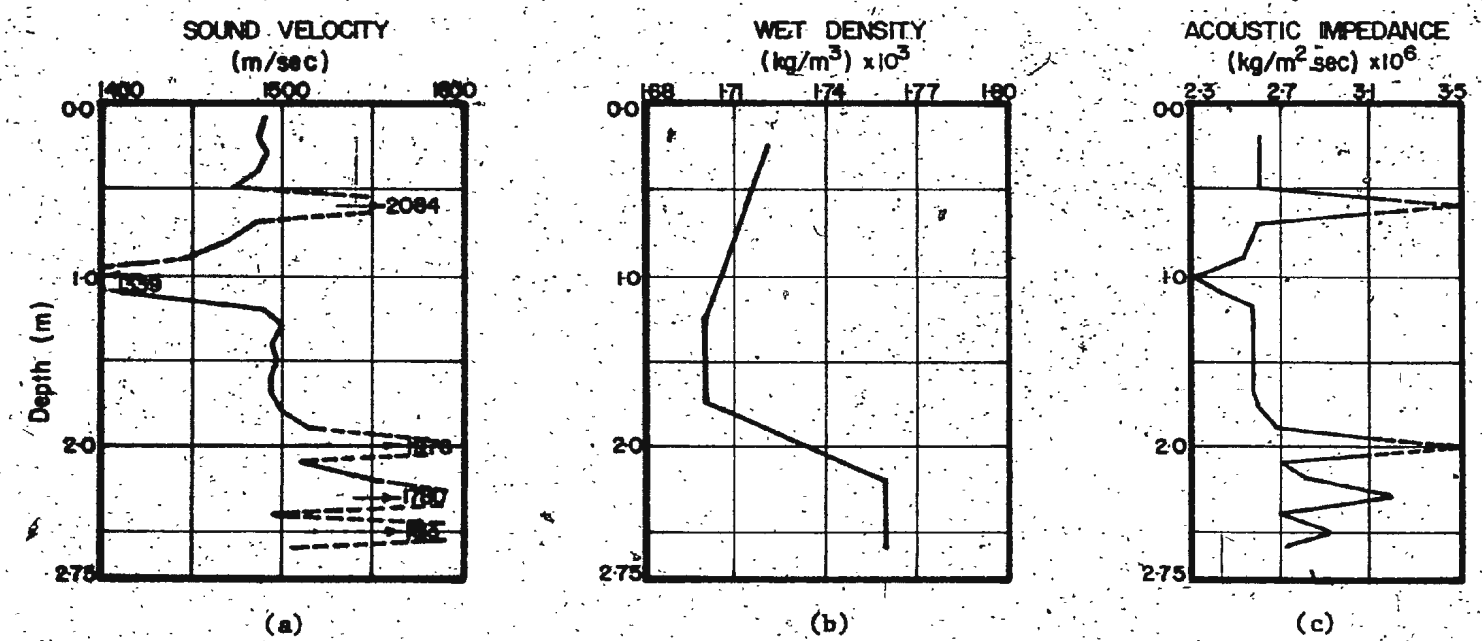

(a) (b) (c)

Fig. 33. Measured Acoustic Properties along Core G 243, (a) Acoustic Sound Velocity (uncorrected), (b) Wet Density and (c) Acoustic Impedance

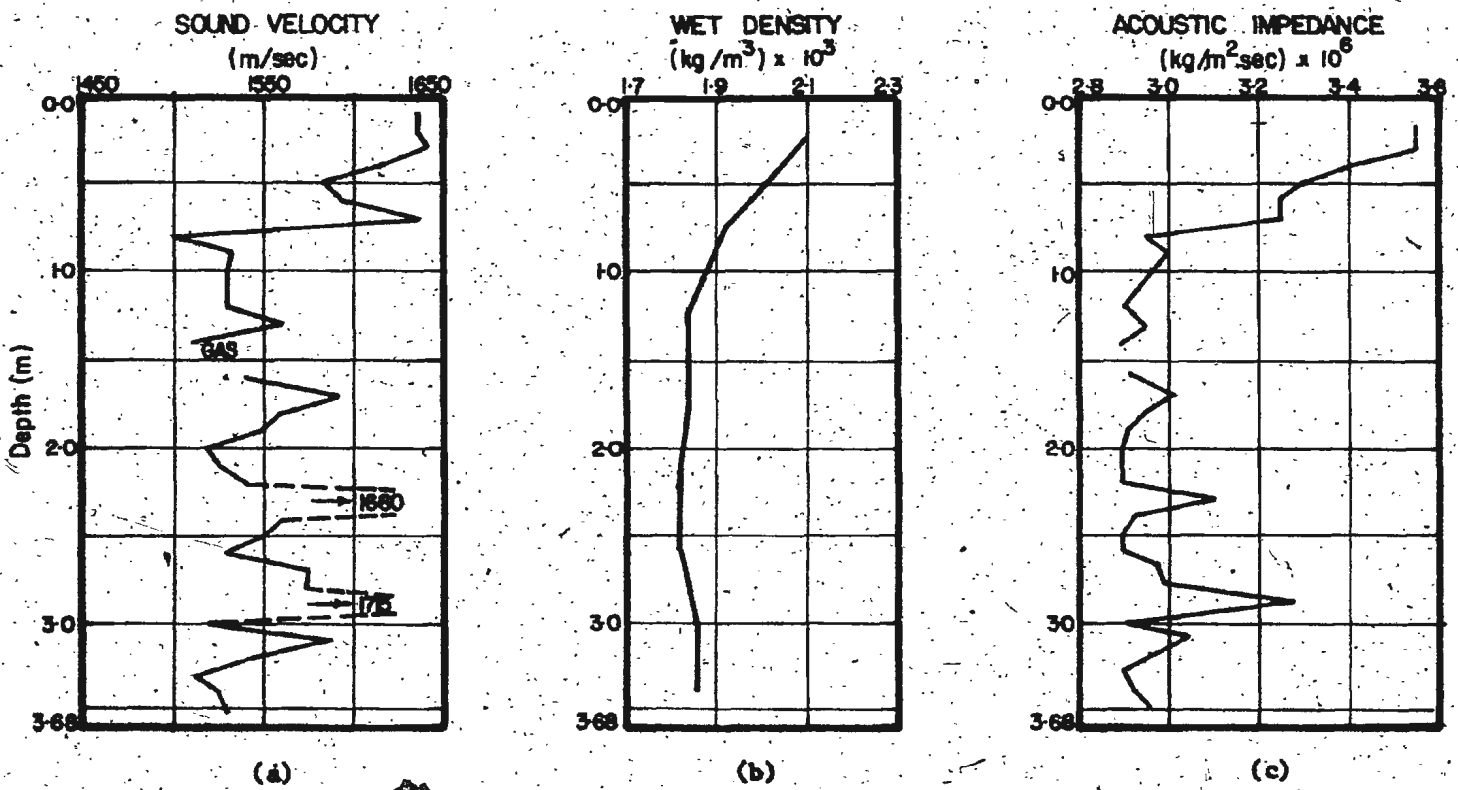

Fig. 34. Measured Acoustic Properties along Core G 332, (a) Acoustic Sound Velocity (uncorrected), (b) Wet Density and (c) Acoustic Impedance

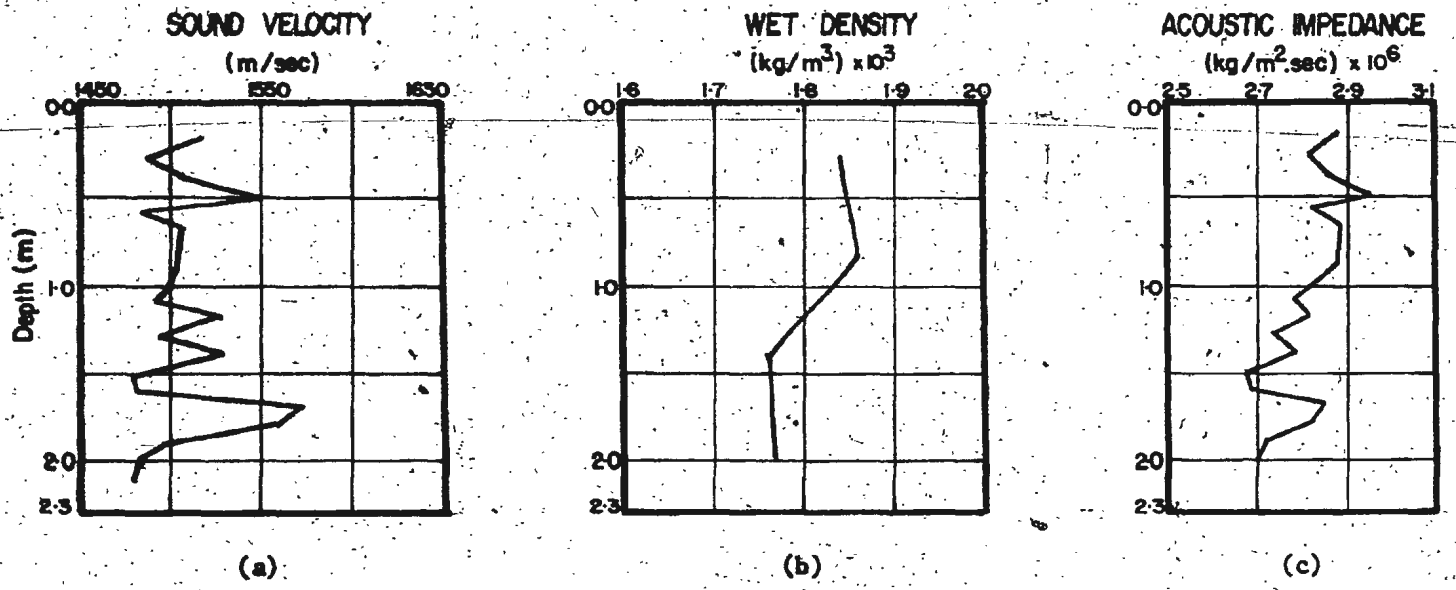

Fig. 35. Measured Acoustic Properties along Core G 341, (a) Acoustic Sound Velocity (uncorrected), (b) Wet Density and (c) Acoustic Impedance

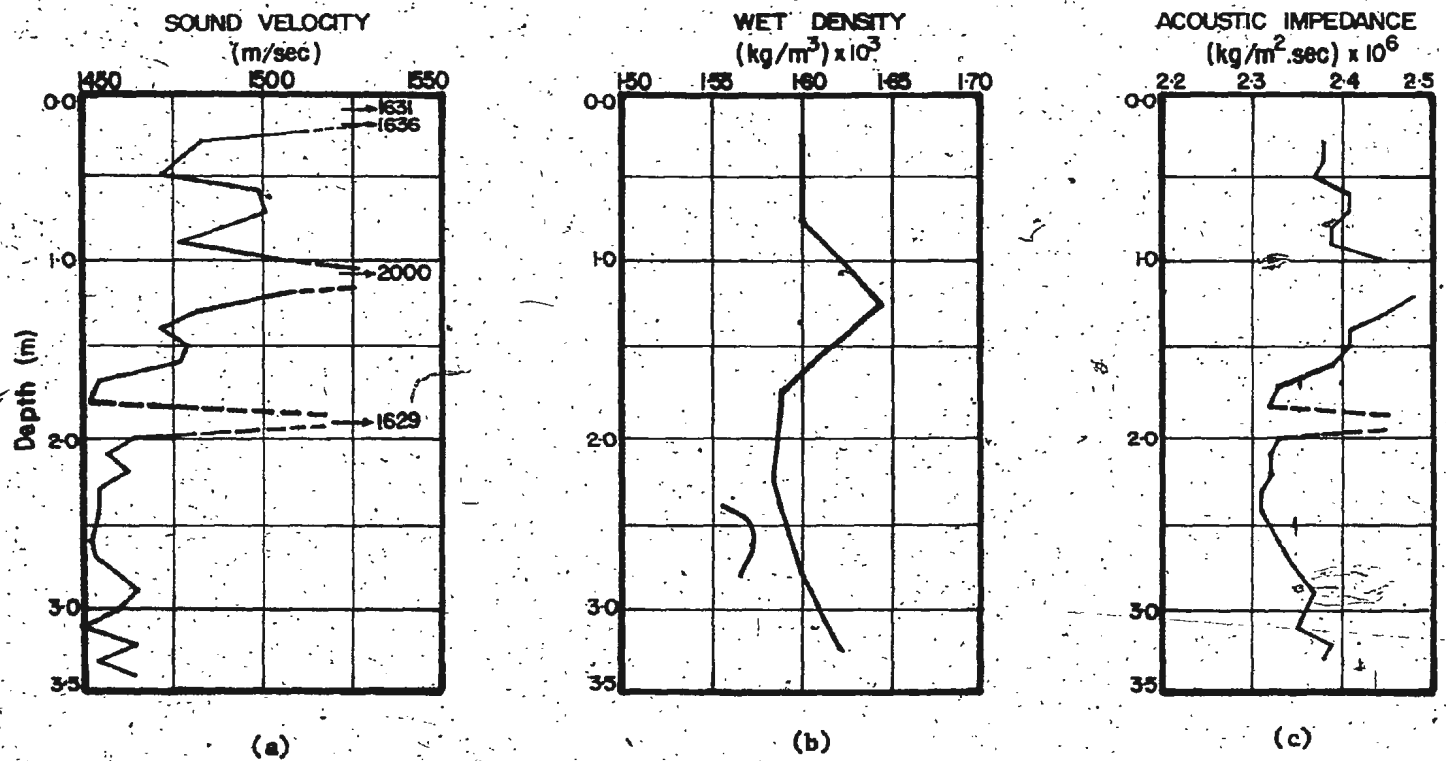

Fig. 36. Measured Acoustic Properties along Core G 432, (a) Acoustic Sound Velocity (uncorrected), (b) Wet Density and (c) Acoustic Impedance

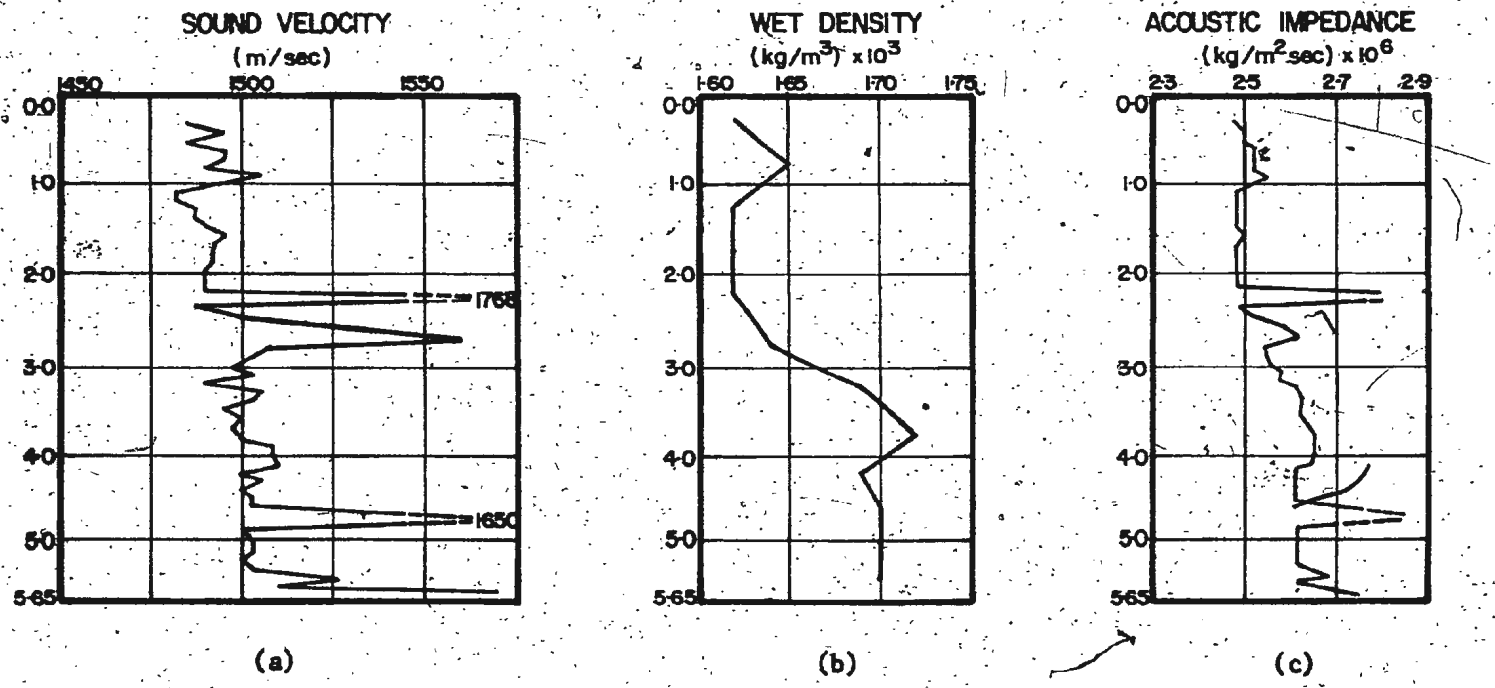

Fig. 37. Measured Acoustic Properties along Core G 441A, (a) Acoustic Soumd Velocity (uncorrected), (b) Wet Density and (c) Acoustic Impedance

CHAPTER V

ANALYSIS AND DISCUSSION OF TEST RESULTS

5.1. Introduction

Available data, presented in Chapter IV, have been analyzed to establish relationships between the various properties of the submarine soils encountered and other parameters which were measured.

This chapter presents: a) basic relationships between the various geotechnical properties of the soils, b) correlations between the acoustic and geotechnical properties of the soils, and c) relationships between the measured geotechnical and acoustic properties and parameters measured by the free fall penetrometer. The shear strength and consolidation characteristics of the sediments investigated are also discussed. In addition, computations of the elastic properties and their inter-relationships with other physical and acoustical properties are reported. In the final section, an evaluation of the impact penetrometer output characteristics is presented to facilitate interpretation of the data obtained.

The degree of correlation has been obtained by regression analyses with results presented in both numerical and graphical forms. Both linear and non linear regression analyses have been used to analyse the data using a computer program which is described in Appendix C. A regression equation was obtained for each case considered. The correlation coefficient was also computed to permit comparison of the equations and to give a quantitative indication of the degree of correlation. Table 6 lists the variables considered in the regression analyses.

TABLE 6. VARIABLES CONSIDERED IN REGRESSION ANALYSES

Variables	Symbols	Units
sound velocity	v_s	km/s
acoustic impedance	Z	$kg/m^2 \cdot s \times 10^6$
moisture content	w	%
liquid limit	w_L	%
plastic limit	w_P	%
plasticity index	I_P	%
liquidity index	I_L	%
Activity	a_c	-
bulk density	ρ_s	kg/m^3
porosity	n	%
void ratio	e	-
clay fraction	u_1	%
sand fraction	u_2	%
silt fraction	u_3	%
median diameter	$M_{d\phi}$	mm
mean diameter	M_ϕ	mm
graphic mean diameter	M_z	mm
phi deviation	σ_ϕ	mm
undrained shear strength	S_u	kN/m^2
compression index	C_c	-
coefficient of consolidation	c_v	$cm^2/s \times 10^{-4}$
cone tip resistance	Q_d	kN/m^2
sleeve friction	F_s	kN/m^2

5.2. Correlation of the Geotechnical Properties

Correlations which identify the relationships between soil properties can be of significant benefit to the engineering designer. This is particularly true in connection with marine geotechnical studies because of the great difficulties encountered in obtaining sufficient data.

Correlations between various geotechnical properties are well established in the literature. In this investigation, an attempt is made to determine these relations for the soils encountered. Hence, a linear regression analysis, using digital computation, has been used for 114 sets of data points, representing the eight cores at 0.25 m intervals. The regression equations obtained and the related correlation coefficients comprise Table 7, with graphical plots of the variables compared are presented on Figs. 38 to 42. The results obtained can be summarized as follows:

1. Observed bulk densities range from 1440 to 2100 kg/m^3. As may be seen in Figs. 38 a,b, density decreases as both moisture content and plasticity index increase. The regression analysis gives negative correlation coefficients of 0.854 and 0.70 respectively.

2. A decrease in porosity occurs with an increase in wet density and a decrease in moisture content (Figs. 39a,b). These relations are already well documented (Buchan et al. 1972). High correlation coefficients of 0.96 and 0.925 have been obtained for these two relations.

3. The plasticity characteristics of the surface sediments have been investigated in this study. Plasticity data are presented in the plasticity chart (Fig. 19a) in Chapter IV. Plots of this data are

distributed along a straight line called the "A - Line" which represents the relationship of

$$I_p = 0.73\ (w_L - 20) \quad \ldots\ldots\ldots \quad (6)$$

The regression analysis for this data gives a linear relationship in the form of

$$I_p = -\ 10.875 + 0.658\ w_L \quad \ldots\ldots\ldots \quad (12)$$

or $$I_p = 0.658\ (w_L - 17) \quad \ldots\ldots\ldots \quad (12')$$

Plasticity data of soil samples taken from the Atlantic Ocean have been reported by Buchan et al. 1972, with an approximate relationship of

$$I_p = 0.73\ (w_L - 15) \quad \ldots\ldots\ldots \quad (13)$$

4. An increase of compression index C_c can be reasonably correlated with an increase in moisture content, an increase in liquid limit, an increase in void ratio, an increase in porosity and a decrease in wet density. These are illustrated in Figs. 40a,b and 41a,b. The regression equations and correlation coefficients are presented in Table 7. The relationship between compression index and liquid limit generally falls within the range:

$$C_c = 0.007 — 0.012\ (w_L - 10) \quad \ldots\ldots\ldots \quad (14)$$

As indicated in Fig. 40b, this range is within the correlation suggested by Terzaghi and Peck (1967) which is

$$C_c = 0.009\ (w_L - 10) \quad \ldots\ldots\ldots \quad (15)$$

No meaningful correlation was found between the coefficient of consolidation c_v and any of the other geotechnical properties.

5. The undrained shear strength, as measured by the laboratory vane, was treated as a dependent variable in the regression analysis to relate this parameter with other geotechnical properties. Low correlation coefficients were obtained between shear strength and moisture content, liquid limit, wet density, porosity and compression index. No meaningful correlation was obtained between shear strength and the coefficient of consolidation. Figs. 42a,b show the variation of undrained shear strength with moisture content and porosity.

5.3. Correlation Between Acoustic and Geotechnical Properties

The inter-relationships between acoustic and geotechnical properties of submarine sediments are multivariate. Previous work (Sutton et al. 1957 and Buchan et al. 1967) has shown that most of the relationships tend to be linear over the range of observations. Hence, the linear regression analysis as well as non - linear analysis, using digital computation, have been used in this data analysis.

The regression equations of the acoustic properties -the dependent variables- and the geotechnical properties -the independent variables- have been computed. The correlation coefficient was also computed for each case. The relationships between sound velocity and index properties, textural properties and engineering properties are presented as well as the variation of acoustic impedance with these properties. Tables 8 and 9 give the computed prediction equations and their correlation coefficients for 114 sets of data points evaluated.

TABLE 7. REGRESSION EQUATIONS FOR GEOTECHNICAL PROPERTIES

Regression Equations	Correlation Coefficients
$\rho_s = 2218.1 - 9.715\ w$	- 0.854
$\rho_s = 1924.68 - 9.8\ I_p$	- 0.70
$n = 131.99 - 0.043\ \rho_s$	- 0.96
$n = 33.45 + 0.472\ w$	0.925
$w = 9.956 + 0.824\ w_L$	0.92
$w_L = 3.208 + 1.812\ w_P$	0.739
$I_P = - 10.875 + 0.658\ w_L$	0.91
$C_c = - 0.1 + 0.0096\ w$	0.873
$C_c = - 0.029 + 0.0083\ w_L$	0.843
$C_c = - 0.012 + 0.288\ e$	0.838
$C_c = - 0.63 + 0.018\ n$	0.828
$C_c = 1.675 - 0.0007\ \rho_s$	- 0.766
$S_u = 2.91 + 0.075\ w$	0.48
$S_u = 2.986 + 0.073\ w_L$	0.524
$S_u = 17.23 - 0.006\ \rho_s$	- 0.44
$S_u = - 2.44 + 0.16\ n$	0.52
$S_u = 4.02 + 7.14\ C_c$	0.50
S_u & c_v	no correlation
S_u / p_o & I_P , I_L	no correlation
$u_1 = 1.426 + 0.495\ w_P$	0.19
u_1 & w_L	no correlation
a_c & I_P	no correlation

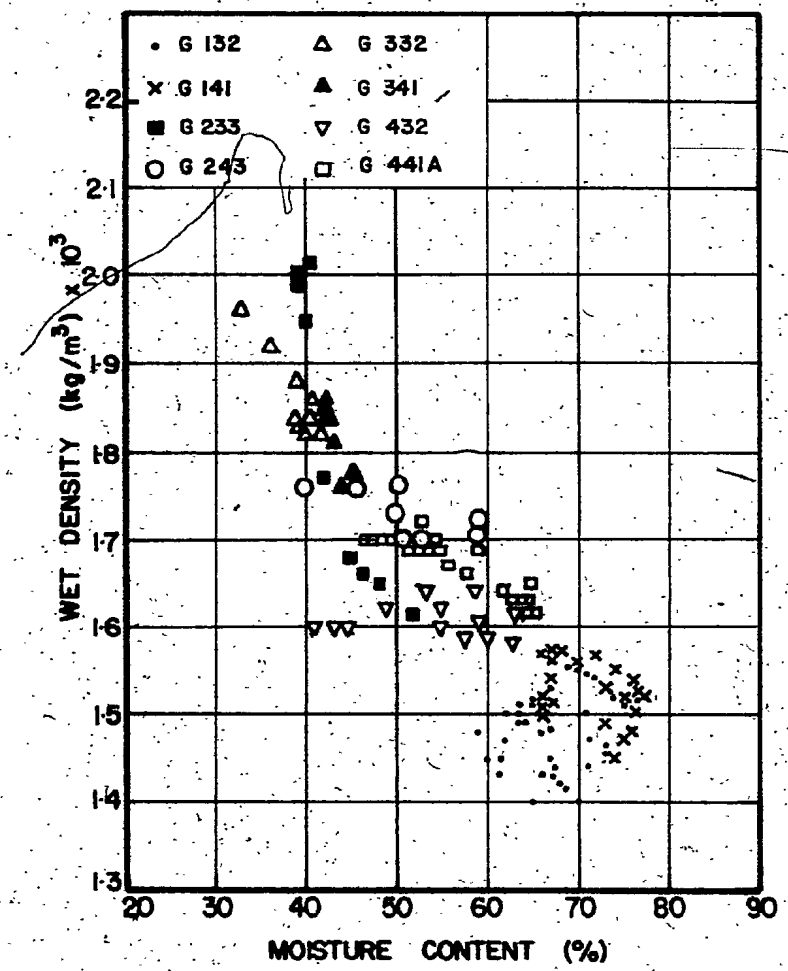

Fig. 38a. Variation of Wet Density with Moisture Content

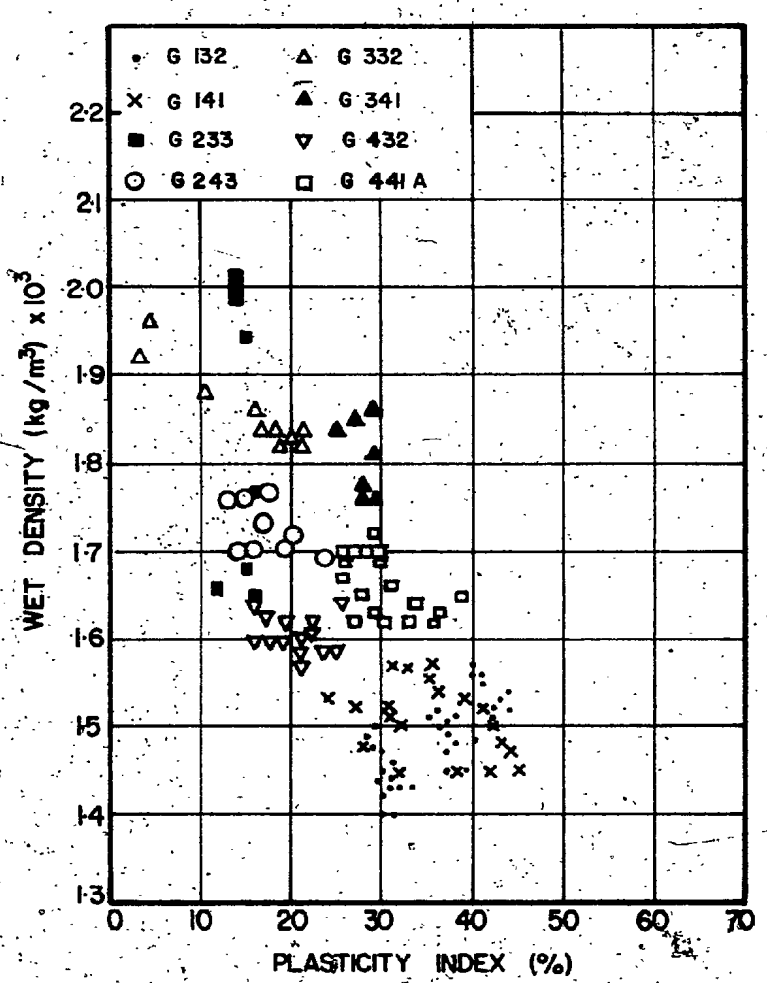

Fig. 38b. Variation of Wet Density with Plasticity Index

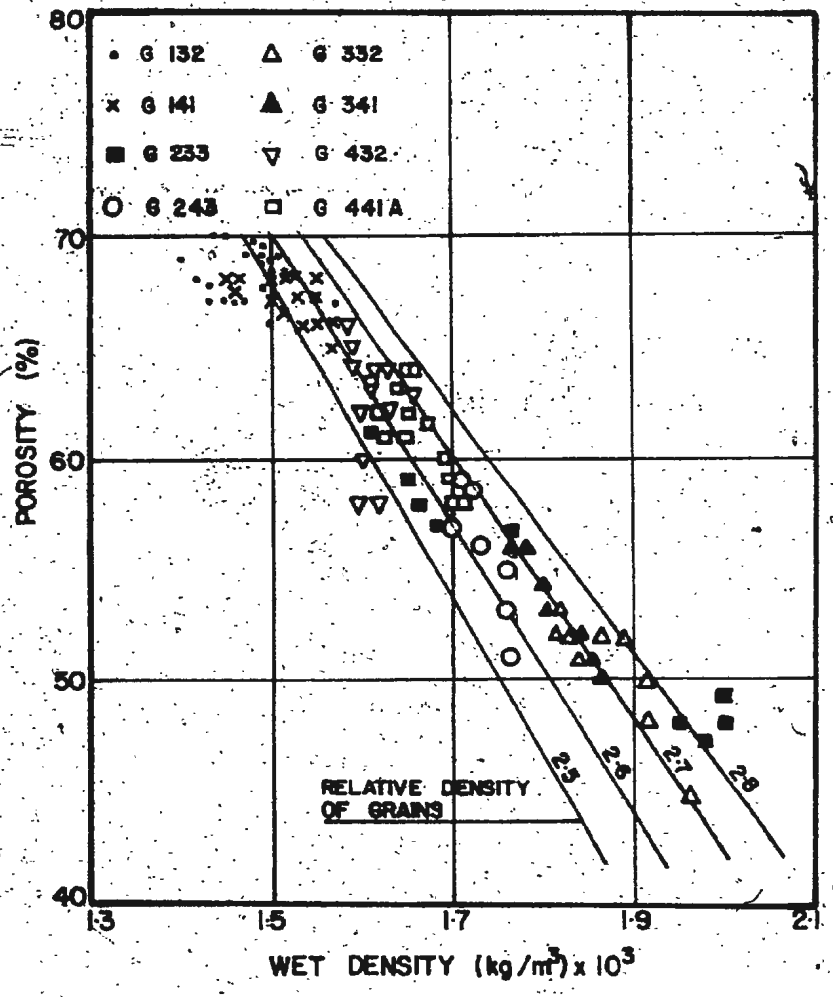

Fig. 39a. Variation of Porosity with Wet Density

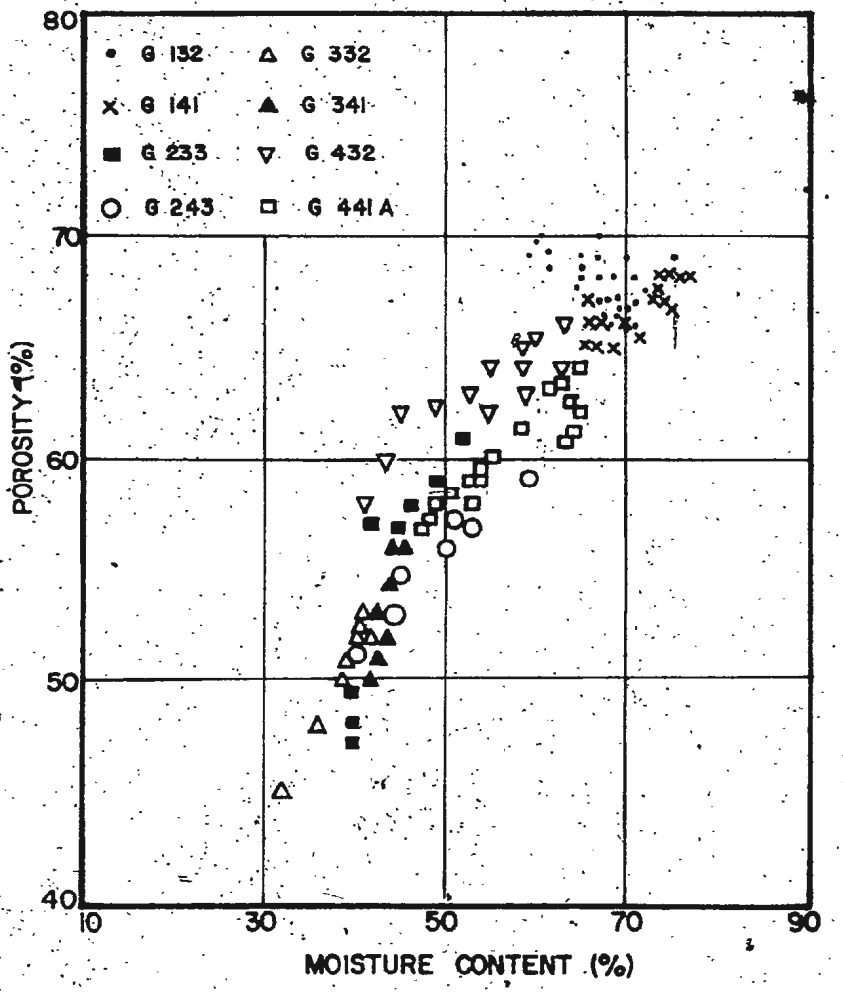

Fig. 39b. Variation of Porosity with Moisture Content.

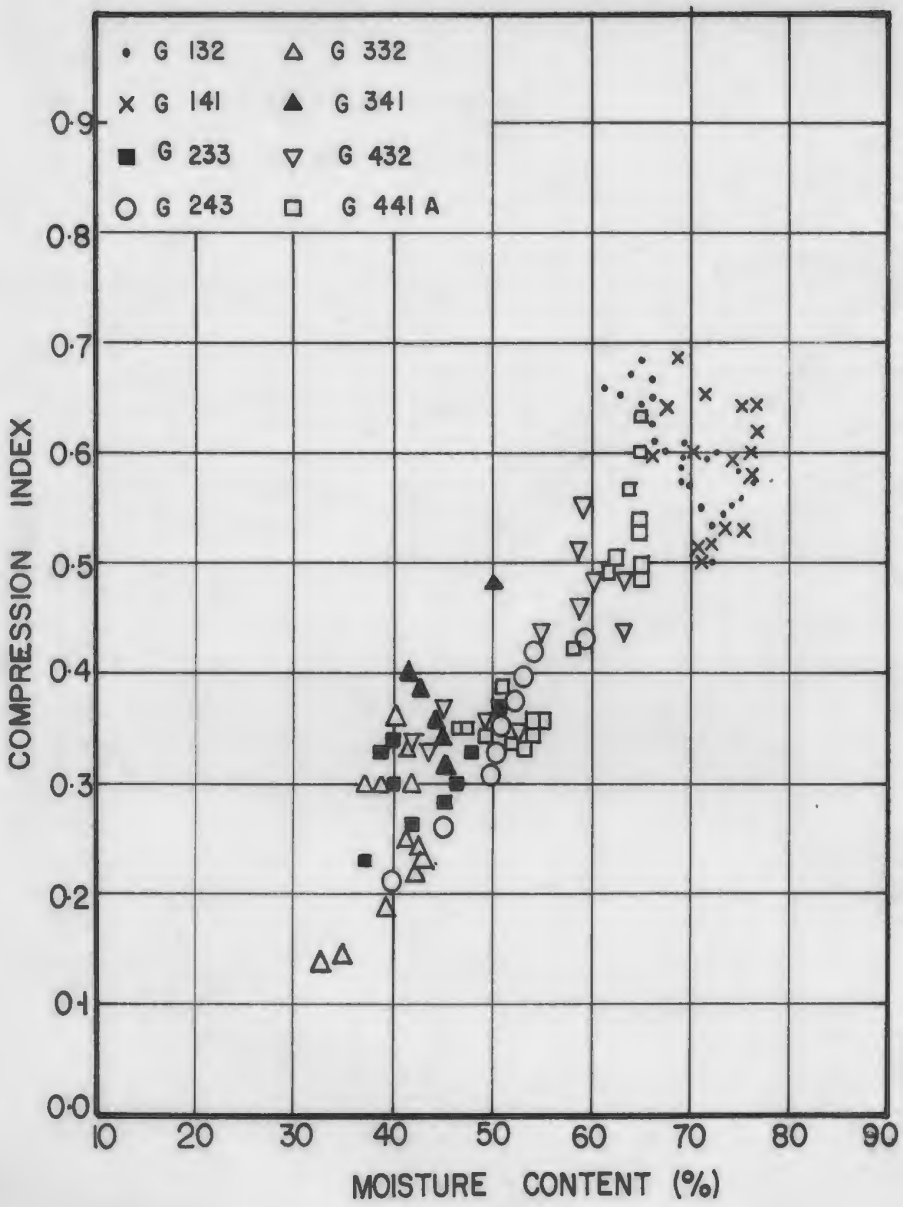

Fig. 40a. Variation of Compression Index with Moisture Content

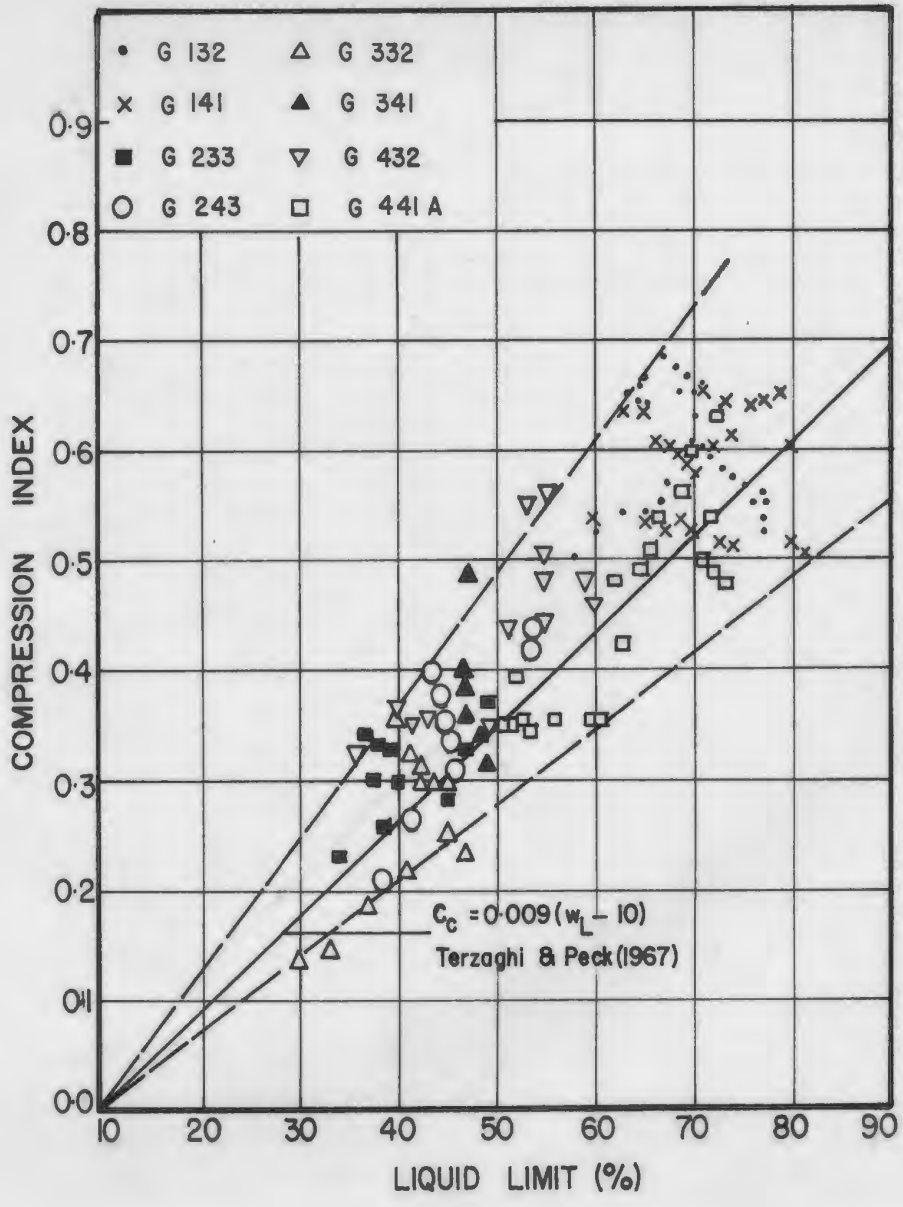

Fig. 40b. Variation of Compression Index with Liquid Limit

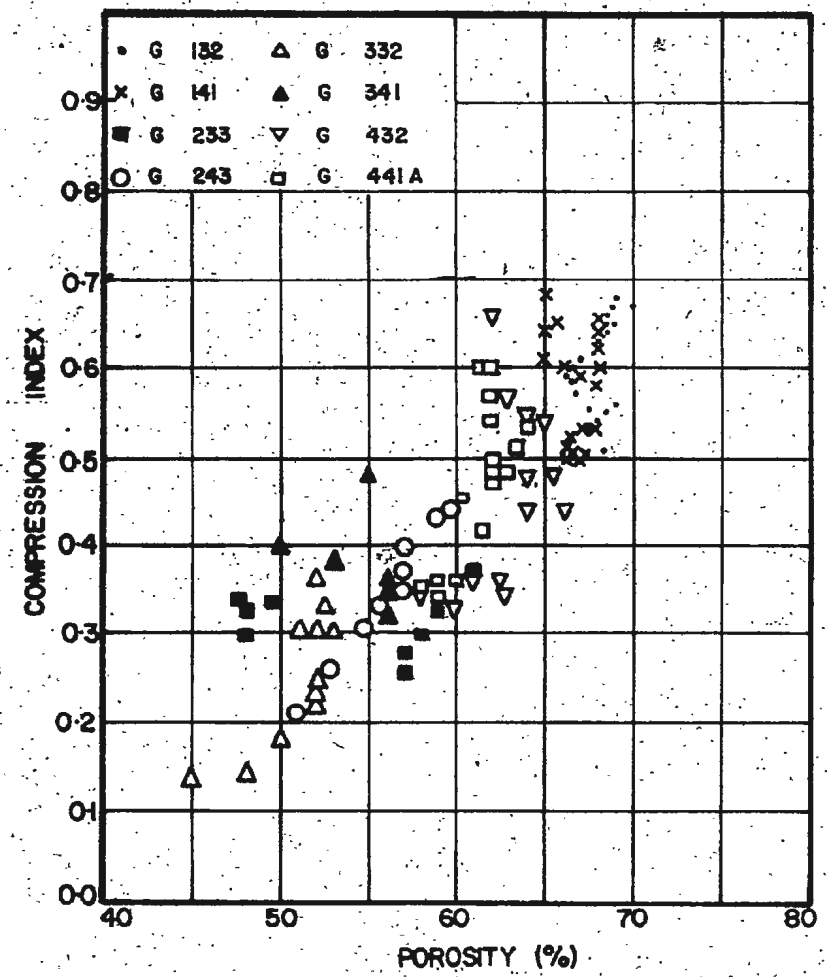

Fig. 41a. Variation of Compression Index with Porosity

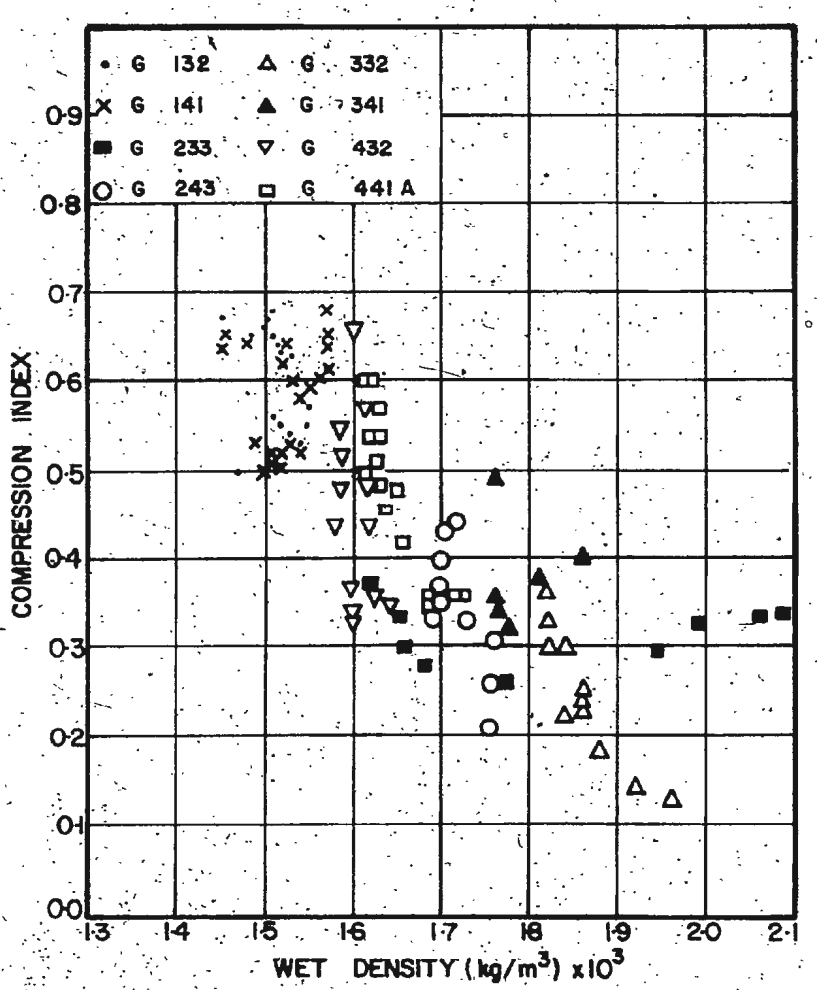

Fig. 41b. Variation of Compression Index with Wet Density

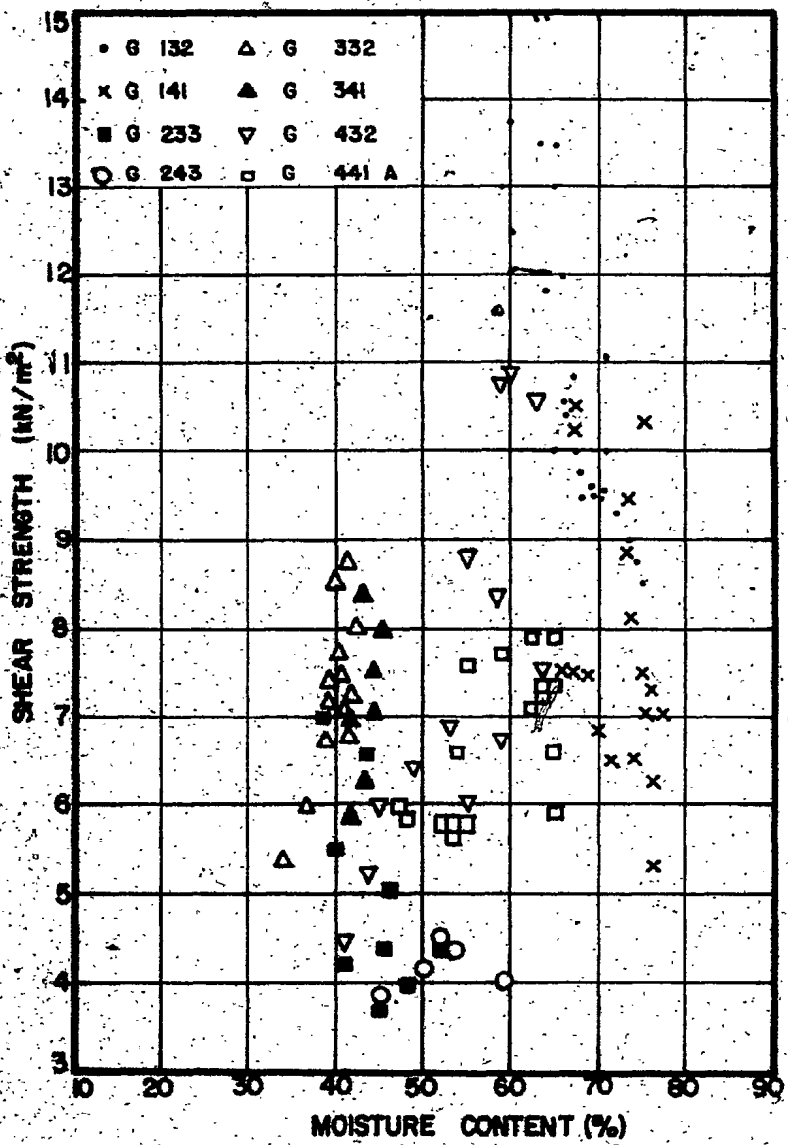

Fig. 42a. Variation of Shear Strength with Moisture Content

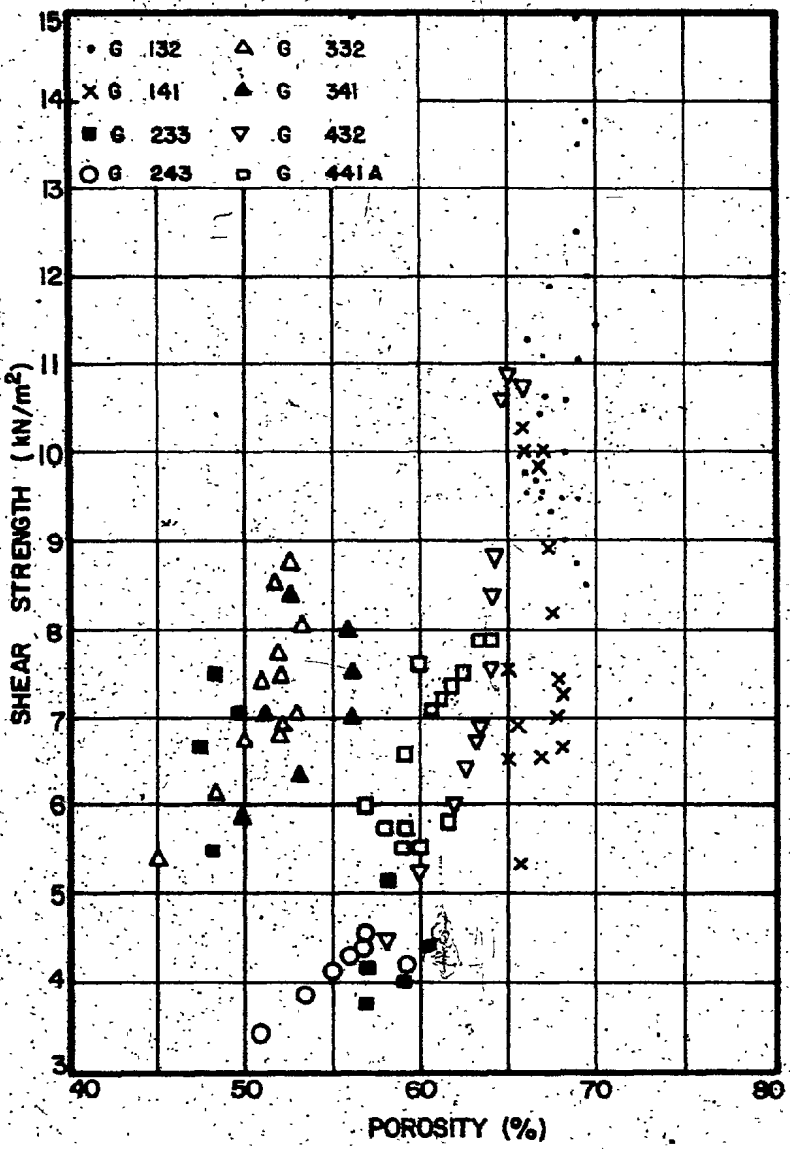

Fig. 42b. Variation of Shear Strength with Porosity

5.3.1. Relationships between Sound Velocity and Index Properties

a. Porosity

The relationship between sound velocity and porosity has received considerable attention in the past. It is generally accepted that sound velocity increases as porosity decreases. However, most authors (Sutton et al. 1957 and Hamilton 1965) indicated that porosity in itself is only a first approximation of several inter-related physical properties. When combined, these properties affect the transmission of sound through a sediment. This relation is illustrated in Fig. 43a where the regression analysis gives a negative correlation of - 0.786. The decrease of sound velocity with increase in porosity is clearly apparent. Data points fall along a gently arcuate trend. The closely clustered points at the low velocity end of the trend represent samples of submarine mud and clay that are products of slow settling of fine particles from suspension. A similar relationship was reported by Buchan et al. 1972 with a negative correlation of - 0.787.

The maximum sound velocity (1.709 km/s) was recorded in a layer of silt with a porosity of 42%. The lowest sound velocities (1.515 - 1.530 km/s) occur in a layer with relatively high percentage of clay with porosities ranging from 66% to 69%.

b. Moisture Content

The relationship between sound velocity and moisture content is illustrated in Fig. 43b. The regression analysis gives a negative correlation coefficient of - 0.745. Buchan et al. 1972 have reported a negative correlation coefficient of - 0.566. Examining Fig. 43b, it is noted that the trend of moisture content variation is nearly parallel

to the trend of porosity variation with sound velocity. This can be explained by the fact that both the moisture content and void ratio of water-saturated sediments are, in the main, functions of available pore space. Sediments containing from 33 to 77% moisture show a progressive decrease in sound velocity with increase in moisture content.

c. Atterberg Limits

Reasonable correlations were obtained between sound velocity and liquid limit, plastic limit and plasticity index. The regression analyses show an increase in sound velocity with a decrease in liquid limit, plastic limit and plasticity index with respective correlation coefficients of - 0.684, - 0.616 and - 0.567. While, no significant correlation was obtained between sound velocity and liquidity index. Figs.44a,b show the relations between sound velocity and liquid and plastic limits.

d. Density

There is an increase in sound velocity with an increase in wet density (Fig. 45a). This relationship is already well documented in the literature. High correlation was obtained between these two parameters with a positive correlation coefficient of 0.794.

5.3.2. Variation of Sound Velocity with Textural Properties of Sediments

The most important factor in the variability of the acoustic data is that of particle size. But in this study, the sound velocity did not correlate significantly with any of the particle size parameters, i.e. % clay, % silt, % sand, median diameter, mean diameter, graphic mean and phi deviation. An attempt was also made using the non - linear regression analysis, and again no meaningful correlation was observed between sound

velocity and % clay, % silt and % sand. However, high correlation was obtained between sound velocity and the logarithm of median diameter yielding a correlation coefficient of 0.72 (Fig. 46). A similar relationship was reported by Sutton et al. (1957) and Hamilton (1963). The relationship obtained between sound velocity and median diameter using the non-linear regression analysis is as follows:

$$M_{d\phi} = (2.95 \times 10^{-12}) (758575)^{v_s} \quad \ldots\ldots\ldots \quad (16)$$

or $$\log M_{d\phi} = - 11.53 + 5.88\, v_s \quad \ldots\ldots\ldots \quad (16')$$

5.3.3. Variation of Sound Velocity with Engineering Properties

a. Shear Strength

Of all the mass physical properties investigated in this study, it is felt that the vane shear measurements were considered the most significant measurements which will offer the greatest potential for establishing correlations between the mass physical properties and acoustic properties.

Analysis of the vane shear profiles yielded an unexpected pattern for most of the cores. The values of the shear strength did not progressively increase towards bottom of the core. Instead, the maximum shear strength was measured at an intermediate depth in all cores with the exception of cores G 141 and 233 (Figs. 3b to 10b). It is felt that, the occurance of the highest value of shear strength at the intermediate depth is quite possibly the result of disturbance of the sediment during the coring process.

The relationship between sound velocity and shear strength is not a simple one. Attempts to relate compressional wave velocity in some

manner with the elastic moduli, and hence to the strength of the sediment, have not met with unqualified success. Most previous attempts used empirical modifications to the Wood (1940) equation for velocity to bring this up to the measured value of the velocity, and then ascribe the modifications to the presence of rigidity in the sample. This however, is only partly true, for some of the difference between the two velocities is undoubtedly due to the presence of a frame compressibility within the sample (Buchan et al. 1972). It is to be expected therefore that vane shear strength does not correlate directly with any acoustic parameter. However, in this study, a low correlation coefficient of - 0.326 was found between sound velocity and the shear strength.

b. Compression Index and Coefficient of Consolidation

The compression index C_c correlates well with sound velocity, it decreases significantly with increasing sound velocity, with a correlation coefficient of - 0.734 (Fig. 45b). In contrast to C_c, the coefficient of consolidation c_v increases with an increase in sound velocity, but a correlation coefficient of only 0.413 was obtained.

5.3.4. Variation of Acoustic Impedance with Geotechnical Properties

The acoustic impedance, Z, is the product of sound velocity and bulk density of the sediment. This important property determines the amount of energy reflected when sound passes from one medium into another.

Similar correlations have been attempted between acoustic impedance and geotechnical properties as were considered for sound velocity. The results of 114 sets of data were analyzed, with the resulting prediction equations and their correlation coefficients presented in Table 9.

TABLE 8. REGRESSION EQUATIONS FOR SOUND VELOCITY

Regression Equations	Correlation Coefficients
$v_s = 1.87 - 0.005\ n$	- 0.786
$v_s = 1.19 + 0.00023\ \rho_s$	0.794
$v_s = 1.706 - 0.0024\ w$	- 0.745
$v_s = 1.682 - 0.002\ w_L$	- 0.684
$v_s = 1.699 - 0.0044\ w_p$	- 0.616
$v_s = 1.628 - 0.0023\ I_p$	- 0.567
$v_s = 1.525 + 0.039\ I_L$	0.278
$v_s = 1.575 - 0.00055\ u_1$	- 0.202
$v_s = 1.561 + 0.00056\ u_2$	0.11
$v_s = 1.537 + 0.00039\ u_3$	0.15
$v_s = 1.615 - 0.007\ S_u$	- 0.326
$v_s = 1.66 - 0.217\ C_c$	- 0.734
$v_s = 1.534 + 0.0028\ c_v$	0.412
$\log M_{d\phi} = - 11.53 + 5.88\ v_s$	0.72

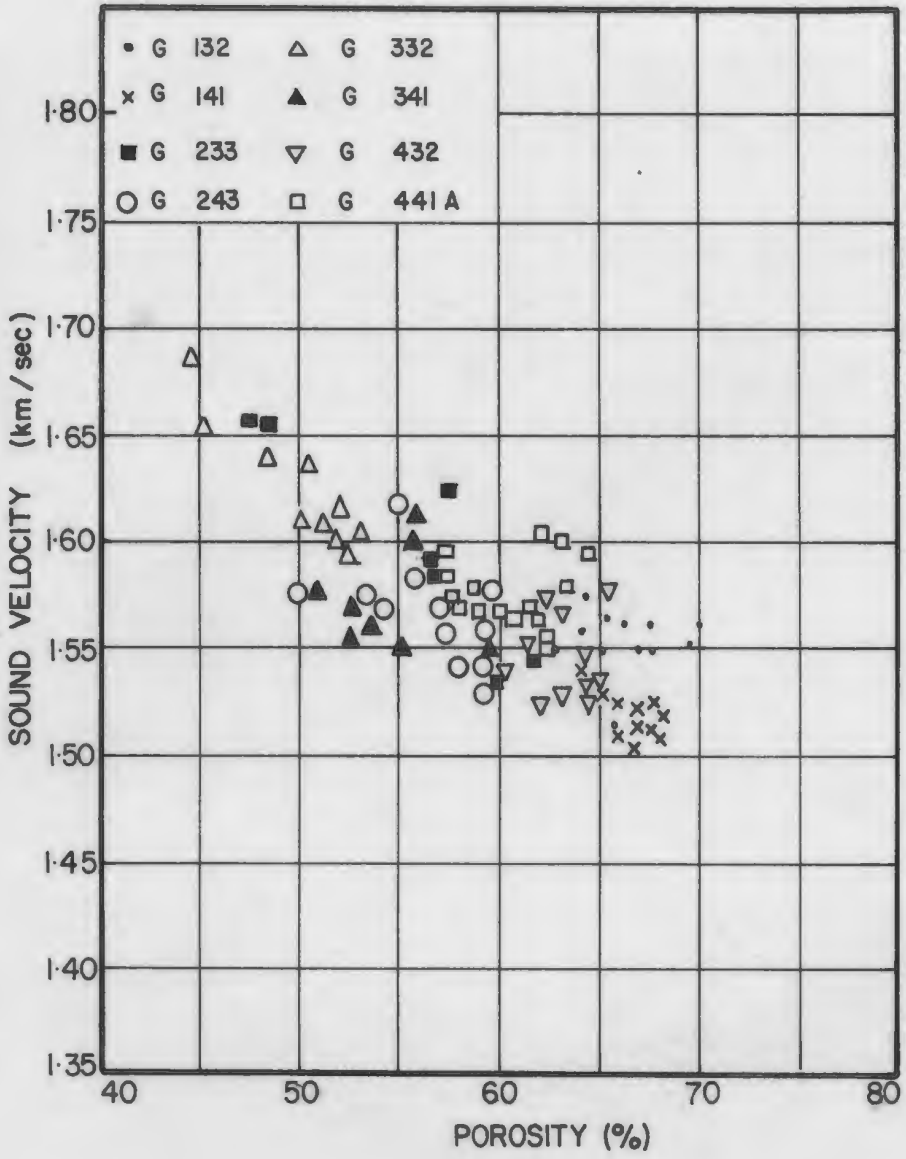

Fig. 43a. Variation of Sound Velocity with Porosity

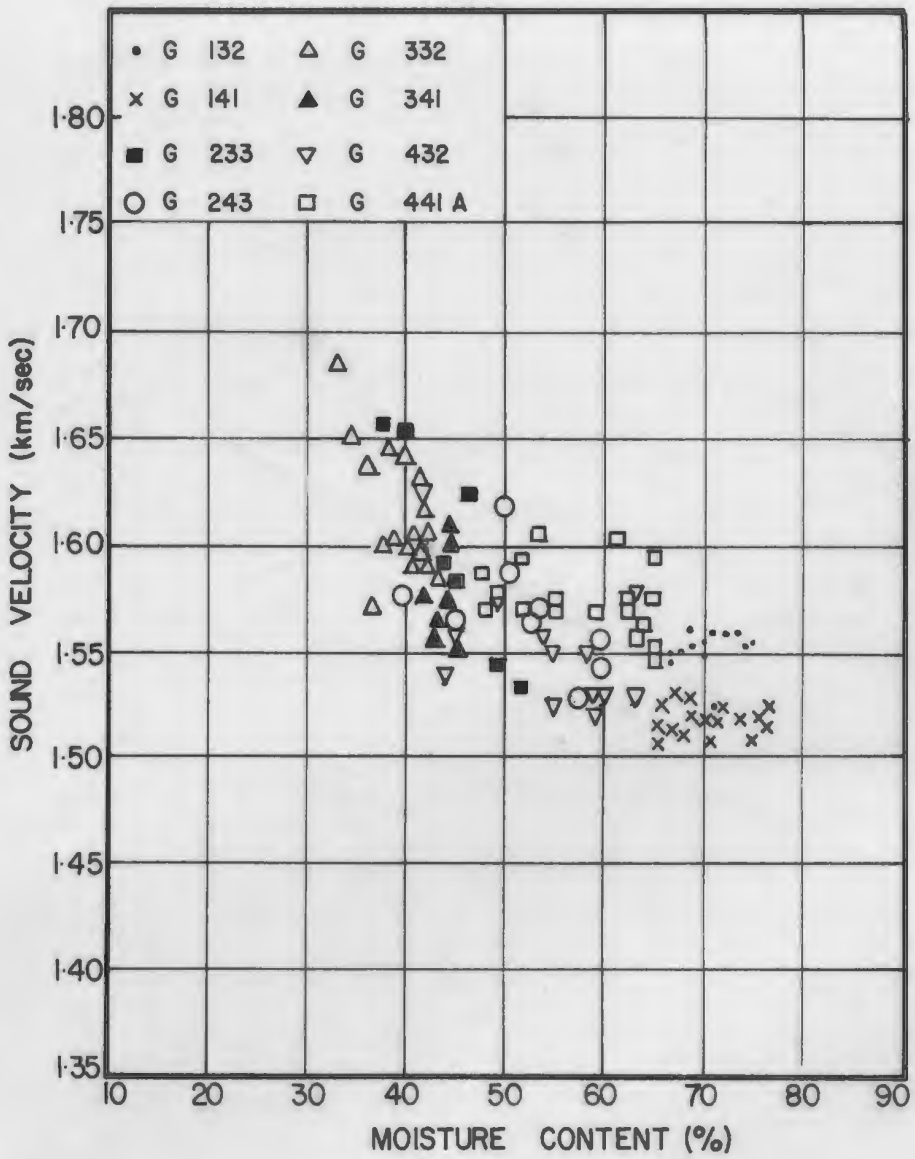

Fig. 43b. Variation of Sound Velocity with Moisture Content

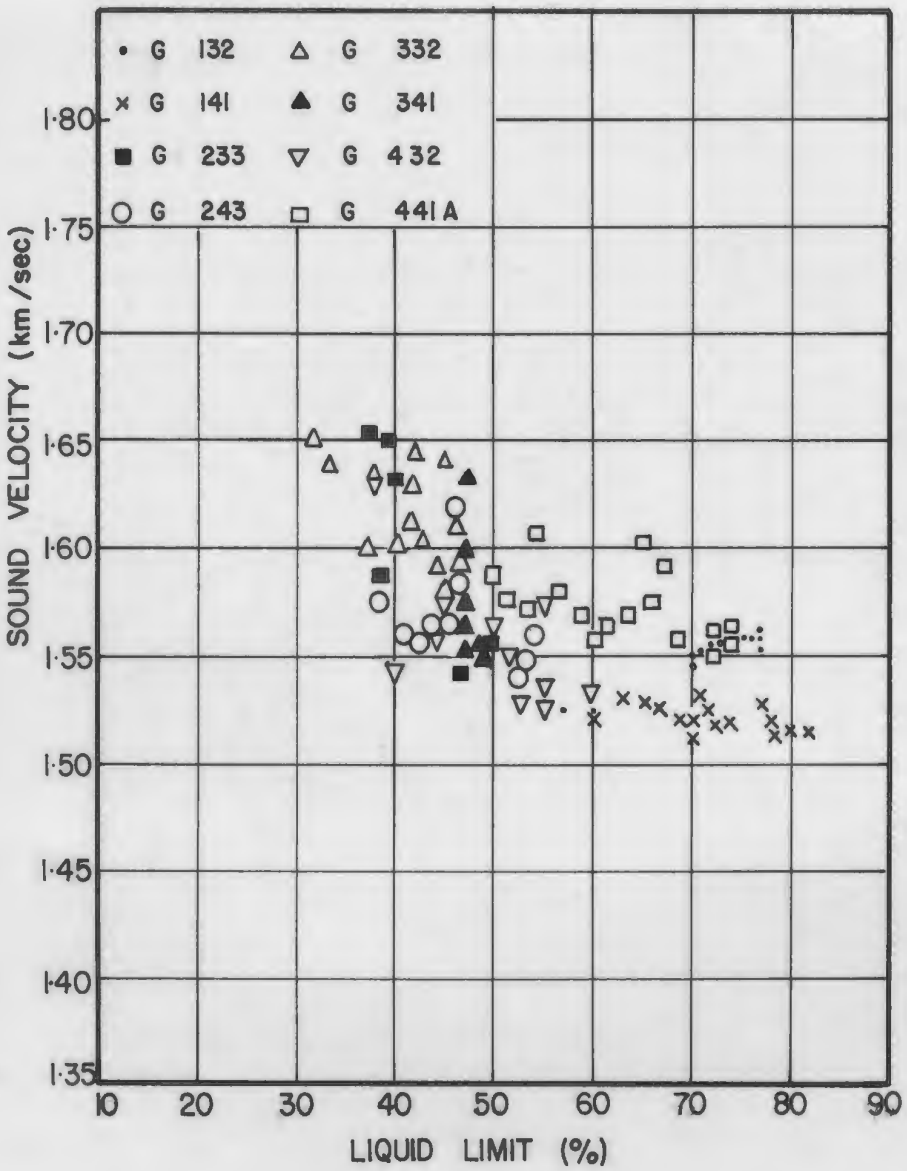

Fig. 44a. Variation of Sound Velocity with Liquid Limit

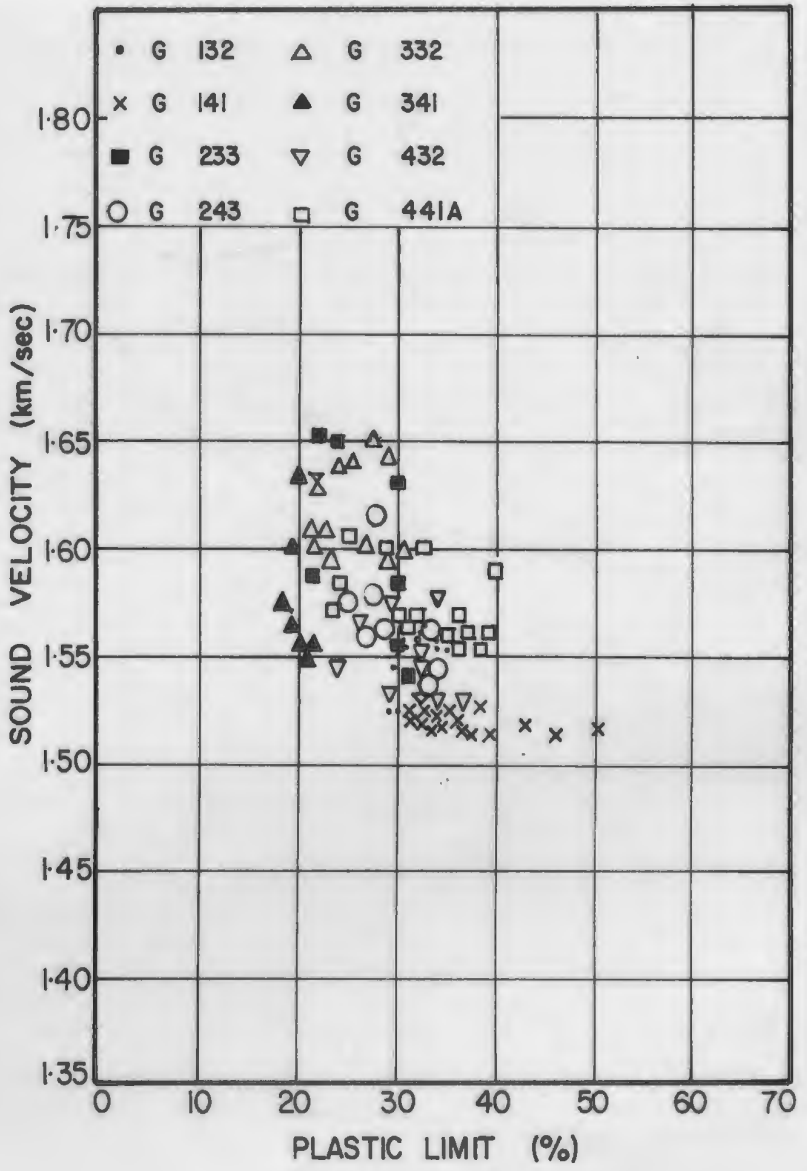

Fig. 44b. Variation of Sound Velocity with Plastic Limit

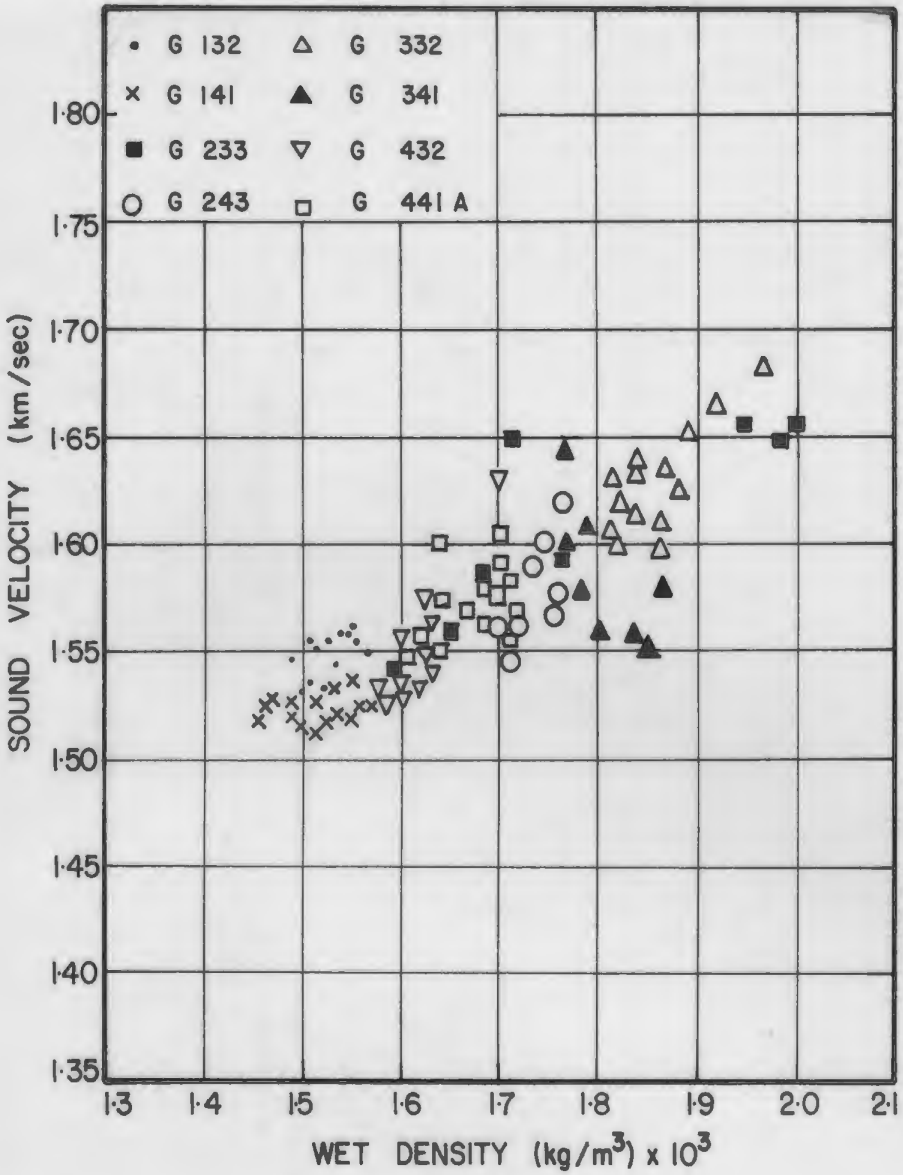

Fig. 45a. Variation of Sound Velocity with Wet Density

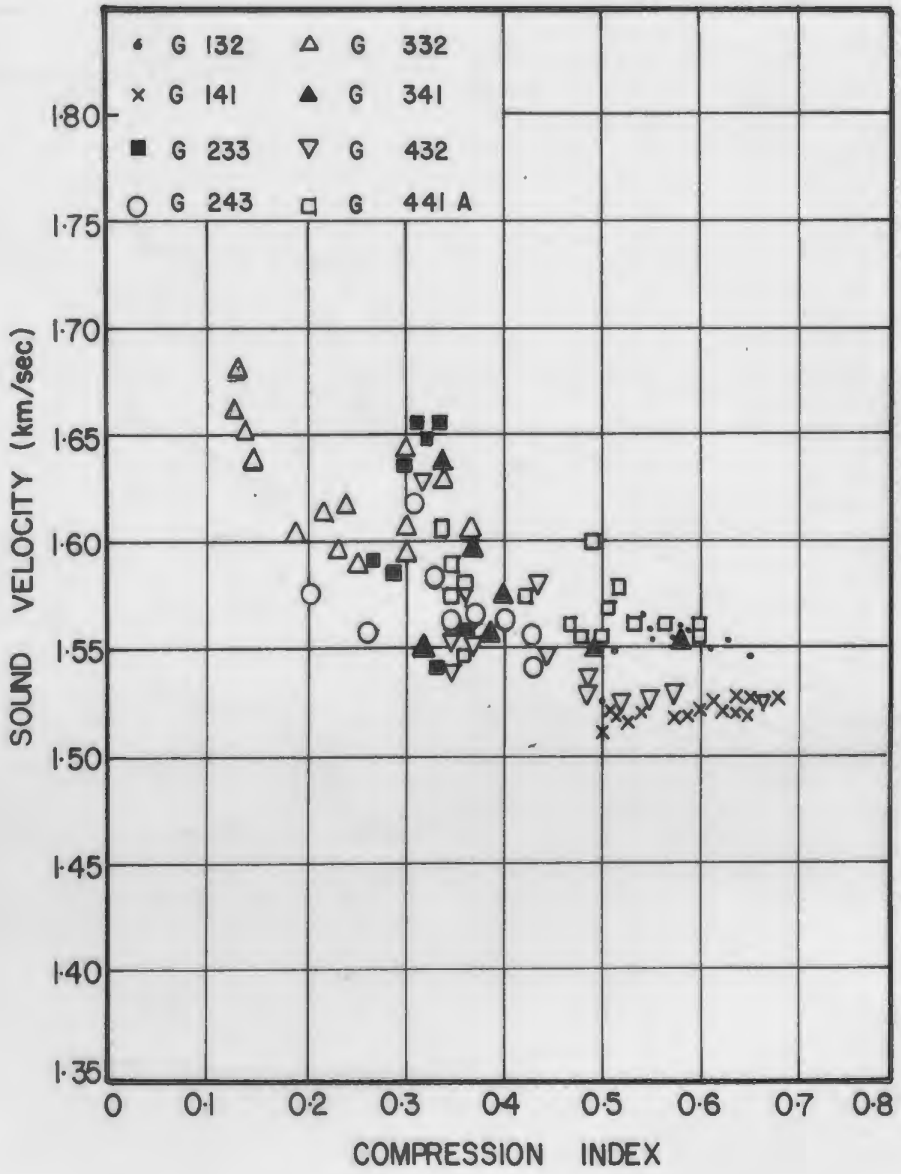

Fig. 45b. Variation of Sound Velocity with Compression Index

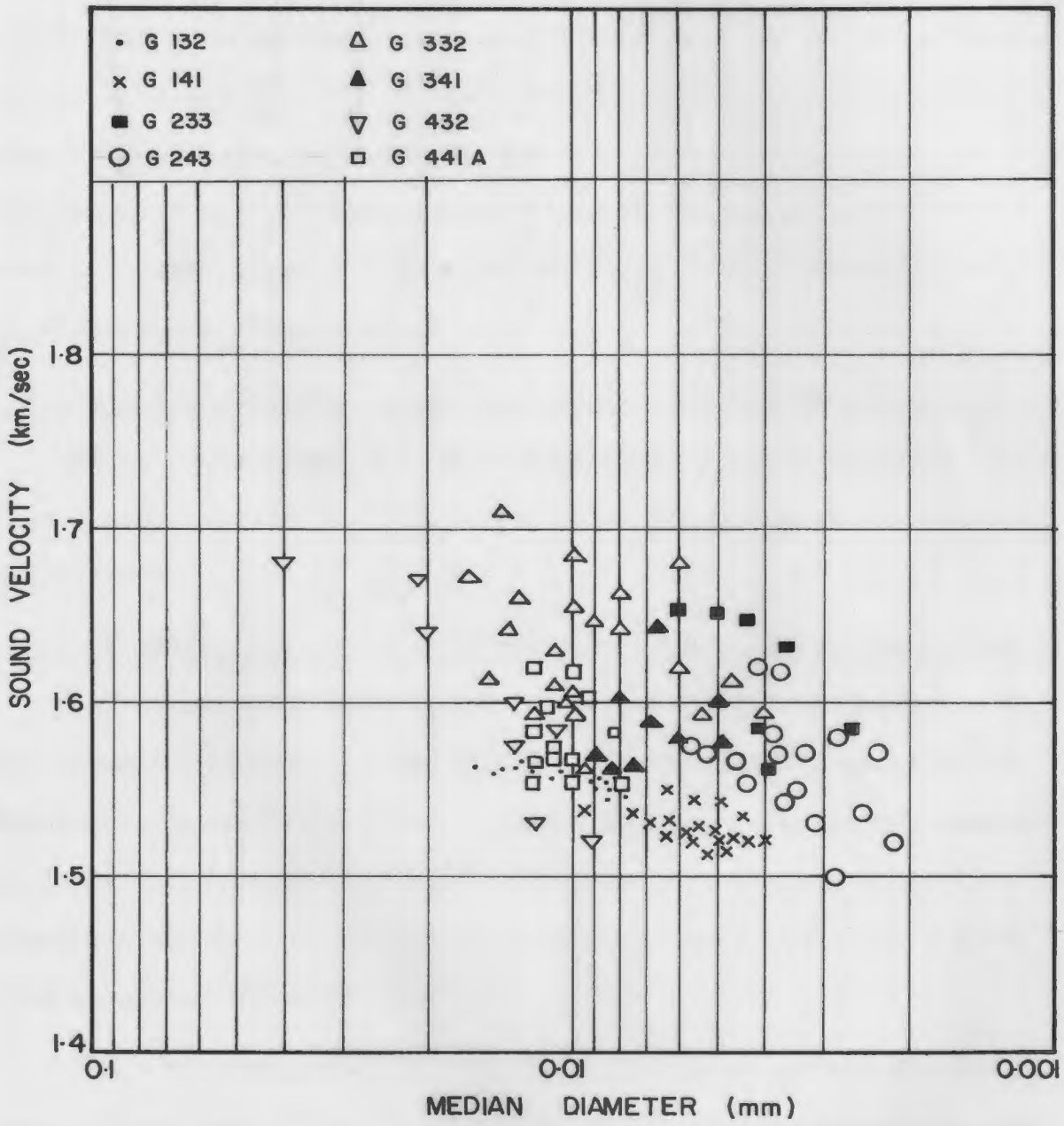

Fig. 46. Variation of Sound Velocity with Logarithm of Median Diameter

a. Relationships between Acoustic Impedance and Index Properties

A decrease in acoustic impedance occurs with an increase in porosity, a decrease in wet density, an increase in moisture content, an increase in liquid limit and an increase in plastic limit. Examining Table 9, it is obvious that a very good correlation exists between acoustic impedance and wet density. Because of the relationships between wet density, porosity and moisture content, very good correlation is observed also between acoustic impedance and the latter two parameters. High correlation coefficients of 0.979, 0.954 and 0.85 have been obtained for these variables.

b. Relationships between Acoustic Impedance and Textural Properties

No correlations were observed between acoustic impedance and the textural properties of the sediments either using linear or non - linear analyses.

c. Relationships between Acoustic Impedance and Engineering Properties

Low correlation was obtained between acoustic impedance and shear strength yielding a negative correlation coefficient of 0.43. A reduction in acoustic impedance occurs with an increase in compression index and a decrease in the coefficient of consolidation. The regression analysis gives correlation coefficients of 0.78 and 0.405 for these variables respectively.

Figs. 47, 48 and 49 present graphical plots of the data showing the relationships between acoustic impedance and various geotechnical properties. Examining Tables 8 and 9, it is obvious that the correlation coefficients obtained for acoustic impedance are generally 15 to 20% higher than between sound velocity and the same geotechnical

TABLE 9. REGRESSION EQUATIONS FOR ACOUSTIC IMPEDANCE

Regression Equations	Correlation Coefficients
$Z = 5.207 - 0.042\ n$	- 0.954
$Z = -0.582 + 0.00195\ \rho_s$	0.979
$Z = 3.75 - 0.019\ w$	- 0.85
$Z = 3.565 - 0.016\ w_L$	- 0.786
$Z = 3.67 - 0.034\ w_p$	- 0.685
$Z = 3.152 - 0.019\ I_p$	- 0.669
$Z = 2.372 + 0.258\ I_L$	0.263
$Z = 3.09 - 0.062\ S_u$	- 0.43
$Z = 3.37 - 1.61\ C_c$	- 0.78
$Z = 2.42 + 0.02\ c_v$	0.405
Z & u_1, u_2, u_3	no correlation

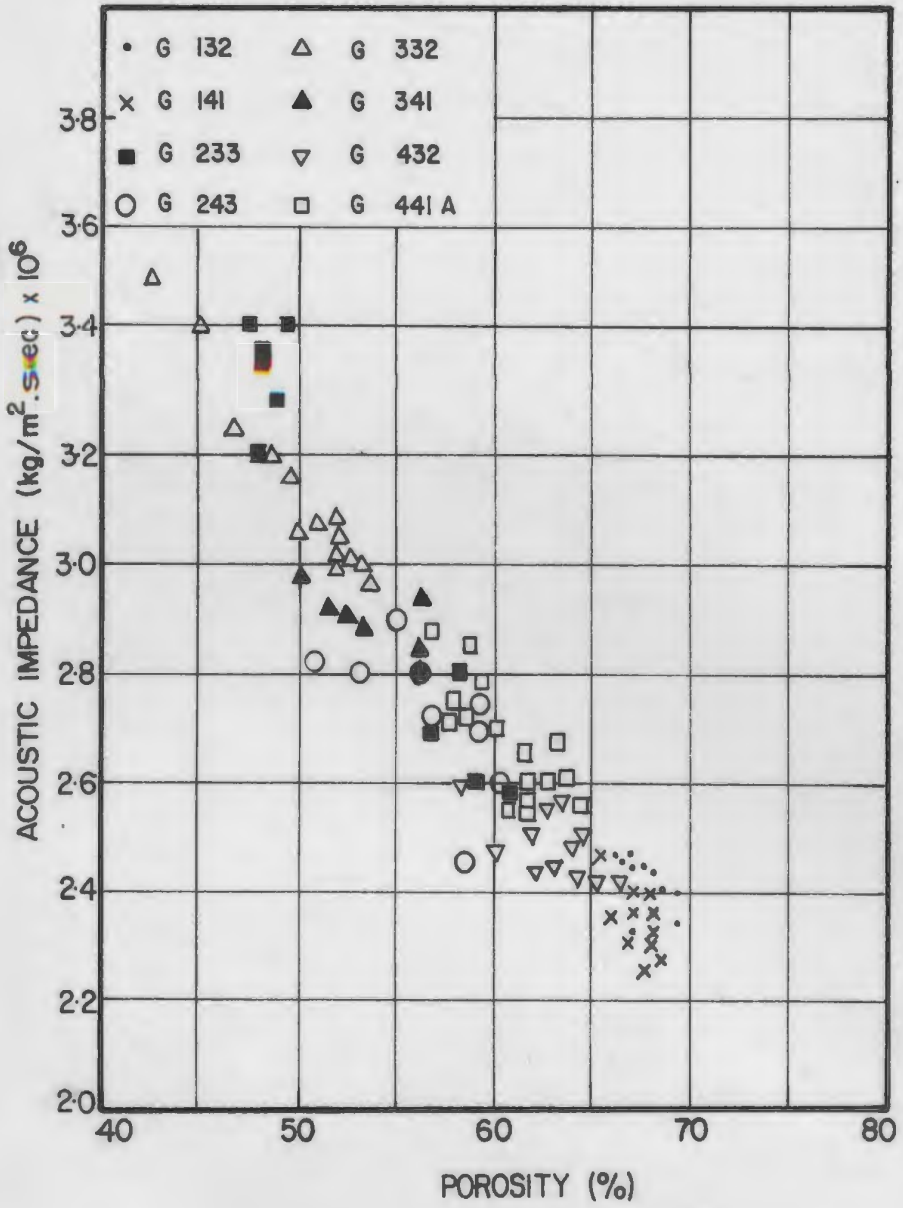

Fig. 47a. Variation of Acoustic Impedance with Porosity

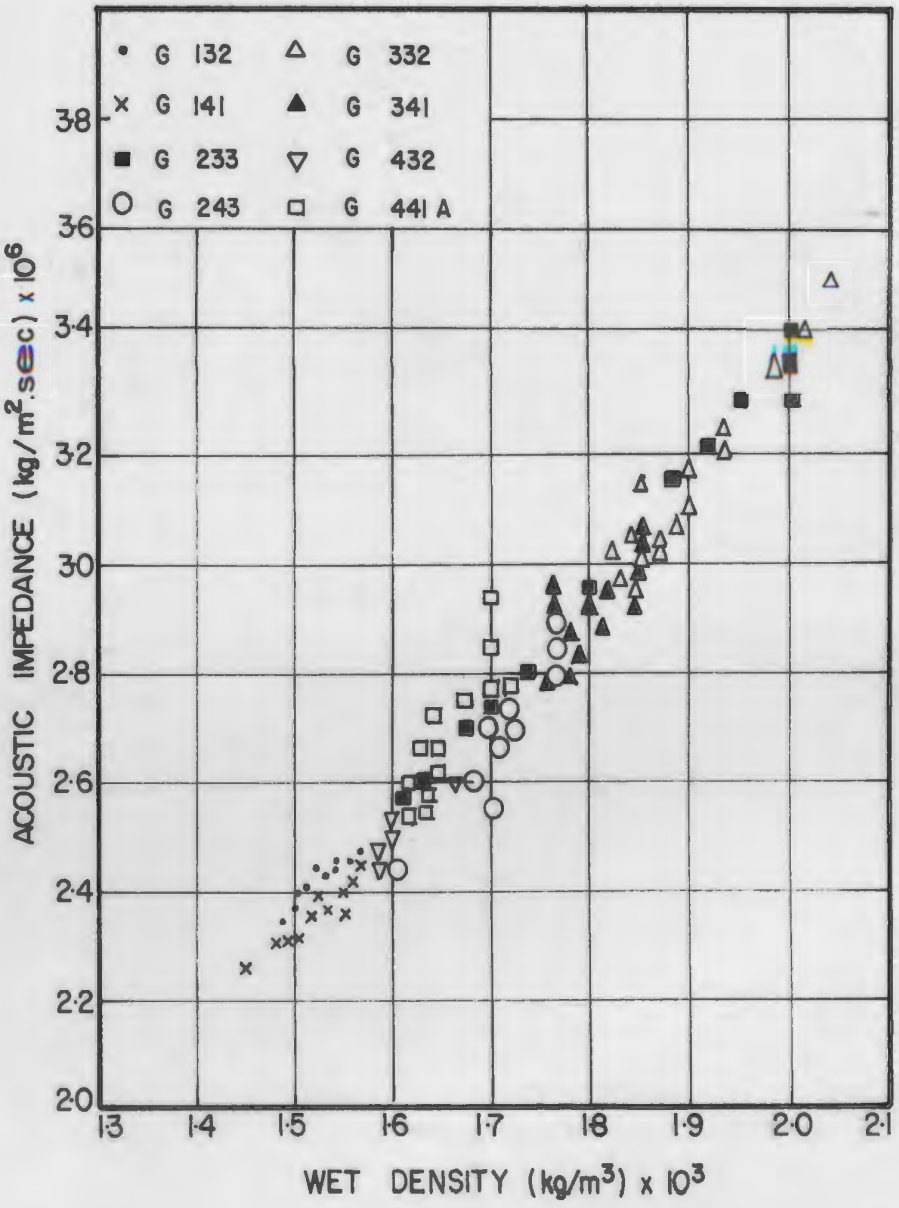

Fig. 47b. Variation of Acoustic Impedance with Wet Density

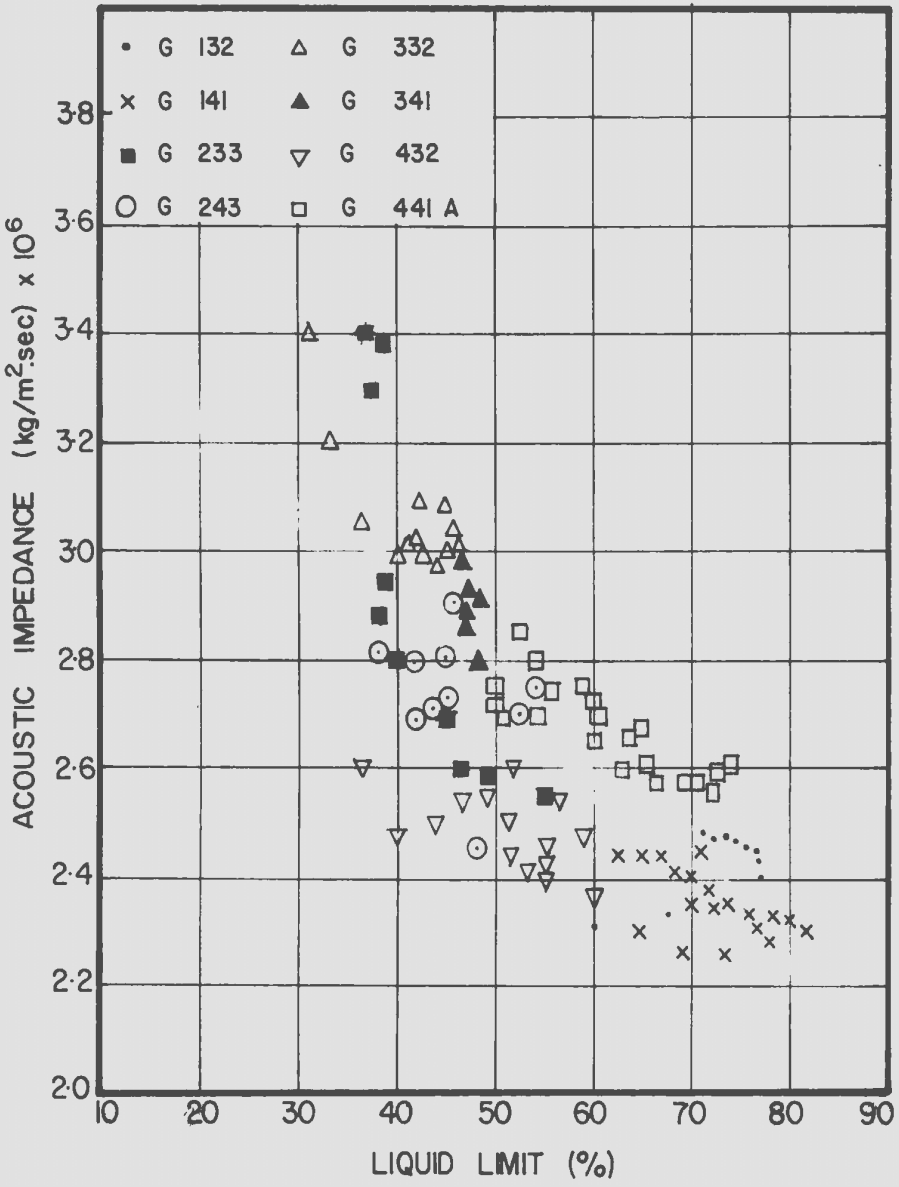

Fig. 48a. Variation of Acoustic Impedance with Liquid Limit

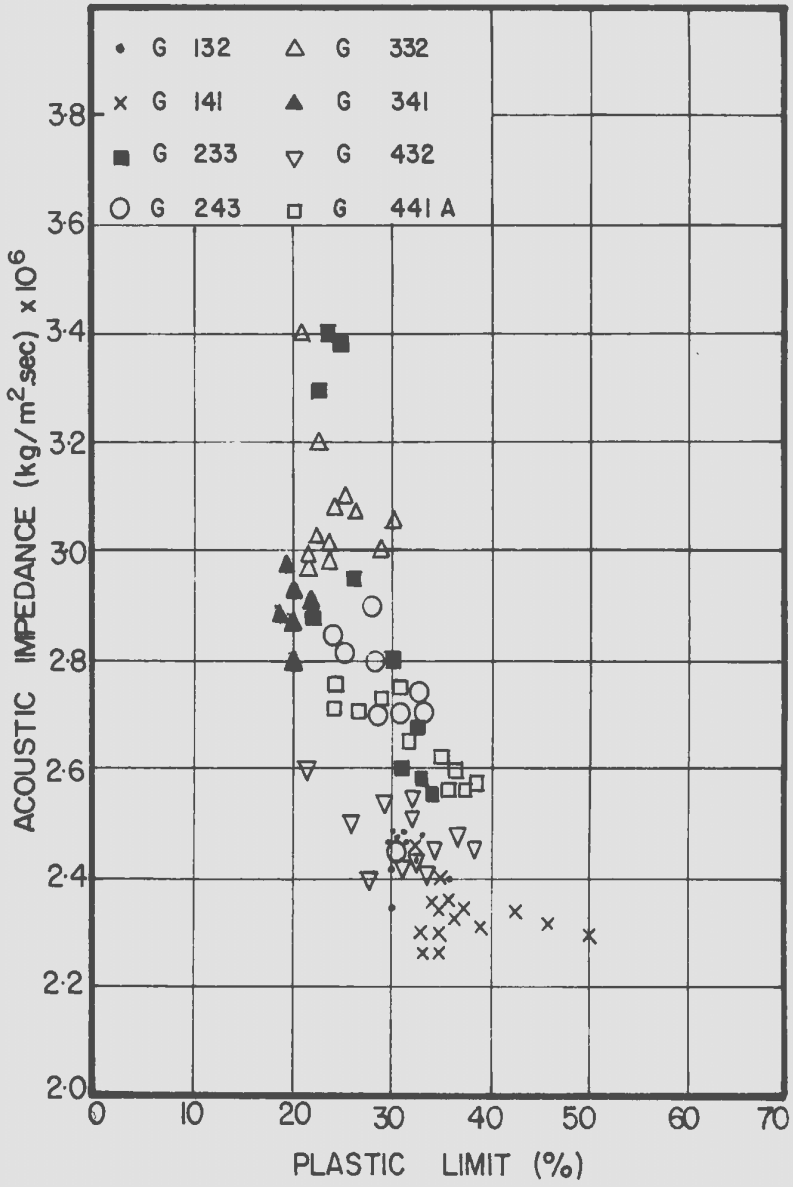

Fig. 48b. Variation of Acoustic Impedance with Plastic Limit

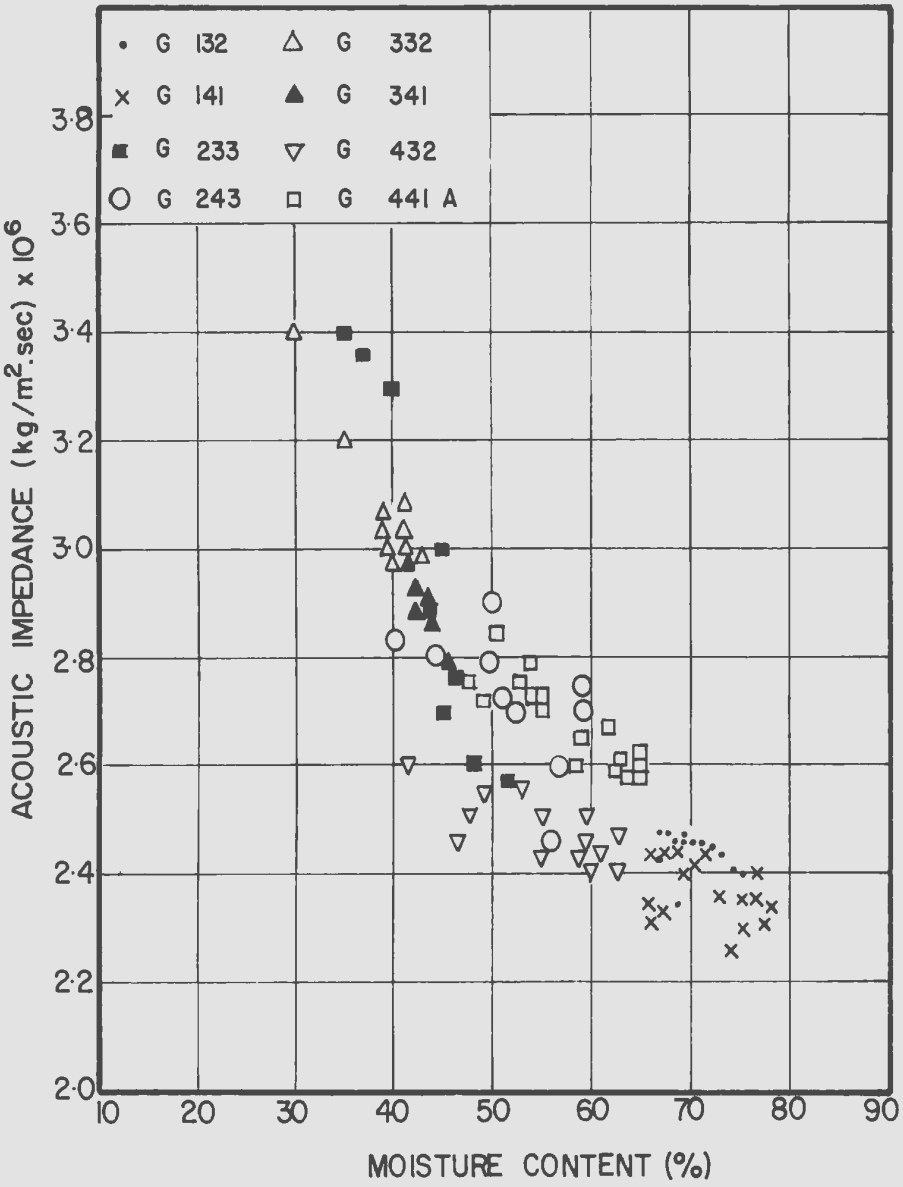

Fig. 49a. Variation of Acoustic Impedance with Moisture Content

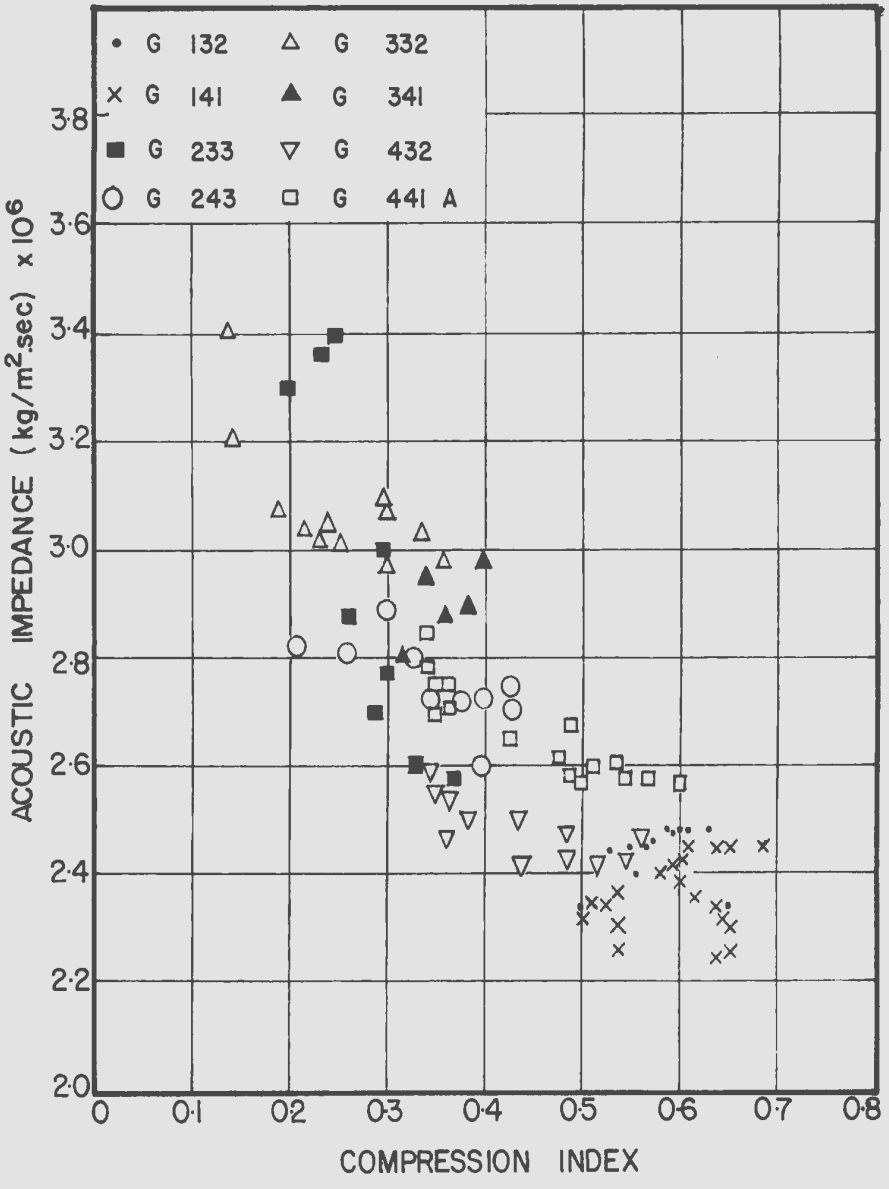

Fig. 49b. Variation of Acoustic Impedance with Compression Index

properties. The improved correlation is due primarily to the fact that acoustic impedance is a function of sound velocity and bulk density. Buchan et al. 1972 have reported similar relationships for shelf sediments to those reported herein, with reasonably good agreement noted in the majority of cases.

5.4. Correlation between Impact Penetrometer Output and Acoustic and Geotechnical Properties

One of the main objectives of this investigation is to assess the suitability of the M.U.N. impact penetrometer as a ground truthing tool for evaluating the properties of near surface marine sediments. The main parameters measured by the impact penetrometer are outlined in Chapter IV together with the related instrumentation.

In this study, the output data from the penetrometer obtained under typical field conditions are compared directly with the established geotechnical and acoustic properties of the sediment cores. Such comparisons are considered valid since at each test location the horizontal distance between the piston core and related penetrometer drop is believed to be 100 m or less. The reported results relate the degree of correlation applicable to all the cores. However, the graphical plots of the data presented indicate that for some cores considered individually a somewhat higher correlation may apply.

A linear regression analysis has been applied to 55 sets of data representing output from six penetrometer drops and geotechnical / acoustic data at 0.25 m intervals of depth.

Relatively good correlation was obtained between acoustic impedance and penetrometer sleeve friction. The sleeve friction

increases with an increase in acoustic impedance with a resulting correlation coefficient of 0.73. For sound velocity, the same trend is noted but with a lower correlation coefficient of 0.535 (Fig. 50a,b). No correlation was obtained between sound velocity and cone tip resistance, while very low correlation was obtained between acoustic impedance and cone tip resistance.

To establish the viability of the impact penetrometer as a geotechnical instrument in the ocean environment, relationships with conventional geotechnical test results must be established. Previous investigators have studied these relationships under laboratory conditions (Dayal, 1974, Chaudhuri, 1979). In this section the cone tip resistance and sleeve friction outputs are compared directly with the measured geotechnical properties of the cores.

The most important factor influencing cone penetration resistance is the shear strength of the sediment. Relatively high correlation was found between the cone tip resistance and shear strength. As expected the cone tip resistance increases with an increase in shear strength with a correlation coefficient of 0.89 (Fig. 51). However, low correlation was obtained between cone tip resistance and both wet density and compression index yielding correlation coefficients of 0.31 and 0.30 respectively. The relationship between sleeve friction and shear strength is illustrated in Fig. 52. The sleeve friction increases with a decrease in shear strength with a correlation coefficient of 0.545. Unexpected correlations in excess of 0.7 were obtained between sleeve friction and moisture content, bulk density and compression index. Table 10 summarizes all the relations obtained.

TABLE 10. REGRESSION EQUATIONS FOR PENETROMETER OUTPUT

Regression Equations	Correlation Coefficients
$Q_d = -72.59 + 53.72\ S_u$	0.89
$Q_d = 867.70 - 332.1\ \rho_s$	- 0.31
$Q_d = 189.30 + 273.85\ C_c$	0.30
Q_d & w , c_v	no correlation
$F_s = 16.3 - 1.023\ S_u$	- 0.545
$F_s = 24.4 - 0.257\ w$	- 0.763
$F_s = -33.48 + 25.76\ \rho_s$	0.773
$F_s = 19.34 - 21.67\ C_c$	- 0.764
$F_s = 5.18 + 0.32\ c_v$	0.49
$v_s = 1.53 + 0.0042 F_s$	0.535
v_s & Q_d	no correlation
$Z = 2.24 + 0.044\ F_s$	0.73
$Z = 2.75 - 0.0004 Q_d$	- 0.202

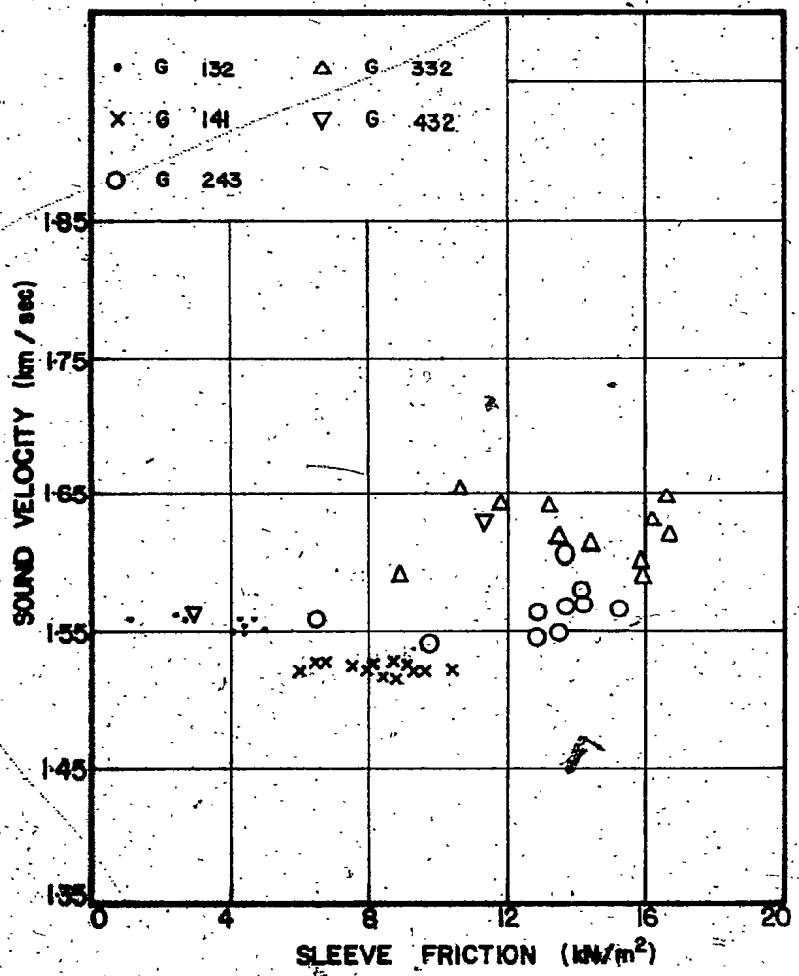

Fig. 50a. Variation of Sound Velocity with Sleeve Friction

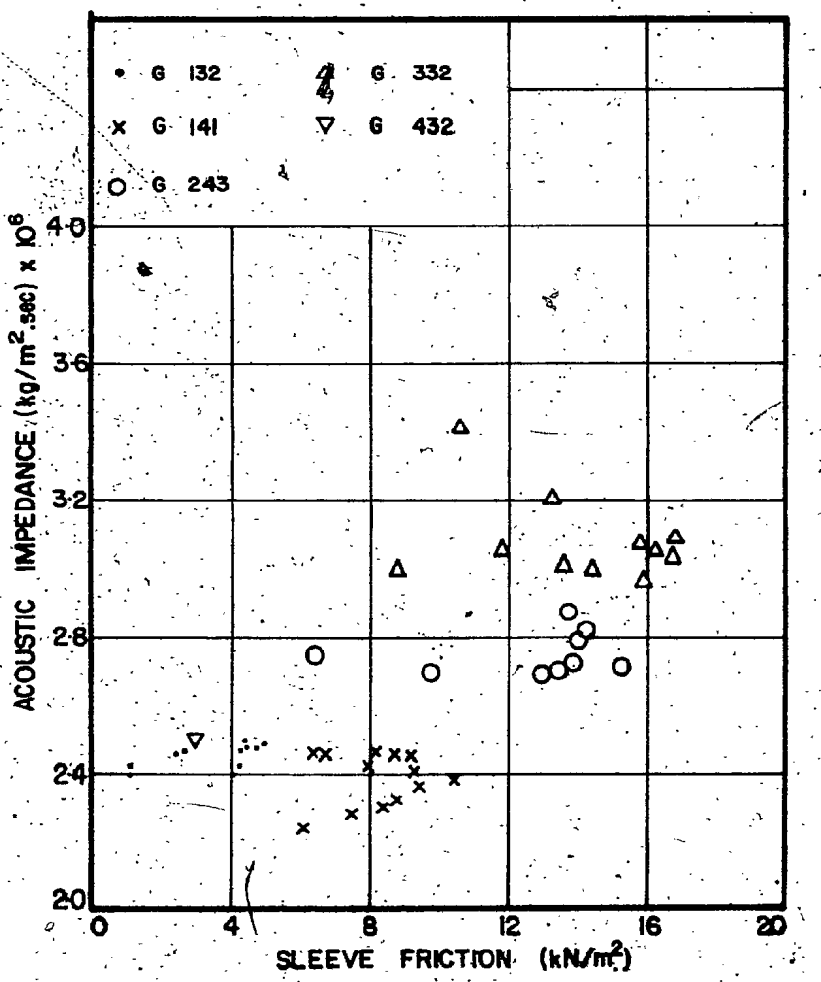

Fig. 50b. Variation of Acoustic Impedance with Sleeve Friction

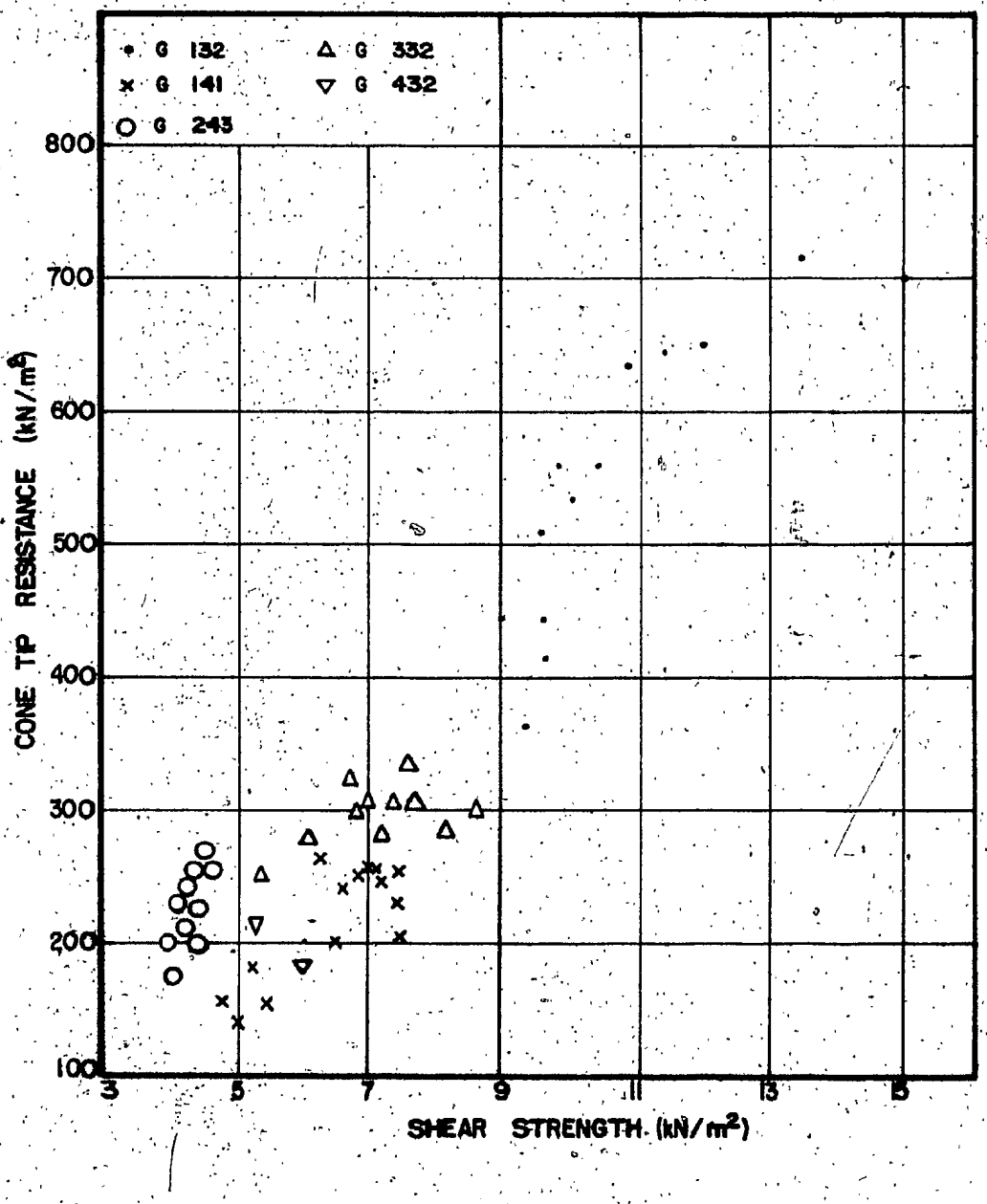

Fig. 51. Variation of Cone Tip Resistance with Shear Strength

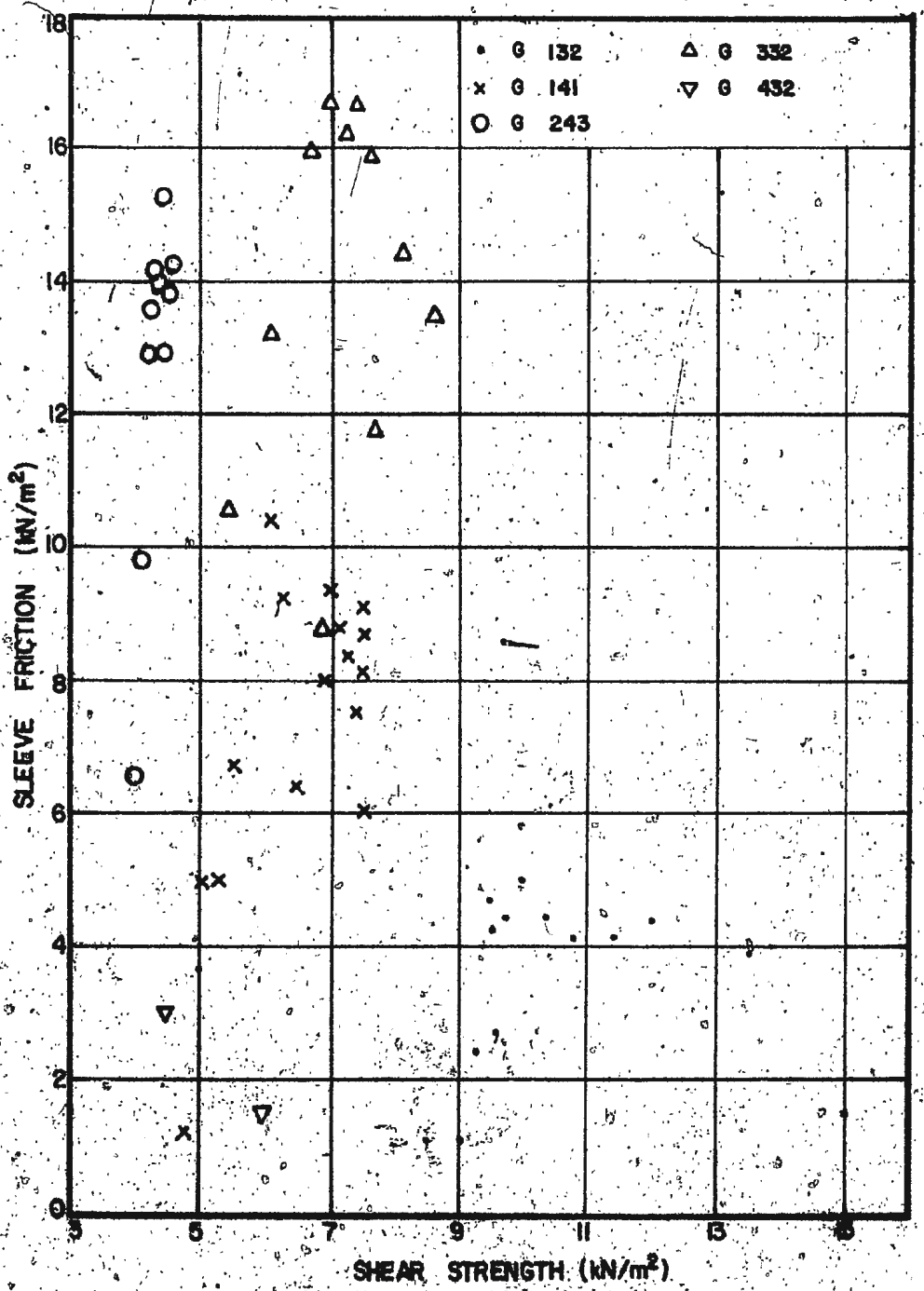

Fig. 52. Variation of Sleeve Friction with Shear Strength

5.5. Strength and Consolidation Characteristics of Investigated Soils

The mechanical behaviour of submarine soils, in particular of cohesive soils, is largely determined by the rate of deposition and by the degree of consolidation; underconsolidated, normally consolidated and overconsolidated states respectively. Identification of the degree of consolidation is commonly made by a) comparing the effective overburden pressure in-situ ,p_o, with the preconsolidated pressure ,p_c, determined from laboratory consolidation tests, and b) by examining the distribution of the undrained shear strength ,S_u, with depth. In normally consolidated soils, the effective overburden pressure ,p_o, is equal to the preconsolidated pressure ,p_c, and the ratio of the undrained shear strength to the effective overburden pressure ,S_u/p_o, has been found to generally fit the following empirical relationship (Skempton 1957) for many terrestrial soils

$$S_u/p_o = 0.11 + 0.0037\, I_P \qquad \ldots\ldots\ldots \quad (17)$$

In underconsolidated soils, p_c is smaller than p_o and S_u/p_o values are also smaller than those for normally consolidated soils. The opposite trends typically occur in the case of overconsolidated soils.

The effect of sample disturbance has a direct influence on the result of consolidation and shear tests, in particular on undrained shear test results. The mechanical disturbance depends on many factors such as the core and technique in sampling and testing operations, the rigidity of core tube relative to stiffness of the soil and the burial depth of sample. As the sample is disturbed, the undrained shear strength tends to decrease and the compression index obtained from consolidation tests also tends to decrease.

Measured shear strength of the Placentia Bay sediments ranged from 3.4 to 15.0 kN/m^2 (Figs. 3b to 10b). Sediments from stations G 132, 141 and 332 have the highest values of shear strength. Examining these figures, the values of the shear strength did not progressively increase towards the bottom of the cores possibly due to sampling disturbance. A comparison of measured ratios of undrained shear strength to the effective overburden pressure (S_u/p_o ratios) with both plasticity index and liquidity index is shown in Fig. 53. Using the regression analysis, no meaningful correlations were obtained between S_u/p_o ratios and both plasticity and liquidity indices.

The results of 73 consolidation tests carried out on the samples were plotted as void ratio (e) versus the logarithm of the pressure (p). It appears from these test results that considerable disturbance has occured in the cores, particularly towards the bottom, as if the lower material had been sucked downward by the upward movement of the corer. The consolidation curves (Figs. 54 and 55) provide additional evidence of disturbance. The flatness of the curves and the lack of definition of the point of maximum curvature, point to either very underconsolidated or disturbed samples.

The interesting feature of the sediments of the Placentia Bay is that the extensive area is underconsolidated. Underconsolidated conditions exist for the samples as the preconsolidation pressure (p_c) is smaller than the actual overburden pressure (p_o) and the S_u/p_o values are also smaller than those calculated from eqn. 17.

The underconsolidation characteristics of these sediments are assumed to be the results of extremely rapid deposition and the delay

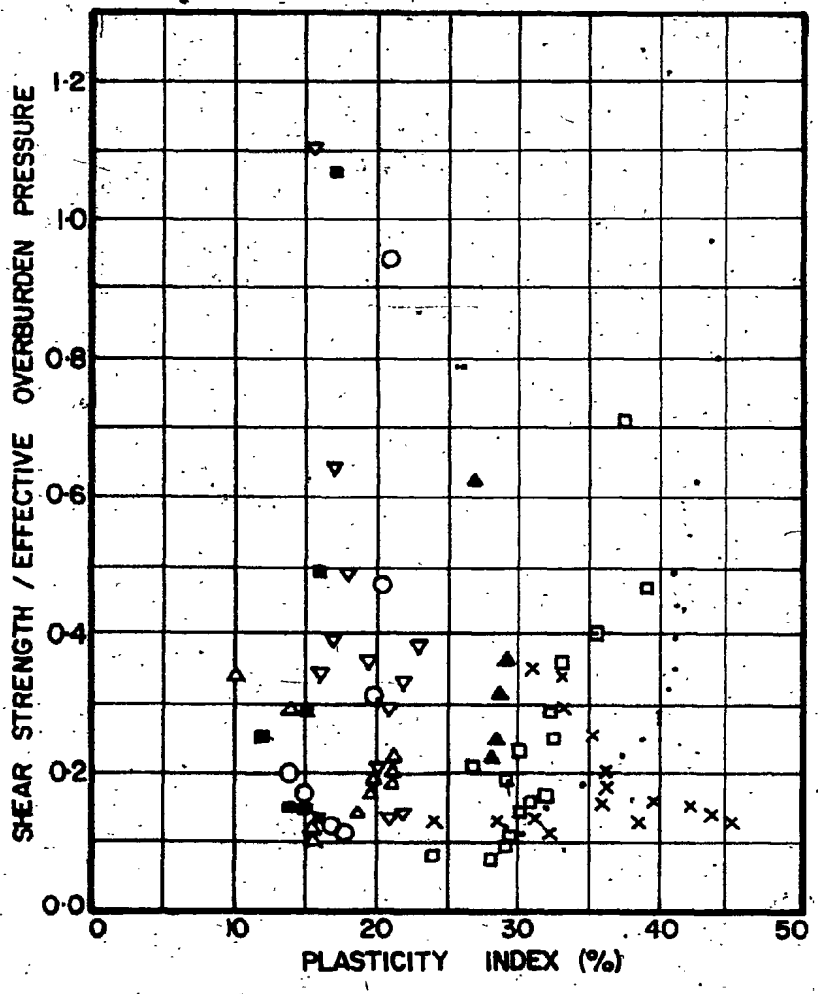

Fig. 53a. Relationship Between Shear Strength/ Effective Overburden Pressure and Plasticity Index

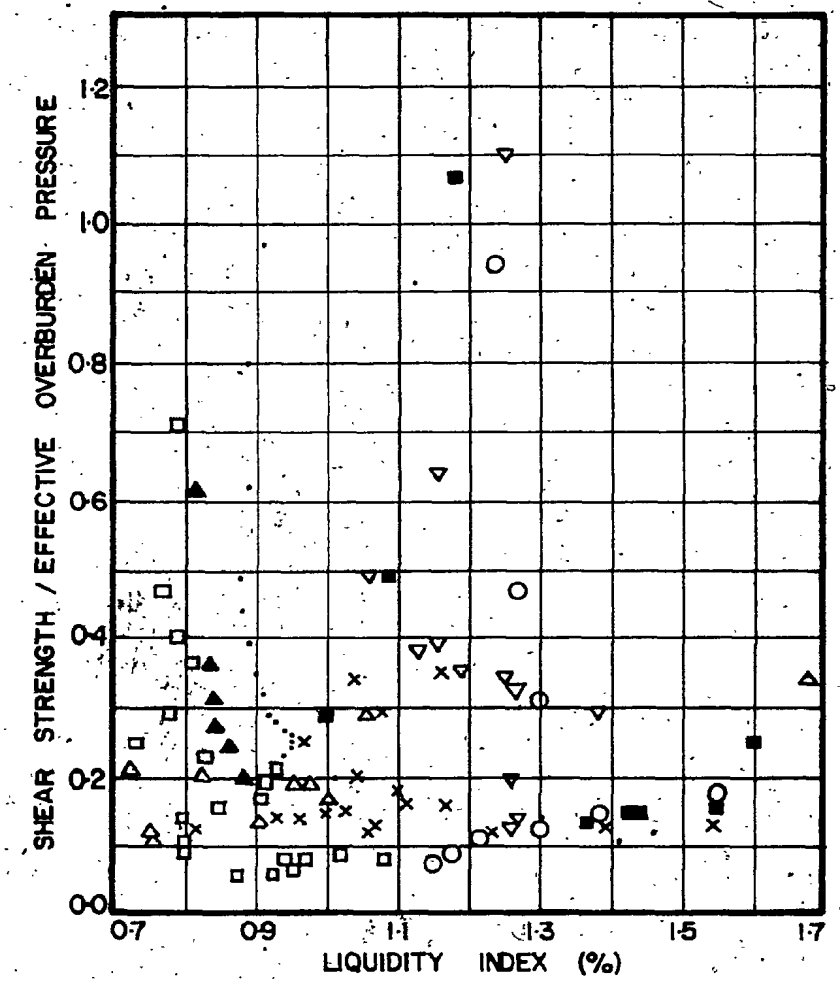

Fig. 53b. Relationship Between Shear Strength/ Effective Overburden Pressure and Liquidity Index

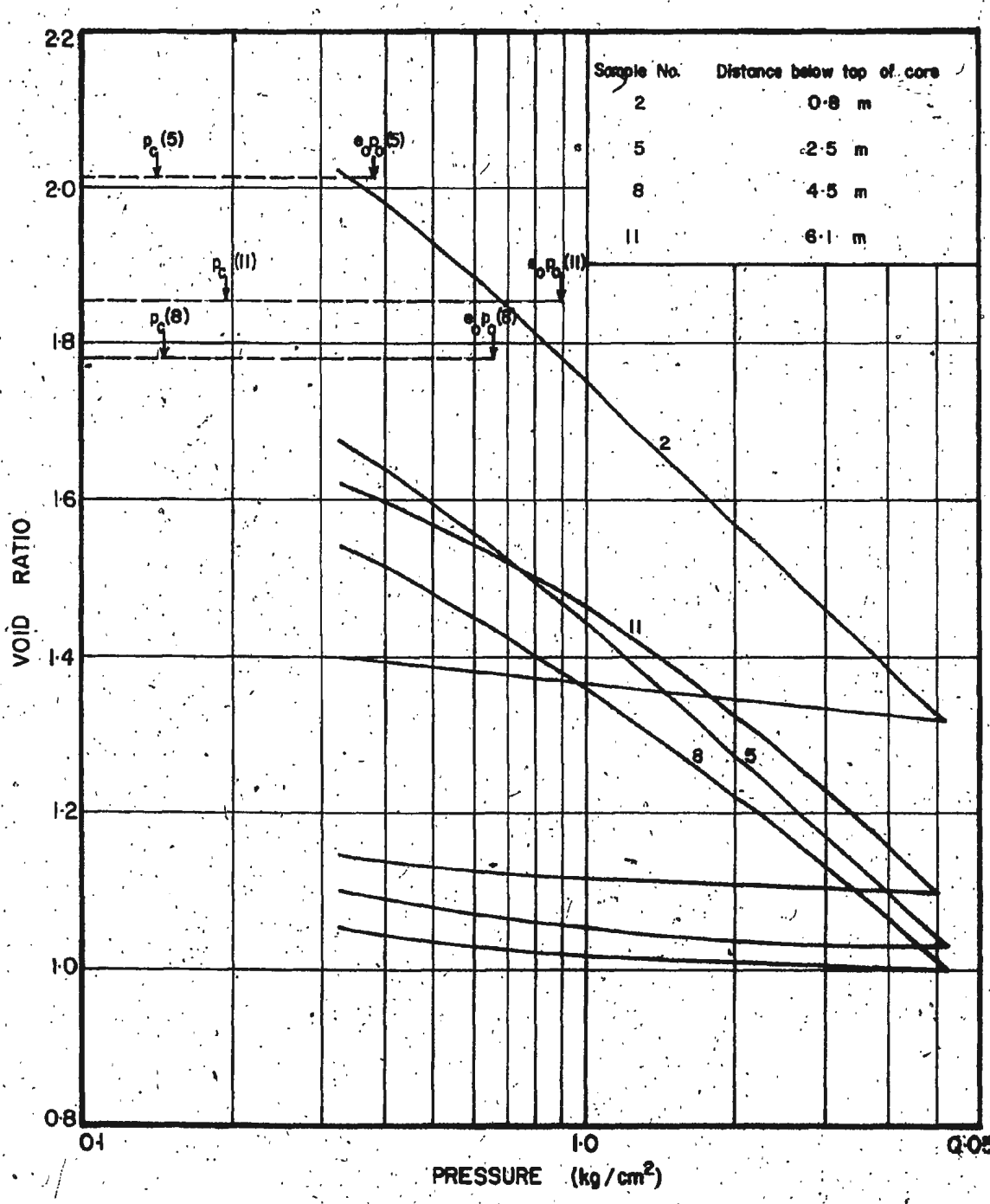

Fig. 54. Void Ratio Change With Logarithm of Pressure - Station G 141

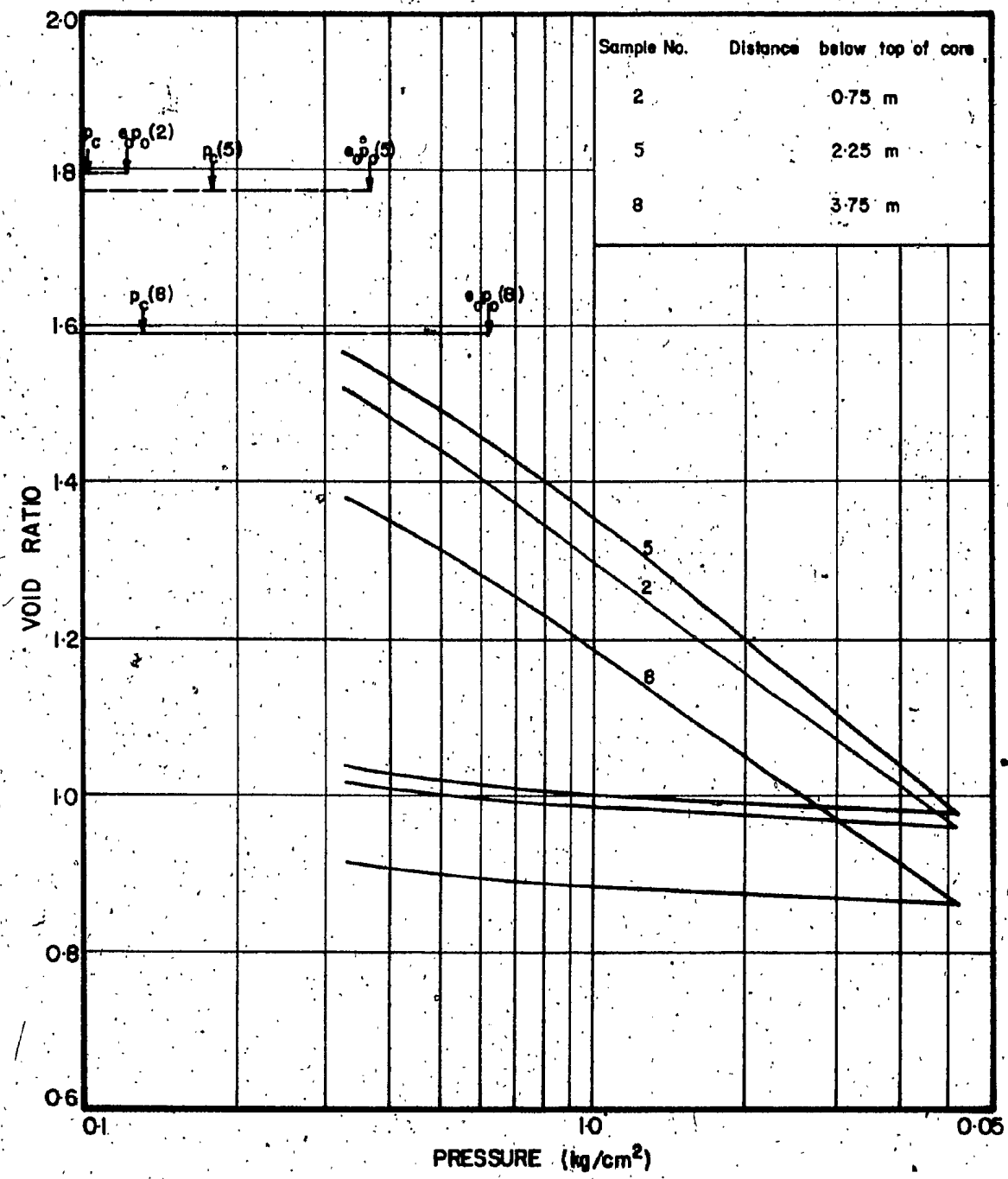

Fig. 55. Void Ratio Change With Logarithm of Pressure - Station G 441A

in pore pressure dissipation. The practical significance of under-consolidated soils is that the engineering properties of the materials are poor, both from an absolute point of view and in comparison with normally consolidated soils.

5.6. Elastic Properties of Sediments

This part of the thesis is concerned with the elastic properties of the sediments. It includes measurements and computations of the elastic constants and their inter-relationships with other physical and acoustical properties. These constants are compressibility, bulk modulus, rigidity (shear) modulus, Lame's constant, Poisson's ratio and Young's modulus.

To compute these elastic constants with the equation of elasticity, the bulk density and any two other elastic constants are required. In the case of marine sediments, the bulk density and sound velocity can be easily measured. The preferred third variable would be the shear wave velocity, at least for the purposes of underwater sound and geophysics.

Information on the velocity of shear waves in marine sediments is rare and should be obtained by measurement. Lacking sufficient information on shear wave velocities, the third constant selected for use in computing the elastic constants, suggests the use of the bulk modulus, K, of the water-mineral system comprising the sediments. This constant was selected because it appears possible to compute, in a logical manner, the bulk modulus of the sediment from its components requiring only minor estimates of one component. The theoretical basis of this computation follows that of Gassman (1951) and used by Hamilton (1969).

The components of the computed system bulk modulus ,K, are porosity (n), the bulk modulus of pore water (K_w), an aggregate bulk modulus of mineral grains (K_s) and the bulk modulus of the sediment structure (K_f) formed by the mineral grains. Good values for the bulk modulus of distilled and sea water and for the common minerals comprising sediments have previously been established. This leaves only a value for the frame-bulk modulus (K_f) needed to compute a bulk modulus for the water-mineral system.

A contribution of Hamilton (1969) was the derivation of a relationship between sediment porosity and the dynamic frame-bulk modulus. Using this relationship, the frame-bulk modulus can be derived and used with the bulk moduli of pore water and the minerals to compute the system bulk modulus. This computed bulk modulus along with the measured bulk density and sound velocity are then used to compute the other elastic constants.

An outline of the computation procedures of the basic constants from laboratory data is presented in Appendix B, together with the mathematical definitions for the elastic constants. Each of the basic constants has been calculated and averaged for each core since the variability of the soil types and properties is limited. These basic constants are listed in Table 11 together with the calculated elastic constants for these soils. Hamilton (1969) has reported the elastic properties of submarine soils and the results presented for silt and clayey silt sediments agree well with the results obtained from this study.

TABLE 11. ELASTIC PROPERTIES OF THE CORE SAMPLES

core no.	K	β	λ	ν	μ	E
G 132	314.01	0.32	292.756	0.451	31.859	92.449
G 141	320.47	0.312	304.65	0.464	23,727	69.467
G 233	395.24	0.253	359.57	0.435	53.5	153.58
G 243	387.14	0.258	368.654	0.465	27.73	81.249
G 332	443.02	0.226	418.43	0.460	36.885	107.248
G 341	410.56	0.244	404.54	0.489	9.03	28.893
G 432	342.33	0.292	320.494	0.454	32.753	95.22
G 441A	356.21	0.281	328.415	0.444	41.693	120.38

Notes:

K = water-mineral system bulk modulus, $kN/m^2 \times 10^4$

β = compressibility, $m^2/kN \times 10^{-6}$

λ = Lame's constant, $kN/m^2 \times 10^4$

ν = Poisson's ratio,

μ = rigidity (shear) modulus, $kN/m^2 \times 10^4$

E = Young's modulus, $kN/m^2 \times 10^4$

5.7. Analysis of M.U.N. Free Fall Penetrometer Output Results

5.7.1. Introduction

Laboratory tests using the redesigned version of M.U.N. penetrometer in free fall mode on cohesionless and cohesive soils, together with an interpretation and analysis of the results, were presented by Chaudhuri (1979). He concluded that the results of free fall penetration tests exhibited a substantially increased penetration resistance, compared to the standard quasi-static tests. However, when the results were translated into computation of the angle of shear resistance, the difference was insignificant. For cohesive soils, penetration resistance is dependent on the velocity of penetration. The "strain-rate effect" was found to influence the results; however, the "static" strength for clays can be derived from dynamic strength profiles by taking into account the "strain-rate effect".

5.7.2. Interpretation of the Results

An attempt is made in this dissertation to interpret the free ~~fall~~ penetrometer results quantitatively, and to suggest values for a dynamic bearing capacity factor (N_d) based on the vane shear strength and cone resistance values obtained. Within the scope of this investigation, the primary objective is to compare the results of the penetrometer outputs from the sea trials with the behaviour under laboratory conditions.

It is generally assumed that the penetrometer is similar to a pile foundation loaded to its ultimate bearing pressure. The general formation for bearing capacity of cohesive soils is:

$$Q_s = C. N_c + \sigma_v \qquad \ldots\ldots\ldots\ldots \quad (18)$$

where σ_v = vertical stress

Meyerhof (1961) recommended $N_c = 9.0$ for statically-loaded deep foundations with $\alpha/2 = 30^{\circ}$ and roughness $\delta/\phi = 0.5$. In view of the analogy between a cone penetrometer and the bearing capacity of deep foundations, Baligh et al. (1979) have suggested values of $N_c = 14 \pm 6$ at a depth of 7.6 m and $N_c = 14 \pm 3$ at a depth of 30.0 m for quasi-static penetrometer tests.

a. Relationship of Static and Dynamic Cone Penetration Resistance

It has been long recognized that the "strain-rate effect" is an important factor which must be considered in the shear strength of cohesive soils. Casagrande and Wilson (1951) and Whitman (1957) have studied this effect and concluded that shear strength gradually increase with an increasing rate of shear strain. The phenomena controlling the shear strain rate effect is considered too complex to permit mathematical definition. However, a successful approach to the shear rate effect for saturated clays for both small and large strain loading apparently has been accomplished by Turange and Freitage (1970). They observed that, for saturated clays, a quantity termed the cone index varied with penetration rate according to the relation

$$\frac{C_{Ix}}{C_{Is}} = \frac{(v/d)_x}{(v/d)_s}^M \qquad \ldots\ldots\ldots\ldots (19)$$

where C_{Ix} = cone index of penetration velocity v_x with diameter d_x

C_{Is} = cone index of a standard cone with velocity v_s and diameter d_s

M = exponent of shear rate factor

The above expression was found to hold good for velocities ranging from 0.05 to 432 cm/s. and cone base diameters from 2.7 to 77 mm. and for saturated soils ranging from silt to heavy clay. The exponent M ranged from 0.091 to 0.109 for the conditions considered by Turnage and Freitage (1970).

In connection with tests on bulldozer blades, Wismar and Luth (1972) attempted to quantify the strain-rate effects using eqn. 19 and suggested a value of 0.1 for the exponential.

From eqn. 19 , the theoretical value of cone resistance for varying impact velocity and cone diameter can be calculated using the quasi-static penetration test as the reference or vice-versa. If the penetrometer diameter is the same for both cases, and applying the upper limit of the exponent, eqn. 19 reduces to

$$Q_s = \left(\frac{v_s}{v_d}\right)^{0.109} Q_d \qquad \ldots\ldots\ldots \quad (20)$$

where Q_s = theoretical quasi-static cone resistance for a standard penetrometer with velocity v_s and diameter d.

Q_d = dynamic cone resistance for impact velocity v_d and diameter d

Chaudhuri (1979) used a similar procedure to determine the dynamic cone resistance which was then compared with the results of quasi-static penetration tests by Abdel-Gawad (1979). He showed that the strain rate effect caused an 84% increase in the soil resistance at a velocity of 7.75 m/s. He also concluded that there is a good correlation between the resistance actually measured in a free fall penetration test and the theoretical cone resistance curve obtained after correcting for the strain - rate effect.

The above procedure can also be applied to field data to determine the theoretical quasi-static penetration resistance corresponding to the field measured dynamic resistance. Once, the quasi-static penetration resistance is obtained, the bearing capacity factor (N_c) and consequently the predicted shear strength can be calculated using any of the available theory in the literature.

Eqn. 20 was applied to the field results obtained from Hudson cruise (78-012), using the approach of Baligh (1979) to determine the static bearing capacity factor (N_c) and the predicted shearing strength. The agreement between the predicted shear strength derived from static cone theory and the measured vane shear strength was not good. This is due to the nonhomogeneity of the soil and the high values of the impact velocity which apparently exceeds the limits of eqn. 19. The penetrometer has recorded a maximum penetration velocity of 9.0 m/s. A correction factor (R) is suggested for eqn. 20, and the form of this equation is thus modified to:

$$Q_s = R \left(\frac{2}{v_d}\right)^{0.109} Q_d \qquad \ldots\ldots\ldots \quad (21)$$

where the standard static velocity of penetration is taken as 2 cm/s. Using the Baligh approach for purely cohesive soils

$$Q_s = 14\, C_{predicted} \qquad \ldots\ldots\ldots \quad (22)$$

The above procedure was applied to the available field data and a comparison of the measured and predicted shear strength is shown in Fig. 56. The correction factor (R) ranges between 0.45 and 0.9 with a mean value of 0.6. Eqn. 21 can now be rewritten after rearranging as:

$$Q_d = \left(\frac{v_d}{2}\right)^{0.109} \left(\frac{Q_s}{0.6}\right) \qquad \ldots\ldots\ldots \quad (23)$$

b. Dynamic Bearing Capacity

For purely cohesive soils, the dynamic cone resistance can be expressed as:

$$Q_d = C N_d \quad \ldots\ldots\ldots\ldots \quad (22')$$

where N_d is the dynamic bearing capacity factor.

Using eqns. 22,23 and making substitutions, an expression for the dynamic bearing capacity factor can be written as:

$$N_d = 22 (v_d)^{0.109} \quad \ldots\ldots\ldots\ldots \quad (24)$$

Fig. 57 shows the relation between dynamic bearing capacity factor and penetration velocity.

It may be relevant to point out here, that the values of sleeve friction measured do not appear to show a significant effect due to strain-rate. This is an area that should be investigated further.

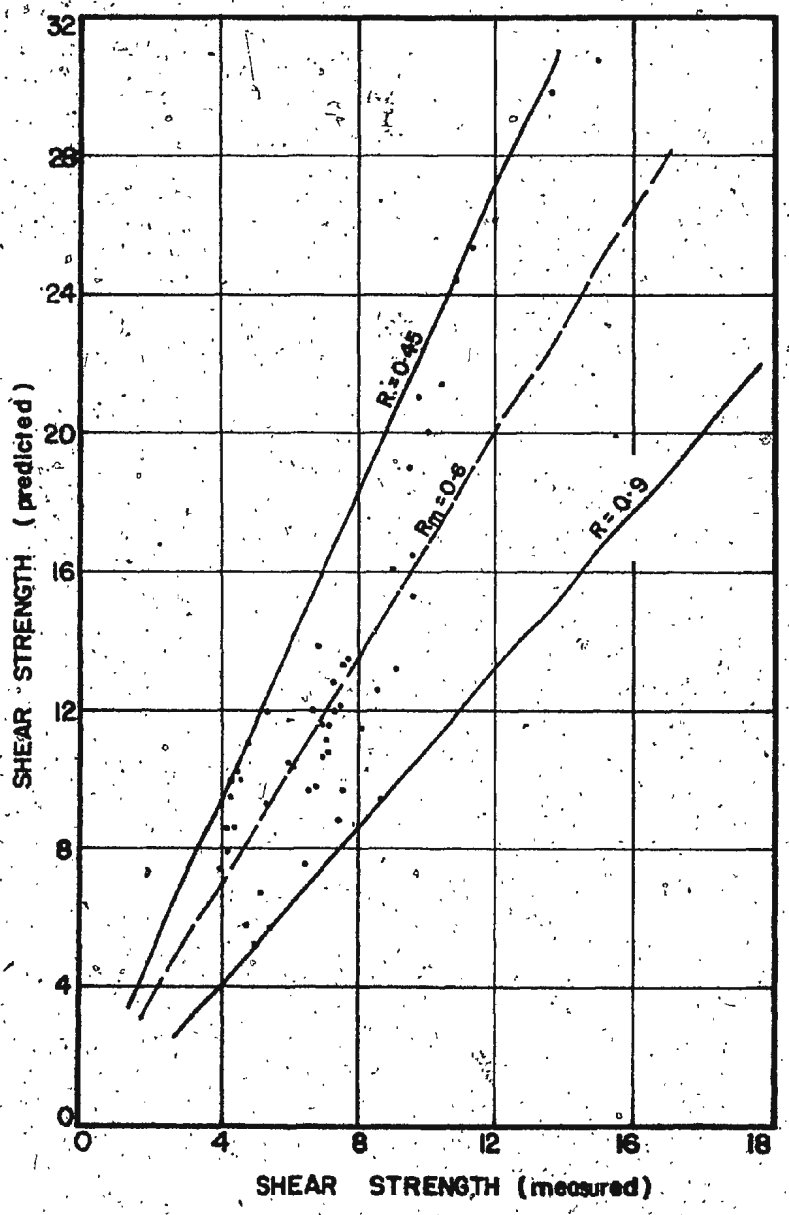

Fig. 56. Comparison of the Measured and Predicted Shear Strength from Cone Tip Resistance.

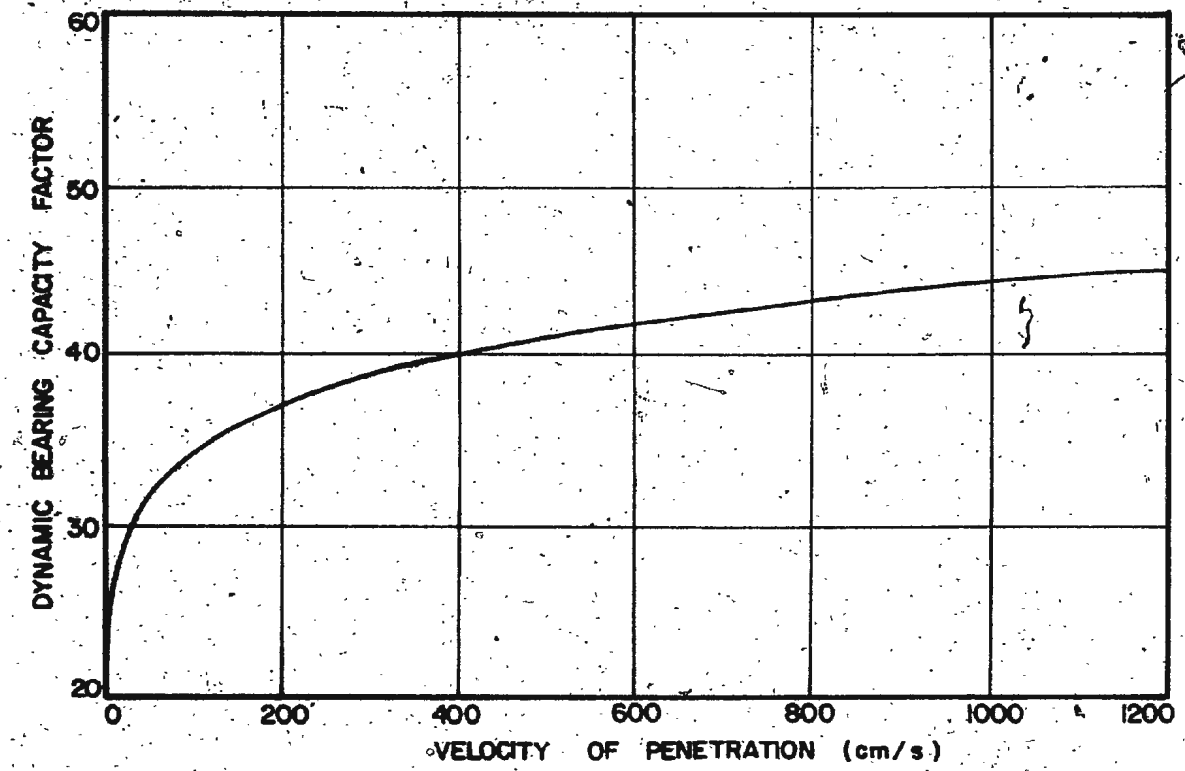

Fig. 57. Relationship Between Dynamic Bearing Capacity Factor and Penetration Velocity.

CHAPTER VI

SUMMARY AND CONCLUSIONS

6.1. Summary

The research reported here is part of an ongoing program to determine the definitive acoustic parameters of ocean bottom sediments which correlate with geotechnical properties, and to develop alternate systems of measuring engineering properties of sediments. An attempt is also made to relate impact cone penetrometer test results to both acoustic and geotechnical properties of the sediments at the test areas. A comprehensive study has been undertaken to evaluate data from the M.U.N. free fall penetrometer deployed in an ocean environment of moderate water depth.

Data obtained during the Hudson cruise 78 - 012 in outer Placentia Bay is analyzed to relate acoustic measurements on cores to data obtained from conventional investigation methods. It is expected that this information will be useful to extend and develop techniques which will permit the rapid differentiation of bottom sediment types and the engineering properties of these materials.

Data presented and evaluated in this study have been obtained from 8 piston cores, 10 grab samples and 6 free fall penetrometer test locations. Standard laboratory tests were conducted on the cores and the following geotechnical properties were determined: natural moisture content, Atterberg limits, wet density, relative density, particle size distribution by wet analysis, vane shear strength and

consolidation characteristics. Other basic parameters were calculated from the properties measured such as: plasticity index, liquidity index, degree of saturation, activity, void ratio and porosity. Velocity measurements were made on the cores immediately after removal from the core barrel.

Cone tip resistance, sleeve friction and deceleration records were obtained using the free fall penetrometer for different soil targets. A Doppler telemetry technique was used during each penetrometer drop to measure the velocity of penetration.

Laboratory and field measurements on the cores subjected to regression analyses show that the principal acoustic properties of sea-floor sediments correlate well with some of their geotechnical properties. Sound velocity and acoustic impedance provide the most reliable information about the following geotechnical properties: porosity, density, Atterberg limits, shear strength and compressibility. The output from impact cone penetrometer has been evaluated and significant correlations were obtained between cone tip resistance and sleeve friction and both geotechnical and acoustic properties.

The graphic determination of preconsolidation pressure, from laboratory consolidation curves, indicates that the sediments of the Placentia Bay area are underconsolidated.

The basic elastic constants of the sediments such as: compressibility, bulk modulus, rigidity modulus, Lame's constant, Poisson's ratio and Young's modulus have been calculated for each core.

6.2. Conclusions

The following conclusions have been drawn from the results of

the present investigation and previous efforts of a similar type:

1. The geotechnical properties are highly inter-correlated. The most pronounced relationship was found between porosity and wet density. The relatively good correlations obtained between most geotechnical properties indicate that the parameters are inter-dependent and that several parameters may be adequately predicted from a few basic properties.
2. Certain index and textural properties of the Placentia Bay sediments have a definite influence on the sound velocity through such marine deposits. For index properties, a decrease in porosity and moisture content is related to an increase in sound velocity. Sound velocity has a positive correlation with wet density and a negative correlation with compression index. A definite relationship exists between sound velocity and the logarithm of median particle diameter. The coarser the sediment is, the higher its' sound velocity.
3. There is no reliable relationship between sound velocity and undrained shear strength (cohesion) as measured in soil mechanics tests. This is apparently because cohesion from a static test can not be compared with dynamic rigidity.
4. Earlier studies to determine sound velocity – porosity relationships produced generalized equations and curves over a full range of sediment velocities and porosities (Hamilton, 1965 and Horn et al. 1968). Data now available from different sediment locations indicate that important environmental differences due to sediment structural rigidity occur. General equations and diagrams relating velocity and porosity should be replaced where possible by diagrams or equations applicable to the local environment. When no sediment data are

available, velocity should be predicted directly rather than, for example, predicting porosity and then velocity.

5. The correlations between acoustic impedance and various geotechnical properties of the sediments follow the same trends as determined for sound velocity with higher degree of correlation in most cases.
6. The reliability of laboratory test results on marine sediment samples from a free fall piston corer is always questionable. In fact, this is one of the main reasons for an increased demand for in-situ tests in the ocean environment.

In the absence of more refined samples, comparison of the free fall penetrometer results with the geotechnical properties of the available core samples does, however, show a significant relationship between cone tip resistance and shear strength with a correlation coefficient of 0.89. No meaningful relationship was obtained between cone tip resistance and any of the other geotechnical properties, while the sleeve friction was found to correlate well with the majority of the other geotechnical parameters.

7. No apparent relationship was obtained between cone tip resistance and any of the acoustic properties. However, significant relationships were obtained between sleeve friction and both sound velocity and acoustic impedance with correlation coefficients of 0.535 and 0.73.
8. The sea trials of the M.U.N. free fall penetrometer indicate that this instrument has merit as a practical method of conducting a rapid and preliminary evaluation of soft surficial ocean sediments to about 10 m depth. The interpretation of the penetrometer results and the relatively high correlation coefficient obtained between the cone tip resistance and shear strength, suggests that the penetrometer could

be used with considerable confidence as a very useful ground truth instrument.

9. It should be emphasized that because of the degree of disturbance of the cores, natural soil variability and probable variations in laboratory techniques, it is impossible to specify all the correlations absolutely. All the above conclusions are based mainly on an examination of the relative trends between the parameters obtained during this analysis.

6.3. Recommendations for Further Work

a. Continued studies of the geotechnical properties of sediments, from a range of marine environments, are required to define the parameters and statistical variations of these properties with an improved degree of reliability. Both laboratory and in-situ measurements should be carried out to refine suitable correlations. Samples of the highest quality should be obtained to ensure that the most representative values of the measured parameters are obtained. Laboratory test results are needed since at present they are the basis of property evaluation and in-situ prediction. Furthermore, an investigation of apparent underconsolidation of sediments should be continued.

b. Vane shear testing is generally a reliable method for measuring shear strength. However, in view of sample disturbance, it is recommended that vane shear testing should be carried out in-situ when possible to minimize the effects of disturbance of the sediment from coring operations. Furthermore, research emphasis must also be placed on the development of methods to adequately define and express values of shear strength determined by dynamic measurements.

c. Ensure that measurements of the mass properties of sediments, as discussed in this investigation, are made a routine part of core laboratory procedures in addition to the detailed logging of cores.

d. In view of the sediment characteristics, exhibited information on the chemical, mineralogical and organic composition of the soils investigated should be obtained and evaluated in further studies to correlate geotechnical properties with other characteristics.

e. Continued efforts towards interpretation and application of results from the Deep-Tow Seismic system (DTS) should be pursued. Considerable research on relating the DTS data to geotechnical properties and penetrometer results is still required.

f. Various indirect methods of analyzing sediment cores, i.e., scanning acoustic, high resolution x-rays and electrical resistivity, together with further development of acoustic and geotechnical inter-relationships should be pursued.

g. Additional theoretical and laboratory work is required for improved correlation of the penetrometer output results with acoustic and geotechnical sediment properties. Furthermore, an evaluation of the strain-rate effect on sleeve friction is an area that should be investigated further.

h. In this investigation, Doppler telemetry was used to obtain velocity profiles directly for comparison with the integrated results of the accelerometer records. The good correlation between the two velocity profiles suggests that research on Doppler telemetry should be continued further.

REFERENCES

1. Abdel-Gawad, S.M.,"Static Penetration Resistance of Soils", Master Thesis, Memorial University of Newfoundland, July, 1979.

2. Allen, J.H., Dayal, U., and Jones, J.M., "Development of Marine Sediment Impact Penetrometer", Proceedings, Oceanology International Conference, pp. 244-248, 1975.

3. Anderson, A., and Hampton, L.D., "In-Situ Measurement of Sediment Acoustic Properties During Coring", Marine Science 2, pp. 327-345, 1974.

4. Baligh, M.N., and Vivatrat, V., "In-Situ Measurements in a Marine Clay", Proceedings of the 2nd International Conference on the Behaviour of Offshore Structures, Vol. 1, pp. 151-174, 1979.

5. Beard, R.M., "Expendable Doppler Penetrometer; A Performance Evaluation", Civil Engineering Laboratory, U.S. Naval Facilities Eng. Command, Technical Report 855, July, 1977.

6. Buchan, S., Dewes, F.C.D., McCann, D.M., and Smith, D.T., "Measurement of the Acoustic and Geotechnical Properties of Marine Sediment Cores", Marine Geotechnique, pp. 65-92, 1967.

7. Buchan, S., McCann, D.M., and Smith, D.T., "Relations Between the Acoustic and Geotechnical Properties of Marine Sediments", Quarterly Journal of Engineering Geology, Vol. 5, pp. 265-284, 1972.

8. Canada, Hydrographic Service, Chart L-4016, Saint Pierre to St. John's, 1973.

9. Casagrande, A., and Wilson, S.D., "Effect of Rate Loading on the Strength of Clays and Shales at Constant Water Content", Geotechnique, Vol. II, pp. 251-263, 1951.

10. Chari, T.R., "Problems Related to Instrumentation for Determining Geotechnical Properties", IEEE, Journal of Oceanic Engineering, OE-3(4), pp. 120-127, May, 1978.

11. Chari, T.R., Smith, W.G., and Zielinski, A., "Use of Free Fall Penetrometer in Sea Floor Engineering", Conf. Rec., Ocean '78, IEEE-MTS Conf., pp. 686-691, 1978.

12. Chari, T.R., Dunsiger, A.D., Fader, G., Peters, G.R., Simpkin, P., and Zielinski, A., "Ocean Sediments - A Study Relating Geophysical, Geotechnical and Acoustic Properties", 1st. Canadian Conf. on Marine Geotechnical Engineering, Calgary, April, 1979, (preprint, 12 pp.).

13. Chari, T.R., Muthukrishnaiah, K., and Zielinski, A., "Performance Evaluation of a Free Fall Penetrometer", 1st. Canadian Conf. on Marine Geotechnical Engineering, Calgary, April, 1979, (preprint, 8pp).

14. Chari, T.R., Abdel-Gawad, S.M., and Chaudhuri, S.N., "Geotechnical Survey of the Sea Floor With a Free Fall Penetrometer", Proceedings, 5th. Int. Conf. Port and Ocean Engineering Under Artic Conditions (POAC), Norway, August, 1979.

15. Chatfield, C., "Statistics for Technology", John Wiley and Sons, New York, 1976.

16. Chaudhuri, S.N., "Free Fall Impact Penetration Tests on Soils", Master Thesis, Memorial University of Newfoundland, August, 1979.

17. Colp, J.L., Coudle, W.N., and Schuster, C.L., "Penetrometer System for Measuring In-Situ Properties of Marine Sediments", Proceedings, IEEE Conf., pp. 405-411, 1975.

18. Dayal, U., "Instrumented Impact Cone Penetrometer", Ph.D. Thesis, Memorial University of Newfoundland, 1974.

19. Denness, B., McCann, D.M., and Fairlie, A., "Geotechnical Studies of the Sea Floor Sediments Around Arran", Offshore Structures, ICE, London, pp. 21-26, 1975.

20. De Ruiter, J., "Electrical Penetrometer for Site Investigations", Journal of Soil Mechanics and Foundations Division, Proc. ASCE, Vol. 90, No. SM2, pp. 457-473, 1971.

21. De Ruiter, J., "The Use of In-Situ Testing for North Sea Soil Studies", Proc. Offshore Europe '75, Aberdeen, pp. 219.1-219.10, 1975.

22. Doyle, E.H., McClelland, B., and Ferguson, G.H., "Wire Line Vane Probe for Deep Penetration Measurement of Ocean Sediment Strength", 3rd. Offshore Technology Conf., Houston, OTC 1327, Vol. I, pp. 121-127, 1971.

23. Emrich, W.J., "Performance Study of Soil Sampler for Deep Penetration Marine Borings", Sampling of Soil and Rock, ASTM STP 483, American Society for Testing and Materials, pp. 30-50, 1971.

24. Erchul, R.A., "In-Situ Determination of Marine Sediment Properties and Engineering Characteristics - Ocean Engineering Applications for Electrical Resistivity Techniques", Proc. 6th. Offshore Technology Conf., OTC 2012, Vol. I, pp. 733-739, 1974.

25. ESOPT, "Proceedings of the European Symposium on Penetration Testing", Vol. I, Stockholm, 1974.

26. Fenske, C.W., "Deep Vane Tests in Gulf of Mexico", Symposium on Vane Shear Testing of Soils, ASTM STP 193, pp. 19-25, 1957.

27. Ferguson, G.H., McClelland, B., and Bell, W.D., "Sea Floor Cone Penetrometer for Deep Penetration Measurements of Ocean Sediment Strength", Proc., 9th. Offshore Technology Conf., OTC 2787, Vol. I, pp. 471-478, 1977.

28. Folk, R.L., "A Review of Grain Size Parameter", Sedimentology, 6 pp. 73-94, 1966.

29. Fukuoka, M. and Nakase, A., "Problems of Soil Mechanics of Ocean Floor", Proc., 8th. international Conf. on Soil Mechanics and Foundation Engineering, Moscow, Vol. 4.2, pp. 205-222, 1973.

30. Gambin, M.Ph., "Discussion on Engineering Properties of Submarine Soils: State-Of-The-Art Review", Journal of Soil Mechanics and Foundations Division, Proc. ASCE, Vol. 97, No. SM6, pp. 937-939, 1971.

31. Gassman, F., "Über Die Elastizität Poröser Medien", Vierteljahrsschrift Der Naturforschenden Geselischaft in Zürich, Vol. 96. pp. 1-23, 1951.

32. Hamilton, E.L., "Sediment Sound Velocity Measurements Made In-Situ From Bathyscaph Trieste", Journal of Geophysical Research, Vol. 68, pp. 5991-5998, 1963.

33. Hamilton, E.L., "Sound Speed and Related Physical Properties of Sediments from Experimental Mohole", Geophysics, Vol. 30, pp. 257-261, 1965.

34. Hamilton, E.L., "Sound Velocity, Elasticity and Related Properties of Marine Sediments, North Pacific, Part I: Sediment Properties, Environmental Control, and Empirical Relationships", Naval Undersea Research and Development Centre, Technical Report 143, 1969.

35. Hampton, L., "Physics of Sound in Marine Sediments", Plenum Press, 1974.

36. Harrison, W., and Richardson, A.M., "Plate-Load Tests on Sandy Marine Sediments, Lower Chesapeake Bay", Marine Geotechnique, Ed. Richars, A.F., Univ. of Illinois Press, pp. 274-290, 1967.

37. Haworth, R.T., and Lefort, J.P., "Geophysical Evidence for the Extent of the Avalon Zone in Atlantic Canada", Canadian Journal of Earth Sciences, Vol. 16, No. 3, pp. 552-567, March, 1979.

38. Henderson, E.P., "Surficial Geology of Avalon Peninsula, Newfoundland", Geological Survey of Canada, Memoir 368, 121 pp. 1972.

39. Hitchings, G.A., Bradshaw, H., and Labiosa, T.D., "The Planning and Execution of Offshore Site Investigations for a North Sea Gravity Plateform", Proc., 8th. Offshore Technology Conference, OTC 2430, Vol. I, pp. 61-74, 1976.

40. Horn, D.R., Horn, B.M., and Delach, M.N., "Correlation Between Acoustical And Other Physical Properties of Deep Sea Cores", Journal of Geophysical Research, Vol. 73, No. 6, pp. 1939-1957, 1968.

41. Jones, J.M., "The Use Of Impact Penetrometer in Remote Sensing Study of the Sea Bed Properties", 2nd. CSCE Hydrotechnical Conference, Atlantic Region, N.S., 1976.

42. Keller, G.H., "Nuclear Density Probe for Inplace Measurement in Deep Sediments", Transactions of the Joint Conference and Exhibit, Marine Technical Society and the American Society of Limnology and Oceanography I, pp. 363-372, 1965.

43. King, L.H., "Aspects of Regional Surficial Geology Related to Site Investigation Requirements - Eastern Canadian Shelf, Int. Conf. on Offshore Site Investigation, Society for Underwater Technology, London, 1979, (preprint, 34pp).

44. Kolbe, R., "The Design and Development of an Ocean Sediment Probe", Ph.D. Thesis, Univ. of New Hampshire, Durham, 1975.

45. Kretschmer, T.R., and Lee, J.H., "In-Situ Determination of Sea Floor Bearing Capacity", Proc., Civil Engineering in the Ocean II, ASCE, pp. 679-702, 1969.

46. Mayer, L., "The Origin of Fine Scale Acoustic Stratigraphy in Deep Sea Carbonates", Journal of Geophysical Research, Vol. 84, No. B11, pp. 6177-6184, 1979.

47. McCann, D.M., and Dewers, F.C.D., "Acoustic Reflectors in the Surface Layers of Deep Sea Sediments", Marine Geophysical Researches, Vol. I, pp. 362-380, 1972.

48. McNary, J.F., and Frolich, H., "An In-Situ Vane Shear Testing Device", Marine Geology, Vol. 8, No. 5, pp. 367-370, 1970.

49. Meyerhof, G.G., "The Ultimate Bearing Capacity of Wedge-Shaped Foundations", Proc., 5th. Int. Conf., Soil Mechanics and Foundation Engineering, Vol. 2, pp. 105-109, Paris, 1961.

50. Noorany, I., "Underwater Sampling and Testing - A State-Of-The-Art Review", Underwater Soil Sampling, Testing and Construction Control, ASTM STP 501, pp. 3-41, 1972.

51. Noorany, I., and Gizienski, S.F., "Engineering Properties of Submarine Soils, State-Of-The-Art Review", Journal of the Soil Mechanics and Foundations Division, ASCE, Vol. 96, No. SM5, Paper No. 7536, pp. 1735-1762, 1970.

52. Peters, G.R., "Cruise Report 78-012 C.S.S. Hudson, May 15 - 30, 1978", Ocean Engineering, Memorial University of Newfoundland, 1978.

53. Preslan, W.L., "Accelerometer-Monitored Coring", Proc., Civil Eng. in the Ocean II, American Society of Civil Engineers, pp. 637-641, 1970.

54. Richards, A.F., "Principle of Piston Coring Fine Grained Sediments with Minimum Deformation", Geological Society of America, Special Paper No. 87, 1966.

55. Richards, A.F., "Marine Geotechnices of the Oslofjorden Region", Marine Geotechnical Laboratory, Lehigh Univ., No. 17, pp. 41-62, 1973.

56. Richards, A.F., McDonald, V.J., Olson, R.E., and Keller, G.H., "In-Place Measurement of Deep Sea Soil Shear Strength", Underwater Soil Sampling, Testing and Construction Control, ASTM STP 501, pp. 55-68, 1972.

57. Rosfelder, A.M., and Marshall, N.F., "Obtaining Large, Undisturbed and Oriented Samples in Deep Water", Marine Geotechnique, Univ. of Illinois Press, pp. 243-263, 1967.

58. Sanglerat, G., "The Penetrometer and Soil Exploration", Elsevier Publishing Company, 1972.

59. Saucier, R.T., "Acoustic Subbottom Profiling Systems, A State-Of-The-Art Survey", Technical Report S-70-1, USAEWES, 1970.

60. Scott, R.F., "In-Place Soil Mechanics Measurements", Marine Geotechnique, Univ. of Illinois Press, pp. 264-271. 1967.

61. Sen Gupta, B.K., and McMullen, R.M., "Foraminiferal Distribution and Sedimentary Facies on the Grand Banks of Newfoundland", Canadian Journal of Earth Science, Vol. 6, No. 3, pp. 475-487, 1969.

62. Silva, A.J., and Hollister, C.D., "Geotechnical Properties of Ocean Sediments Recovered With Giant Piston-Corer: I-Gulf of Marine", Journal of Geophysical Research, Vol. 78, No. 18, pp. 3597-3616, 1973.

63. Silva, A.J., Hollister, C.D., Laine, E.P., and Beverly, B.E., "Geotechnical Properties of Deep Sea Sediments: Bermuda Rise", Marine Geotechnology, Vol. 1, No. 3, pp. 195-232, 1976.

64. Simpkin, P.G., "Geophysical Investigation of Marine Sediments Under In-Situ Conditions", Ph.D. Thesis, University of Wales, England, March, 1975.

65. Simpkin, P.G., "Velocity Scanning of the Piston Cores Collected on the Memorial Cruise, A preliminary Evaluation", Huntec '70 Ltd, Seabed Report #H7807-01/SB/pgs, 1978.

66. Skempton, A.W., "Discussion on the Planning and Design of the New Hong Kong Airport", Proc. of the Institution of Civil Engineers, Vol. 7, pp. 305-307, 1957.

67. Slatt, R.M., and Gardiner, W.W., "Comparative Petrology and Source of Sediments in Newfoundland Fiords", Canadian Journal of Earth Sciences, Vol. 13, No. 10, pp. 1460-1465, October, 1976.

68. Sly, P.G., "Equipment and Techniques for Offshore Survey and Site Investigations", 1st. Canadian Conf. on Marine Geotechnical Eng., Calgary, April, 1979, (preprint, 19pp.).

69. Stehman, C.F., "Pleistocene and Recent Sediments of Northern Placentia Bay, Newfoundland", Canadian Journal of Earth Sciences, Vol. 13, No. 10, pp. 1386-1392, October 1976.

70. Sutton, G.H., Berckhemer, H., and Nafe, J.E., "Physical Analysis of Deep Sea Sediments", Geophysics, Vol. XXII, No. 4, pp. 779-812, 1957.

71. Tayler, R.J., and Demars, K.R., "Naval In-Place Seafloor Test Equipment", U.S. Naval Civil Engineering Laboratory, 1970.

72. Terzaghi, K., and Peck, R.B., "Soil Mechanics in Engineering Practice", John Wiley and Sons, New York, 1967.

73. True, D.G., "Penetration of Projectiles into Seafloor Soils", U.S. Naval Civil Engineering Laboratory, Technical Report R822, 1975.

74. Turnage, G.W., and Freitage, D.R., "Effects of Cone Velocity and Size on Soil Penetration Resistance", Paper no. 69-670, American Society of Agricultural Engineering, 1969.

75. Wang, M.C., Nacci, V.A., and Market, C.D., "Electrical Resistivity Method for Marine Sediment Consolidation Study", Proc., 8th. Offshore Technology Conf., OTC 2623, Vol. III, pp. 45-54, 1976.

76. Whitman, R.V., "The Behaviour of Soils Under Transient Loadings", Proc., 4th. Int. Conf., Soil Mechanics and Foundations Engineering, London, Vol. I, pp. 207-210, 1957.

77. Williams, H., "Applachian Orogen in Canada", Canadian Journal of Earth Sciences, Vol. 16, No. 3, pp. 792-807, March 1979.

78. Wismar, R.D., and Luth, H.J., "Rate Effects in Soil Cutting", J. Terramechanics, Vol. 8, No. 3, pp. 11-21, 1972.

79. Zuidberg, H.M., "The Seacalf, A Submersible Cone Penetrometer Rig", Marine Geotechnology, Vol. I, No. 1, pp. 15-32, 1975.

APPENDIX A

LABORATORY TEST PROCEDURES

This part of the thesis presents details of test procedures and methods used for measuring laboratory geotechnical properties and velocity logging of the cores. Also included are detailed test results of some of the parameters determined. Summarized results of the data are presented in Chapter IV.

1. Geotechnical Properties of the Sediments

The geotechnical properties of the sediments are divided into three main categories; a) particle size characteristics, b) index properties, and c) engineering properties.

a. Particle Size Characteristics

The core samples collected have been analyzed by a combination of sieving and hydrometer analysis according to ASTM - D 422. Data from particle size analyses were presented in the form of a cumulative frequency curve. From this curve, the following information were taken:

- Median diameter $M_{d\phi} = \Phi_{50}$ . . . . . (A.1)
- Mean diameter $M_{\phi} = 1/2\ (\Phi_{16} + \Phi_{84})$ . . . . . (A.2)
- Graphic mean diameter $M_z = 1/3\ (\Phi_{16} + \Phi_{50} + \Phi_{84})$ . . . . . (A.3)
- Phi deviation $\sigma_{\phi} = 1/2\ (\Phi_{84} - \Phi_{16})$ . . . . . (A.4)

These quantities are defined by Folk (1966) and may be quoted in phi units where the phi diameter is given by:

$$\Phi = -\log_2 d \quad \text{. . . . . (A.5)}$$

where: d = particle diameter in mm.

Tables 12 to 19 present detailed particle size compositions as determined at 0.5 m intervals along the eight cores, as well as their median diameter, mean diameter, graphic mean and phi deviation.

b. Index Properties -

A typical element of marine sediment comprises three distinct phases; solid, liquid and gas. The more common geotechnical parameters are defined below:

Colour: wet sediment colour is determined in the laboratory by examining sections sliced from the core immediately after extraction from the core tube.

Moisture content: is the weight of water per unit dry weight of solid particles, and determined by finding loss of weight on drying in an oven at 105 ^{o}C $\pm$ to constant weight according to ASTM - D 2216.

Wet density: is the ratio of the total weight of the sample to the total volume.

Relative density of solids: is the ratio of the weight in air of a given volume of sample to the weight in air of an equal volume of distilled water. (ASTM - D 2049)

Void ratio: is the ratio of the volume of the voids to the volume of the solids, and can be calculated using the following equation:

$$e = \frac{1 + w}{\rho_s} D_R \rho_w - 1 \qquad \ldots\ldots\ldots\ldots \text{(A.6)}$$

where: w = moisture content

D_R = relative density of solids

ρ_s = bulk density of soil

ρ_w = density of water

TABLE 12. PARTICLE SIZE CHARACTERISTICS: CORE - G 132

depth below mudline (m)	sand (%)	silt (%)	clay (%)	median diameter (mm)	mean diameter (mm)	graphic mean diameter (mm)	phi deviation (mm)
0.0 - 0.5	5	87.5	7.5	0.01	0.021	0.017	0.017
0.5 - 1.0	3	92	5	0.016	0.02	0.017	0.012
1.0 - 1.5	5	91	4	0.01	0.018	0.015	0.012
1.5 - 2.0	6	82	12	0.009	0.021	0.017	0.019
2.0 - 2.5	2.5	82.5	15	0.008	0.018	0.014	0.016
2.5 - 3.0	4	88	8	0.009	0.018	0.015	0.014
3.0 - 3.5	7.5	76.5	16	0.008	0.019	0.015	0.017
3.5 - 4.0	7	78	15	0.0084	0.021	0.017	0.019
4.0 - 4.5	3	77	20	0.0064	0.016	0.013	0.014
4.5 - 5.0	2.5	77.5	20	0.0064	0.011	0.01	0.01
5.0 - 5.5	6	82	12	0.007	0.018	0.014	0.015
5.5 - 6.0	7	86	7	0.008	0.018	0.015	0.014
6.0 - 6.5	0	91	9	0.0054	0.009	0.009	0.009
6.5 - 7.0	0	83	17	0.006	0.009	0.008	0.007
7.0 - 7.5	3	85	12	0.0055	0.008	0.007	0.0065
7.5 - 8.0	0	80	20	0.005	0.007	0.006	0.006
8.0 - 8.4	0	81	19	0.005	0.007	0.006	0.005
8.4 - 8.82	0	86	14	0.0052	0.007	0.006	0.005

TABLE 13. PARTICLE SIZE CHARACTERISTICS: CORE - G 141

depth below mudline (m)	sand (%)	silt (%)	clay (%)	median diameter (mm)	mean diameter (mm)	graphic mean diameter (mm)	phi deviation (mm)
0.0 - 0.5	12	57	31	0.0056	0.023	0.026	0.022
0.5 - 1.2	18	70	12	0.009	0.034	0.036	0.03
1.2 - 1.7	3	67	30	0.0055	0.012	0.015	0.01
1.7 - 2.2	3	65	32	0.0047	0.011	0.013	0.01
2.2 - 2.8	8	65	27	0.005	0.012	0.013	0.01
2.8 - 3.5	7	62	31	0.0056	0.018	0.021	0.018
3.5 - 4.2	14	53	33	0.0055	0.02	0.021	0.016
4.2 - 4.75	9	55	36	0.0047	0.016	0.018	0.015
4.75- 5.25	8	58	34	0.005	0.015	0.018	0.015
5.25- 5.9	5	71	24	0.005	0.012	0.015	0.01
5.9 - 6.2	2	61	37	0.004	0.01	0.012	0.01
6.2 - 7.06	25	63	12	0.01	0.08	0.07	0.06

TABLE 14. PARTICLE SIZE CHARACTERISTICS: CORE - G 233

depth below mudline (m)	sand (%)	silt (%)	clay (%)	median diameter (mm)	mean diameter (mm)	graphic mean diameter (mm)	phi deviation (mm)
0.0 - 0.5	4	82	14	0.004	0.011	0.011	0.01
0.5 - 1.0	10	80	10	0.004	0.016	0.024	0.013
1.0 - 1.5	10	66	24	0.0035	0.013	0.018	0.012
1.5 - 2.0	5	54	41	0.0028	0.009	0.0095	0.009
2.0 - 2.5	6	58	36	0.0043	0.012	0.014	0.012
2.5 - 3.02	50	34	16	0.06	0.0011	0.031	0.001

TABLE 15. PARTICLE SIZE CHARACTERISTICS: CORE - G 243

depth below mudline (m)	sand (%)	silt (%)	clay (%)	median diameter (mm)	mean diameter (mm)	graphic mean diameter (mm)	phi deviation (mm)
0.0 - 0.5	3	80	17	0.0037	0.0065	0.0084	0.0036
0.5 - 1.0	4	72	24	0.0033	0.0068	0.0085	0.0052
1.0 - 1.5	5	50	45	0.0023	0.01	0.018	0.0076
1.5 - 2.0	4	59	37	0.0033	0.007	0.0087	0.0061
2.0 - 2.4	8	92	0	0.0036	0.009	0.009	0.009
2.4 - 2.75	2	98	0	0.0056	0.008	0.011	0.008

TABLE 16. PARTICLE SIZE CHARACTERISTICS: CORE - G 332

depth below mudline (m)	sand (%)	silt (%)	clay (%)	median diameter (mm)	mean diameter (mm)	graphic mean diameter (mm)	phi deviation (mm)
0.0 - 0.5	11	70	19	0.014	0.024	0.031	0.023
0.5 - 1.0	5	78	18	0.008	0.016	0.024	0.01
1.0 - 1.5	15	70	15	0.015	0.029	0.037	0.027
1.5 - 2.0	12	70	18	0.009	0.023	0.027	0.021
2.0 - 2.4	8	80	12	0.011	0.021	0.026	0.019
2.4 - 2.8	9	79	12	0.011	0.02	0.025	0.018
2.8 - 3.2	5	69	26	0.0054	0.015	0.018	0.013
3.2 - 3.68	6	60	34	0.005	0.011	0.013	0.01

TABLE 17. PARTICLE SIZE CHARACTERISTICS: CORE - G 341

depth below mudline (m)	sand (%)	silt (%)	clay (%)	median diameter (mm)	mean diameter (mm)	graphic mean diameter (mm)	phi deviation (mm)
0.0 - 0.6	9	90	1	0.009	0.022	0.018	0.018
0.6 - 1.1	7	83	10	0.005	0.014	0.011	0.012
1.1 - 1.7	5	95	0	0.005	0.014	0.011	0.011
1.7 - 2.3	7	93	0	0.008	0.024	0.018	0.021

TABLE 18. PARTICLE SIZE CHARACTERISTICS: CORE - G 432

depth below mudline (m)	sand (%)	silt (%)	clay (%)	median diameter (mm)	mean diameter (mm)	graphic mean diameter (mm)	phi deviation (mm)
0.0 - 0.5	18	82	0	0.043	0.066	0.07	0.05
0.5 - 1.0	12	88	0	0.011	0.04	0.043	0.03
1.0 - 1.5	12	88	0	0.013	0.03	0.022	0.02
1.5 - 2.0	8	62	30	0.0095	0.018	0.023	0.016
2.0 - 2.5	8	62	30	0.009	0.016	0.023	0.014
2.5 - 3.0	15	85	0	0.012	0.03	0.036	0.026
3.0 - 3.5	9	91	0	0.0085	0.023	0.02	0.02

TABLE 19. PARTICLE SIZE CHARACTERISTICS: CORE - G 441A

depth below mudline (m)	sand (%)	silt (%)	clay (%)	median diameter (mm)	mean diameter (mm)	graphic mean diameter (mm)	phi deviation (mm)
0.0 - 0.5	7	93	0	0.012	0.02	0.026	0.013
0.5 - 1.0	6	94	0	0.012	0.019	0.025	0.011
1.0 - 1.5	14	82	4	0.009	0.019	0.023	0.016
1.5 - 2.0	4	94	2	0.01	0.039	0.044	0.03
2.0 - 2.5	6	94	0	0.01	0.018	0.023	0.012
2.5 - 3.0	8	92	0	0.01	0.019	0.023	0.014
3.0 - 3.5	8	78	14	0.011	0.018	0.023	0.015
3.5 - 4.0	11	71	18	0.011	0.021	0.027	0.019
4.0 - 4.4	7	91	2	0.011	0.018	0.023	0.013
4.4 -4.8	10	87	3	0.01	0.02	0.024	0.015
4.8 - 5.2	7	80	13	0.011	0.018	0.023	0.015
5.2 - 5.65	12	75	13	0.012	0.025	0.031	0.023

Porosity: is the ratio of the volume of voids to the total volume of sample.

$$n = \frac{e}{1 + e} \qquad \ldots\ldots\ldots \quad (A.7)$$

Degree of saturation: is the ratio of the volume of water to the volume of the voids, and can be calculated by:

$$S_r = w\, D_R\, (1-n) \,/\, n \quad \times 100\ \% \qquad \ldots\ldots\ldots \quad (A.8)$$

$$S_r = w\, D_R \,/\, e \quad \times 100\ \% \qquad \ldots\ldots\ldots \quad (A.8')$$

Atterberg limits: Atterberg limit tests describe the consistency of a cohesive sediment. The Atterberg limits include:

liquid limit, w_L: which is defined as the moisture content at which the sediment stops acting as a liquid and starts acting as a plastic. (ASTM - D 423).

plastic limit, w_p: which is defined as the moisture content which marks the limit between plastic and brittle failure. (ASTM - D 424).

The difference in water content between the liquid and plastic limits is known as the plasticity index, I_p, while the liquidity index, I_L is defined as:

$$I_L = \frac{w - w_p}{I_p} \qquad \ldots\ldots\ldots \quad (A.9)$$

Activity: is the ratio of plasticity index to the clay fraction (less than 2 microns): This ratio represents the surface activity of the clay fraction, such as the increased ion exchange capacity and potential absorption of water with decreasing grain size.

c. Engineering Properties

Shear strength: the shear strength of a sediment is defined as the maximum shear stress which the sediment can withstand. While shear strength can be measured by a number of methods including triaxial

compression and direct shear tests, it was impractical to use these common test methods for the soft material recovered in the cores. A convenient method for measuring the shear strength of fine grained sediments is the vane shear test. Details of the standard field procedure for vane shear testing have been presented by ASTM - D 2573. No standard method for a laboratory vane shear test presently exists and thus the field procedure was generally followed. A four bladed rotor of known dimensions is inserted into the sediment and the undrained shear strength S_u is calculated from the maximum torque required to rotate the vane and produce failure.

Consolidation: The one-dimensional consolidation test is carried out in a consolidometer in which the sample is contained in a rigid circular ring between two porous plates and is loaded axially. Increasing loads are applied to the sample, and the amount and time-rate of compression of the sample for each load increment is measured. As the pore water drains out with time, a pressure difference is produced and the volume of the sediment decreases. These tests followed standard soil mechanics procedures ASTM - D2435. A 63.1 mm sample diameter was used. The starting load was very light, being just the top capacity of the consolidometer cell, on the sample. Each load was allowed to remain on the sample for 24 hours, at which time the next load (apart from the first increment, each successive load was double the preceding one) was added. This gave increasing pressures of 0.326, 0.652, 1.304, 2.608 and 5.216 kg/cm^2. The results were plotted as void ratio, e, against the logarithm of the pressure, p, Figs. 54 and 55 in Chapter V show two examples of such curves representing samples from stations G 141 and 441A. Other data from the

consolidation test can be used to provide more information about the sediment sample such as compression index and coefficient of consolidation. Compression index, C_c is the slope of the linear portion of the pressure-void ratio curve on a semi-log plot. Coefficient of consolidation, c_v is a coefficient utilized in the theory of consolidation, containing the physical constants of a soil affecting its rate of volume change.

Consolidation tests were performed on samples at 0.5 m intervals along each core for a total of 73 tests. In view of the general similarity of the test results, the curve for each test has not been included. Values of the compression index C_c and coefficient of consolidation c_v obtained from the tests have been included in Figs 3 to 10 in Chapter IV for comparison with other test values. In each case, the value of c_v reported has been calculated for the second load increment of the test.

2. Sound Velocity Measurement

The travel time of a sound impulse across a core liner filled with sediment is compared to one filled with water of known velocity. From the time difference obtained, the sound velocity of the sediment is determined. Fig. 58 is a schematic diagram of the electric circuitry in the system used to measure core velocities in this study.

Sound velocity was calculated using an estimate of the arrival time of a pulse at the receiver (Simpkin 1978). If a two phase medium is considered with a transmitter at A and a receiver at B (Fig, 59). Assuming that one phase is the liner plastic and the second phase is water, the time for a pulse to travel from A to B is:

$$T_1 = \frac{L_p}{v_p} + \frac{L_1 - L_p}{v_w} + T_t \qquad \ldots\ldots\ldots\ldots \quad (A.10)$$

where: L_p = 2 x liner wall thickness

L_1 = outside diameter of liner

v_p = sound velocity in plastic

v_w = sound velocity in water

T_t = the fixed delays

Similarly, for sediment

$$T_2 = \frac{L_p}{v_p} + \frac{L_2 - L_p}{v_s} + T_t \qquad \ldots\ldots\ldots \quad (A.11)$$

where: v_s = sediment sound velocity

Subtracting 10 from 11 and rearranging:

$$v_s = \frac{L_2 - L_p}{\Delta T + (L_1 - L_p)/v_w} \qquad \ldots\ldots\ldots \quad (A.12)$$

where: $\Delta T = (T_2 - T_1)$ is the difference in the time for both the sediment and water cases. If L_2 is measured concurrently with T_2 during the scanning period, then estimates of T_1, L_p, L_1 and v_w are required to compute v_s (Simpkin 1978). These parameters can be obtained after calibration and providing the measuring technique remains unchanged throughout the measuring period.

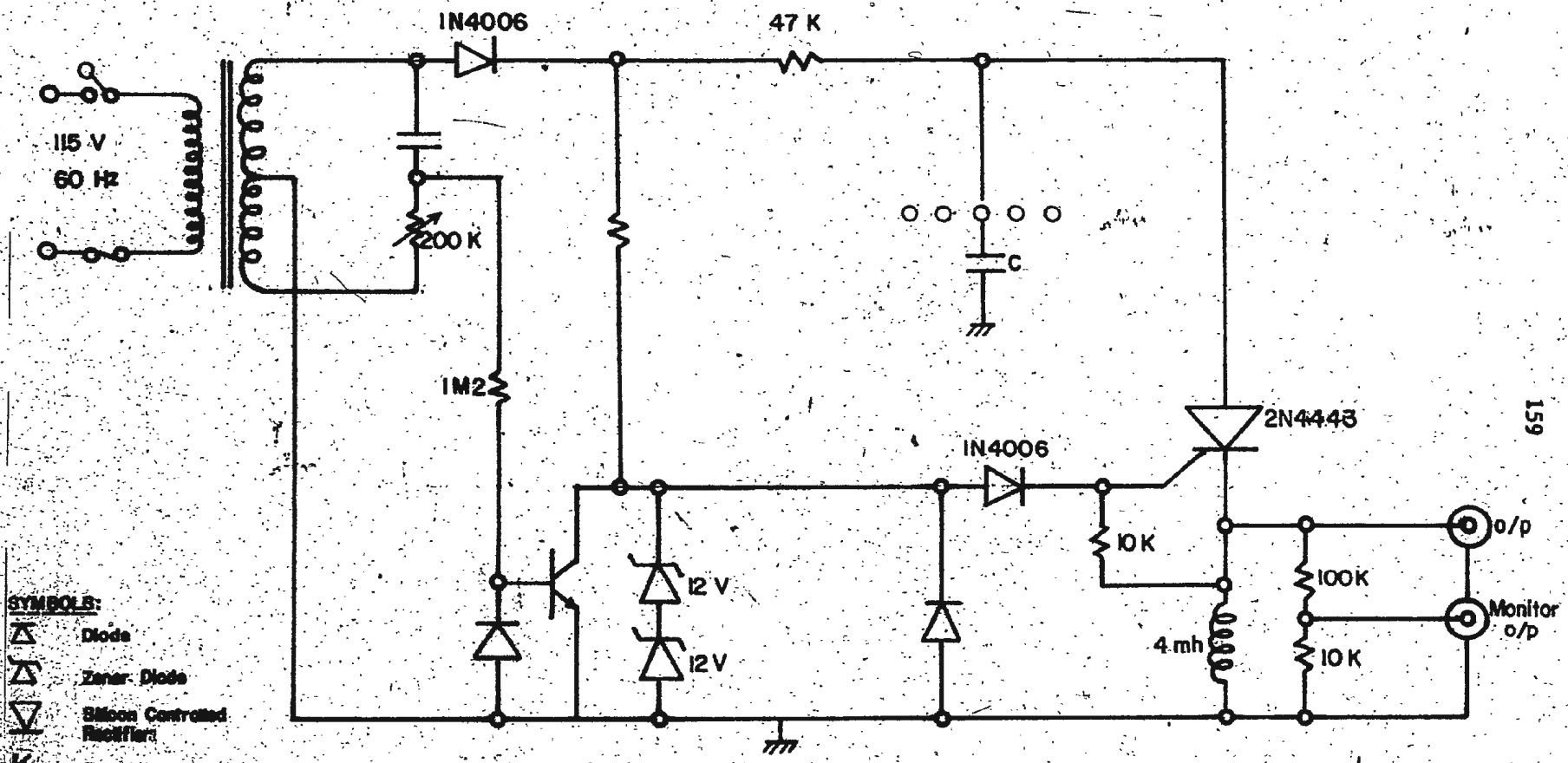

Fig. 58. Schematic of Velocity Scanning System Circuitry (Ref. 65)

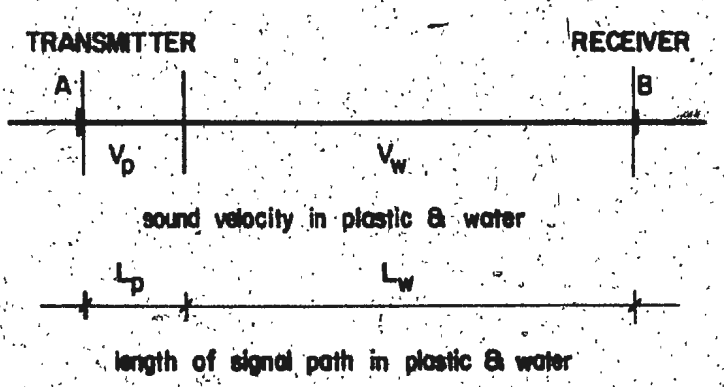

Fig. 59. Comparison of Sound Velocity and Signal Path in Two Phase Medium (Ref. 65)

APPENDIX B

OUTLINE OF COMPUTATION PROCEDURES TO OBTAIN ELASTIC CONSTANTS FROM LABORATORY SEDIMENT DATA

This appendix outlines the procedures used to compute elastic constants from sediment laboratory test data. The following constants have been derived for the samples tested: compressibility, bulk modulus, rigidity (shear) modulus, Lame's constant, Poisson's ratio and Young's modulus. The elastic constants are derived from the following sediment properties, with average values taken for each case:

a. sediment sound velocity, v_s

b. bottom water sound velocity, v_w

c. sediment density, ρ_s

d. density of water, ρ_w

e. sediment porosity, n

The following procedures are applied for each core tested using the equations derived by Gassman (1951) and Hamilton (1969). The results are presented in Table 11 of chapter V.

1. Determination of bulk modulus of pore water (K_w):

Using the equation of sound velocity in a liquid,

$$v_w = (K_w/\rho_w)^{\frac{1}{2}} \qquad (B.1)$$

or $$K_w = \rho_w . v_w^2 \qquad (B.1')$$

The bottom water sound velocity for the Placentia Bay area is about 1444 m/s (Simpkin, 1978), and the density of pore water at an average depth of 10 m below the mud-line is almost 1.024 gm/cm^3. Using these values, an average value of the bulk modulus of the pore water K_w

has been calculated as $K_w = 213.5 \times 10^4$ kN/m^2 for all the cores tested.

2. Determination of aggregate bulk modulus of mineral grains (K_s):

The range of aggregate bulk moduli for most sediments is so small that estimates can be used when the mineralogy is not exactly known. Thus with small error, the aggregate bulk modulus for fine sand, clayey silt, and clay can be assumed from published values (Hamilton, 1969)

- fine sand aggregate $K_s = 5233 \times 10^4$ kN/m^2
- silt aggregate $K_s = 5338.5 \times 10^4$ kN/m^2
- clayey silt aggregate $K_s = 5442 \times 10^4$ kN/m^2
- silty clay aggregate $K_s = 5000 \times 10^4$ kN/m^2.

3. Determination of dynamic frame-bulk modulus (K_f):

Hamilton (1969) provided a derivation of a relationship between dynamic bulk moduli and porosities. These relationships are

- for sands $\log K_f = 2.71405 - 4.12135\ n$ . . . . . (B.2)
- for silts and clays $\log K_f = 3.73807 - 4.2557\ n$ . . . . . (B.3)

where K_f in dyne/cm^2 $\times 10^8$

4. Computation of water-mineral system bulk modulus (K):

Using Gassman's equation (1951)

$$K = K_s \frac{K_f + Q}{K_s + Q} \quad \text{. . . . . (B.4)}$$

where $Q = \text{constant} = \frac{K_w (K_s - K_f)}{n (K_s - K_w)}$ . . . . . (B.5)

K_w = bulk modulus of pore water (from step 1)

K_s = aggregate-bulk modulus of mineral solids (from step 2)

K_f = frame-bulk modulus (from step 3)

n = decimal-fractional porosity of sediment

The results for each of the tested cores are summarized in Table 20.

5. Computation of the elastic constants using the measured values of bulk density (ρ_s), sound velocity (v_s) and the computed system-bulk moduli. These equations are:

- Compressibility, $\beta = \frac{1}{K}$ . . . . . (B.6)

- Lame's constant, $\lambda = \frac{3K - \rho_s v_s^2}{2}$ . . . . . (B.7)

- Poisson's ratio, $\nu = \frac{3K - \rho_s v_s^2}{3K + \rho_s v_s^2}$ . . . . . (B.8)

- Rigidity modulus, $\mu = 3/4\ (\rho_s v_s^2 - K)$ . . . . . (B.9)

- Young's modulus, $E = \frac{9K\ (\rho_s v_s^2 - K)}{(\rho_s v_s^2 + 3K)}$ . . . . . (B.10)

These relationships have been defined by Gassman (1951) and Hamilton (1969).

TABLE 20. SUMMARY OF BULK MODULUS COMPUTATIONS

core description		measured values			computed values			
core no.	sediment type	ρ_s	n	V_s	K_w	K_s	K_f	K
G 132	clayey silt	1.48	0.681	1552	213.5	5442	6.917	314.01
G 141	clayey silt	1.52	0.668	1522	213.5	5442	7.857	320.47
G 233	clayey silt	1.80	0.553	1610	213.5	5442	24.25	395.24
G 243	clayey silt	1.725	0.563	1568	213.5	5442	22.0	387.14
G 332	clayey silt	1.88	0.503	1618	213.5	5442	39.77	443.02
G 341	silt	1.81	0.535	1528	213.5	5338.5	28.92	410.56
G 432	silt	1.606	0.628	1551	213.5	5338.5	11.628	342.33
G 441A	clayey silt	1.606	0.606	1575	213.5	5442	14.425	356.21

Notes:

K_w = bulk modulus of pore water, $kN/m^2 \times 10^4$

K_s = aggregate bulk modulus of mineral grains, $kN/m^2 \times 10^4$

K_f = dynamic frame-bulk modulus, $kN/m^2 \times 10^4$

K = water-mineral system bulk modulus, $kN/m^2 \times 10^4$

APPENDIX C

REGRESSION AND CORRELATION ANALYSIS & PROGRAM

A regression analysis relating the acoustic properties to the physical properties of ocean sediments was obtained by the statistics of multiple regression. The statistical theory applied in such a case is given in most elementary statistics texts (Chatfield 1976) and only a summary of the most important relations will be given here.

Regression Theory:

If several measurements are made on the dependent variables, y, at the same value of the controlled variables, x, then the results will form a distribution. The curve which joins the mean values of these distributions is called the regression curve of y on x. If a straight line can be fitted to the data, then we say that a linear relationship exists between the two variables, otherwise the relationship is non-linear.

a- Linear Regression:

For n pairs of measurements, $(x_1,y_1),\ldots,(x_n,y_n)$, where y are the dependent and x are the independent variables, a straight line can be represented by the equation:

$$y = a_o + a_1 x \qquad \ldots\ldots\ldots \quad (C.1)$$

The task here is to find estimates of a_o and a_1 such that the line gives a good fit to the data. One way of doing this is by the "method of least squares". This method gives values for both a_o and a_1 as:

$$a_o = \bar{y} - a_1\bar{x} \qquad \ldots\ldots\ldots \quad (C.2)$$

$$a_1 = \frac{\Sigma x_i y_i - n\bar{x}\bar{y}}{\Sigma x_i^2 - n\bar{x}^2} \qquad \ldots\ldots\ldots \quad (C.3)$$

where

$$\bar{y} = \frac{1}{n} \Sigma y_i \qquad \ldots\ldots\ldots \quad (C.4)$$

$$\bar{x} = \frac{1}{n} \Sigma x_i \qquad \ldots\ldots\ldots \quad (C.5)$$

After the least squares regression line has been calculated, it is possible to predict values of the dependent variable. At a particular value, x, of the controlled variable, the point estimate of y is given by:

$$y = a_o + a_1 x \qquad \ldots\ldots\ldots \quad (C.1)$$

b- Non-Linear Regression:

In many cases, an inspection of the scatter diagram is sufficient to show that the regression is not a straight line. One way of using linear theory in the linear case is to transform the variables in such a way that a linear relationship results. For example, if two variables are related by the formula:

$$y = a_o x^{a_1} \qquad \ldots\ldots\ldots \quad (C.6)$$

then we have

$$\log y = \log a_o + a_1 \log x \qquad \ldots\ldots\ldots \quad (C.7)$$

So that if log y is plotted against log x, the points will lie on a straight line. Another transformation is:

$$y = a_o a_1^x \qquad \ldots\ldots\ldots \quad (C.8)$$

then we have

$$\log y = \log a_o + x \log a_1 \qquad \ldots\ldots\ldots \quad (C.9)$$

So, if log y is plotted against x, the points will also lie on a straight line.

The Correlation Coefficient:

The purpose of the correlation is to see if the two variables are inter-related and to find a measure of the degree of association or correlation between them.

The correlation is said to be "positive" if large values of both variables tend to occur together, and "negative" if large values of one variable tend to occur with small values of the other variable. The correlation is said to be "high" if the observations lie close to a straight line and "low" if the observations are widely scattered.

The most important measure of the degree of correlation between two variables is a quantity called correlation coefficient. If we have n pairs of measurements, (x_i, y_i), then the observed correlation coefficient given by Chatfield (1976) is:

$$r = \frac{\Sigma(x_i - \bar{x})(y_i - \bar{y})}{\sqrt{\{\Sigma(x_i - \bar{x})^2\}\{\Sigma(y_i - \bar{y})^2\}}} \qquad \ldots\ldots\ldots \quad (C.10)$$

It can be shown that the value of r must lie between -1 and +1. For r =+1, all the observed points lie on a straight line which has a positive slope; for r =-1, all the observed points lie on a straight line which has a negative slope.

The Computer Program:

A computer program was written in Fortran language to find a mathematical relationship between each set of data points, using the regression analysis described previously. The program has the option of doing either linear or non-linear analysis in a manner similar to equations(C.1,6 and 8). The degree of correlation between the variables was established by running a straight forward correlation program which also computes the mean values of each parameter.

The program first reads all the data, accumelating the necessary totals, including sums of squares and products. The regression equation of y, the dependent variables, on x, the independent variables, is computed and the least squares fitting is used to calculate the constant of the equations. The program also computes the correlation coefficient given by equation (C.10).

Input Data:

a- control card (3I10)

columns 1 - 10 Number of simultanious pairs of data set

11 - 20 Number of points of the dependent variable

21 - 30 Option for type of regression

b- dependent variable cards (8F10.0)

c- title card (I8, 18A4)

columns 1 - 8 Number of points of the independent variable

9 - 80 Title of the problem

d- independent variable cards (8F10.0)

Notes:

1- data cards must be in proper sequence.

2- units must be considered.

3- for M sets of data, M cards for the independent variables are required.

4- the options (I CHECK) are as follows:

a) if I CHECK = 1 $y = a_o + a_1 x$ . . . . . (C.1)

b) if I CHECK = 2 $y = a_o x^{a_1}$ . . . . . (C.6)

c) if I CHECK = 3 $y = a_o a_1^x$ . . . . . (C.8)

d) if I CHECK = 4 $x = a_o a_1^y$ . . . . . (C.11)

Program Output:

The output of the program is in the following sequences:

1- problem number and title.

2- number of points used in the regression analysis.

3- printing of dependent versus independent variables,

4- correlation coefficient (r).

5- the equation form.

```
C
C     ************************************************************************
C     * PROGRAM TO FIND A SUITABLE RELATIONSHIP BETWEEN ANY TWO              *
C     * PARAMETERS USING THE REGRESSION ANALYSIS. THE PROGRAM ALSO           *
C     * COPUTES THE CORRELATION COEFFICIENT BETWEEN THESE PARAMETERS         *
C     ************************************************************************
C
      DIMENSION X(200),Y(200),TITLE(18)
C
C     READ TYPE OF REQUIRED REGRESSION AND NUMBER OF SETS OF DATA
C
      READ 1,M,IY,ICHECK
    1 FORMAT(3I10)
C
C     READ THE VALUES OF THE DEPENDENT VARIABLES (Y)
C
      READ 5,(Y(J),J=1,IY)
    5 FORMAT(8F10.0)
      IF(ICHECK.EQ.2) GO TO 70
      IF(ICHECK.EQ. 3) GO TO 70
      GO TO 17
   70 DO 16 II=1,IY
   16 Y(II)=ALOG10(Y(II))
   17 DO 100 K=1,M
C
C     READ AND PRINT TITLE, NUMBER OF DATA SETS AND THE INDEPENDENT
C     VARIABLES AND THE DEPENDENT VARIABLES.
C
      READ 2,N,(TITLE(I),I=1,18)
    2 FORMAT(I8,18A4)
      PRINT 3,K,(TITLE(I),I=1,18),N,ICHECK
    3 FORMAT(//,10X,'PROBLEM NO:',I5,'---',18A4/10X,90(1H*)//,
     15X,'TOTAL NUMBER OF POINTS IS =',I5//,'ICHECK =',I5,//)
      WRITE(6,4)
    4 FORMAT(10X,'Y',10X,'X'/10X,'-',10X,'-'/)
      READ 6,(X(J),J=1,N)
    6 FORMAT(8F10.0)
      Z=FLOAT(N)
      IF(ICHECK.EQ.2) GO TO 71
      IF(ICHECK.EQ.4) GO TO 71
      GO TO 50
   71 DO 15 II=1,N
   15 X(II)=ALOG10(X(II))
   50 XP=0.0
      YP=0.0
      XX=0.0
      YY=0.0
      XY=0.0
      DO 10 I=1,N
      WRITE(6,7)Y(I),X(I)
    7 FORMAT(5X,F10.5,4X,F10.5)
C
```

```
C       USE THE LEAST SQUARE FITTING
C
        XP=XP+X(I)
        YP=YP+Y(I)
        XX=XX+X(I)*X(I)
        YY=YY+Y(I)*Y(I)
        XY=XY+X(I)*Y(I)
   10 CONTINUE
C
C       CALCULATE THE CORRELATION COEFFICIENT (R)
C
        R=(XY-XP*YP/Z)/SQRT((XX-XP*XP/Z)*(YY-YP*YP/Z))
        IF(ABS(R).GE.0.09) GO TO 30
        WRITE(6,20)
   20 FORMAT(5X,'NO CORRELATION BETWEEN THESE TWO PARAMETERS'//)
        GO TO 100
   30 A1=(XY-XP*YP/Z)/(XX-XP*XP/Z)
        A0=YP/Z-A1*XP/Z
C
C       CHECK FOR THE TYPE OF RELATIONSHIP
C
        IF(ICHECK.EQ.2) GO TO 72
        IF(ICHECK.EQ.3) GO TO 73
        IF(ICHECK.EQ.4) GO TO 74
        PRINT 40,R,A0,A1
   40 FORMAT(//5X,'CORRELATIIN COEFFICIENT ....=',F10.7//,5X,
       U'THE RELATIONSHIP IS IN THE FOLLOWING FORM:',//5X,'Y  = ',
       2F10.5,F10.5,'X',//)
        GO TO 100
   72 B0=10**A0
        B1=A1
C
C       PRINT THE FINAL RESULTS.
C
        PRINT 41,R,A0,A1,B0,B1
   41 FORMAT(//,5X,'CORRELATION COEFFICIENT ...= ',F10.7//,5X,
       1'THE LINEAR RELATIONSHIP IS IN THE FOLLOWING FORM ...:',//,5X,
       2'LOG (Y)  =  LOG',F10.5,F10.5,'LOG(X)',//,5X,'OR ON THE FORM .....
       4Y=',F10.5,'X TO THE POWER',F10.5,//)
        GO TO 100
   73 B0=10**A0
        B1=10**A1
        PRINT 42,R,A0,A1,B0,B1
   42 FORMAT(//,5X,'CORRELATION COEFFICIENT....= ',F10.7,//,5X,
       1'THE LINEAR FORM IS :.....LOG(Y)=LOG',F10.5,'X,LOG',F10.5,//,
       2'OR IN THE FORM....Y=',F10.5,'BY',F10.5,'TO THE POWER X',//)
        GO TO 100
   74 B0=0.
        B1=0.0
        PRINT 43,R,A0,A1,B0,B1
   43 FORMAT(//,5X,'CORRELATION COEFFICIENT...=',F10.5,//,5X,
```

```
     1'THE CONSTANTS ARE ...A0= '.F10.5.'...AND...A1 ='.F10.5.//.
     25X.'OR IN THE FORM ....X= '.F10.5.'BY'.F10.5.'TO THE POWER Y'.//)
100  CONTINUE
     STOP
     END
```

PROBLEM NO: 1--- "SOUND VELOCITY VERSUS WET DENSITY "

****

TOTAL NUMBER OF POINTS IS = 114

CHECK = 1

Y	X
1.56000	1510.00000
1.55600	1520.00000
1.56400	1530.00000
1.56300	1540.00000
1.56200	1545.00000
1.55900	1550.00000
1.55700	1553.00000
1.56000	1557.00000
1.55500	1560.00000
1.55300	1565.00000
1.55000	1570.00000
1.55400	1434.00000
1.54700	1486.00000
1.52200	1500.00000
1.52200	1470.00000
1.52800	1570.00000
1.52800	1570.00000
1.52800	1570.00000
1.52700	1570.00000
1.52400	1561.00000
1.52000	1554.00000
1.52100	1545.00000
1.52400	1535.00000
1.52000	1525.00000
1.52000	1520.00000
1.51800	1500.00000
1.52200	1485.00000
1.52800	1465.00000
1.52200	1450.00000
1.52100	1450.00000
1.52300	1458.00000
1.52200	1490.00000
1.52100	1530.00000
1.51500	1520.00000
1.51500	1510.00000
1.52000	1530.00000
1.52000	1520.00000
1.51500	1510.00000
1.51800	1500.00000
1.56200	1615.00000
1.54300	1650.00000
1.58500	1680.00000
1.63700	1660.00000
1.58700	1770.00000
1.65600	1950.00000
1.65600	2130.00000
1.65600	2060.00000
1.65600	1990.00000
1.56000	1720.00000
1.54300	1713.00000
1.54800	1710.00000
1.56500	1700.00000
1.56800	1700.00000
1.56700	1700.00000
1.58200	1733.00000
1.62000	1760.00000
1.56500	1760.00000
1.57500	1760.00000
1.55800	1840.00000

1.55400	1850.00000
1.57400	1660.00000
1.56400	1810.00000
1.60100	1760.00000
1.64400	1765.00000
1.55200	1770.00000
1.65300	1960.00000
1.68900	1920.00000
1.60000	1880.00000
1.61400	1840.00000
1.64500	1840.00000
1.59100	1830.00000
1.61000	1820.00000
1.63100	1820.00000
1.60100	1820.00000
1.64700	1840.00000
1.58900	1860.00000
1.61600	1860.00000
1.59500	1860.00000
1.63000	1600.00000
1.54200	1600.00000
1.56500	1600.00000
1.57500	1622.00000
1.56300	1645.00000
1.55100	1618.00000
1.52300	1590.00000
1.53300	1587.00000
1.57900	1584.00000
1.52300	1590.00000
1.52400	1600.00000
1.52900	1611.00000
1.53300	1623.00000
1.55500	1620.00000
1.55600	1635.00000
1.56300	1650.00000
1.56300	1635.00000
1.55600	1620.00000
1.55900	1620.00000
1.56200	1620.00000
1.56000	1620.00000
1.59000	1620.00000
1.57100	1630.00000
1.60000	1640.00000
1.57000	1665.00000
1.56800	1690.00000
1.56800	1705.00000
1.57000	1720.00000
1.57900	1703.00000
1.57200	1690.00000
1.57200	1695.00000
1.61300	1700.00000
1.64500	1700.00000
1.57200	1700.00000
1.57100	1700.00000
1.58700	1700.00000

CORRELATION COEFFICIENT .....= 0.7940505

THE RELATIONSHIP IS IN THE FOLLOWING FORM:

Y = -1.18993 + 0.00623X